Spring 2013

The Effect of Surface Treatment on Nickel Leaching from Nitinol

Daniel Lawrence Leobrera Madamba
San Jose State University

THE EFFECT OF SURFACE TREATMENT ON NICKEL LEACHING FROM NITINOL

A Thesis

Presented to

The Faculty of the Department of Biomedical, Chemical, and Materials Engineering

San José State University

In Partial Fulfillment

of the Requirements for the Degree

Master of Science

by

Daniel Madamba

May 2013

The Designated Thesis Committee Approves the Thesis Titled

THE EFFECT OF SURFACE TREATMENT ON NICKEL LEACHING FROM NITINOL

by

Daniel Madamba

APPROVED FOR THE DEPARTMENT OF BIOMEDICAL, CHEMICAL, AND MATERIALS ENGINEERING

SAN JOSÉ STATE UNIVERSITY

May 2013

Dr. Guna Selvaduray	Department of Biomedical, Chemical, and Materials Engineering
Dr. Michael Jennings	Department of Biomedical, Chemical, and Materials Engineering
Dr. Gregory Young	Department of Biomedical, Chemical, and Materials Engineering

ABSTRACT

THE EFFECT OF SURFACE TREATMENT ON NICKEL LEACHING FROM NITINOL

by Daniel Madamba

Nitinol is widely used as a biomaterial for implantable medical devices but can be susceptible to nickel leaching. Our research was aimed at determining nickel leaching from surface treated Nitinol samples, treated as follows: mechanical polishing (untreated), oxidation, and nitriding+oxidation (5 different nitriding temperatures). Five specimens from each category were immersed in 40 mL PBS solution and incubated at 37^{o}C over 91 days. Nickel concentration readings were taken at regular intervals. After 91 days, the average nickel concentration in the PBS solution was (a) 0.223 mg/L, SD 0.017, untreated, (b) 7.68 mg/L, SD 6.405, 1000°C nitriding+oxidation, and (c) 3.914 mg/L, SD 1.78, oxidation-only. The concentration readings had large standard deviations implying differences in surface characteristics after treatment. The increased nickel leaching from treated samples was thought to be due to atomic diffusion and exposure of the nickel-rich sublayers to PBS after oxide layer delamination. These sublayers formed after formation of thick (>1 μm) TiO_2 layers during oxidation.

ACKNOWLEDGMENTS

The author would like to thank Dr. Guna Selvaduray for his support and guidance throughout the process and for the encouragement to pursue this research in the first place. Dr. Michael Jennings and Dr. Gregory Young are much appreciated for serving on the Reading Committee and their input and feedback.

The author would also like to thank Intuitive Surgical for their generous financial support.

Many thanks go out to the people at San José State University for their expertise and patience, especially Anastasia Micheals, Christy Peters, Neil Peters, and Craig Stauffer. The invaluable support, advice and hard work of Maleeha Naqvi are also greatly appreciated. Without her, much of this work would not have been possible. Special thanks to Edin Bazochaharbakhsh and Masao Drexel for their help with the experimental setup and materials.

Finally, a huge thank you goes out to my family whose love and support have helped keep me afloat throughout my educational career.

TABLE OF CONTENTS

LIST OF FIGURES

LIST OF TABLES

CHAPTER ONE

INTRODUCTION

Nitinol is an intermetallic compound that is composed of nickel and titanium in a nominally 1:1 stoichiometric ratio. It has wide usage today in medical devices because of its shape memory, superelasticity, and biocompatibility.

1.1 History of Nitinol

Nitinol (**Ni**ckel **Ti**tanium **N**aval **O**rdnance **L**aboratory) was discovered in 1958 by metallurgist William J. Buehler at the Naval Ordnance Laboratory while researching materials for use in the nose cone of the U. S. Navy Polaris reentry vehicle [1]. During his research, he realized that temperature changes in bars of equiatomic nickel-titanium alloy caused major changes in the atomic structure of the material. Further studies into the alloy revealed its excellent fatigue resistance and shape memory characteristics [1]. Although Nitinol was not used for the nose cone, the discovery of its unique properties enabled its future usage in a variety of different applications.

1.2 Properties of Nitinol

Shape memory and superelasticity are two of the key properties of Nitinol that make it so unique and useful. Shape memory refers to the ability of Nitinol to return to a predetermined state after heating, while superelasticity refers to the fact that Nitinol can withstand abnormally large, recoverable strains compared to other alloys. Both of these properties stem from the martensite-austenite phase transformation that occurs when Nitinol changes temperature. The phase transformations due to temperature and applied stress are shown in Figure 1.

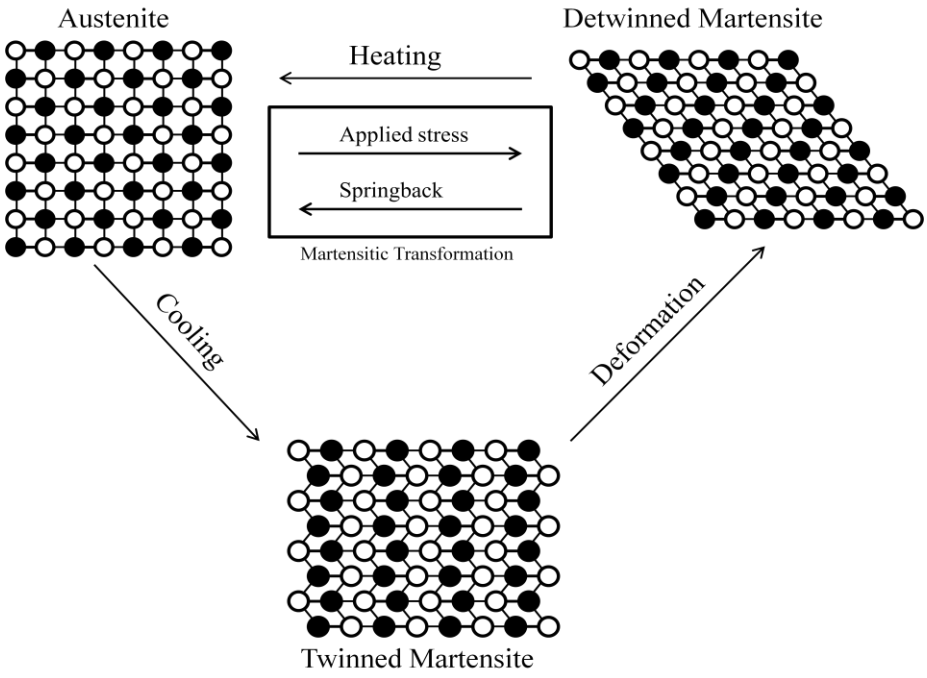

Figure 1. Diagram of Nitinol Phase Transformations.

At high temperatures (100°C), Nitinol exists in its austenite phase, which is body-centered cubic [2]. Cooling austenitic Nitinol causes a change in the crystal structure of the alloy, from austenite to a twinned martensite phase, with a monoclinic crystal structure. In this phase, mechanical deformation of the Nitinol causes the microstructure to change from the twinned martensite phase to a de-twinned martensite. Subsequent heating of the Nitinol to a temperature higher than the austenite finish temperature results in the Nitinol reverting back to its original austenite structure [2]. This martensite-austenite phase transformation may also occur due to applied stress, wherein deformation of austenite causes the formation of de-twinned martensite. Removal of the stress restores the austenite phase. Because of its superelasticity, Nitinol is able to recover strains of up to 8%, compared to other alloys which can recover less than 1% [2].

Another consideration in the use of Nitinol in medical devices is its biocompatibility. This property is derived from the formation of a passive TiO_2 layer on the surface of the alloy [3]. This layer acts as a barrier between the NiTi bulk and the human body, preventing potentially toxic nickel from leaching out. In addition, the layer also helps to prevent corrosion. These phenomena have important implications in the usage of Nitinol in medical devices.

1.3 Applications of Nitinol

One of the main applications of Nitinol in the medical device industry is for stents. Nitinol's superelasticity allows for delivery of stents to the intervention site without kinking or permanently deforming. Nitinol stents are "self-expanding," taking advantage of the shape memory capability, and are made in such a way that the fully-expanded form of the stent is in the austenite phase. The stent is compressed and constrained in the delivery system until time for deployment in the body. Once released from the sheath, the stent expands to its original shape [3]. The same concept has been applied to the delivery of vena cava filters.

The superelasticity of Nitinol also makes it a useful material for guidewires and catheters. As these wires must endure a tortuous path through the vasculature, it is important that the material not deform permanently. Nitinol also has a long history of usage in dental applications where it is used mainly for orthodontic archwires. Compared to stainless steel archwires, Nitinol archwires require fewer changes over the duration of the treatment, reduce the time needed to rotate teeth for improved alignment, and are more corrosion resistant [2].

1.4 Nickel Leaching

Although Nitinol is generally biocompatible, nickel leaching can still be a problem. Nickel present within the oxide layer can lead to release of nickel ions into the surrounding media [4]. The formation of the oxide layer also results in the creation of nickel-rich sublayers which, when exposed, can act as reservoirs of nickel in the body. Nickel atoms are also small in comparison to titanium and oxygen atoms and can thus diffuse interstitially through surface oxide layers [5]. These problems are more pronounced in Nitinol samples that have a native oxide layer, rather than one that has been grown as a result of treatment methods. The formation of a completely nickel-free oxide layer on the surface of Nitinol would help to reduce the problem of nickel leaching.

1.5 Scope of Research

This research was done to characterize nickel leaching from surface treated Nitinol. Exposure of the human body to excess amounts of nickel can lead to adverse effects including allergic reactions, oxidative stress, and DNA damage and is especially harmful to those with hypersensitivity to nickel [6, 7]. Surface treatment of Nitinol reduces nickel leaching as compared to untreated samples [8]. In this study, samples were treated with various methods including oxidation, nitriding and oxidation, and mechanical polishing. The surface treatments were studied to determine whether they were effective in reducing nickel ion release from Nitinol, towards the ultimate goal of improving the safety of Nitinol medical devices.

A review of the literature concerning nickel toxicity and Nitinol treatment methods is contained in Chapter 2. The objectives of the research are outlined in Chapter

3. The materials and methods used to perform the research are described in Chapter 4. The results of the research are presented in Chapter 5. A discussion of the results follows in Chapter 6. The conclusions are presented in Chapter 7, with recommendations for future work following in Chapter 8.

CHAPTER TWO

LITERATURE REVIEW

2.1 Introduction

Nickel is a naturally-occurring element found in the earth's crust and in the natural environment [9]. Human exposure to nickel can occur via food intake, inhalation, or skin contact with nickel-containing alloys, such as those used to make jewelry or coins. For humans, the average daily intake for ingested nickel is 0.1 - 0.3 mg, compared to less than 0.0008 mg per day for inhalation [10]. The nickel content in human serum ranges from 0.0001 to 0.0013 mg/L [11]. As defined by the American Conference of Governmental Industrial Hygenists (ACGIH), the limit for nickel carbonyl exposure in air without adverse effects (Threshold Limit Value, or TLV) is 0.05 ppm for 8 hrs of exposure, or about 0.065 mg/m^3 air. For soluble nickel compounds, this limit is 0.100 mg/m^3 air [12]. The U.S. Environmental Protection Agency (EPA) reference dose for nickel is 0.020 mg/kg/day with a lowest observed adverse effect level (LOAEL) of 50 mg/kg and a "no observed adverse effect level" (NOAEL) of 5 mg/kg [13]. Those in the nickel mining and processing industry see significantly increased exposure to nickel, mostly via inhalation. Nickel is a constituent in a number of metal alloys commonly used in medical devices, including those implanted in the body. They include stainless steel, Nitinol, and cobalt-chromium alloys (Conichrome, Phynox, Elgiloy). The nickel content of medical devices made with such metals presents a safety concern as contact with nickel-containing alloys could lead to problems such as contact dermatitis, inflammation, or even carcinogenic activity [9]. Nickel has not been proven to be an essential element

for human life, and the metabolism of nickel compounds in the body is unknown. Since nickel is abundant in all types of food, nickel deficiency is rare. Its role as a carcinogen and mutagen is currently being studied.

Overall, 8-14% of women and 1-2% of men exhibit hypersensitivity to nickel [14]. For the most part, the immune response is caused by dermal contact with nickel and nickel alloys in common items such as jewelry, implants, or coins. Nickel can cause both a delayed immunologic response (allergic contact dermatitis, ACD) and an immunologic contact urticaria (ICU) [15]. ACD is expressed as cutaneous and mucous membrane eruptions while ICU involves symptoms of respiratory allergy. Nickel has also been shown to induce oxidative stress and DNA damage in cultured lymphocytes [6, 7]. The oxidative stress brought forth by nickel exposure is a precursor to more serious effects such as mutagenesis and carcinogenicity. Examples of the oxidative damage that can occur include modification of transcription, replication errors, and genomic instability. All nickel compounds excluding metallic nickel have also been classified as carcinogenic to humans, according to the International Agency for Research on Cancer (IARC) [9].

There are a number of Nitinol surface treatment methods that have been employed to reduce the amount of nickel leaching that occurs. Many of these have been described by Shabalovskaya *et al.* in 2008 [8]. A selection of previous studies concerning the treatment and nickel leaching of Nitinol is summarized in Table 1 and described in greater detail in this chapter.

Table 1. Summary of Nickel Leaching Test Results.

Treatment Method	Treatment Details	Surface Layer Thickness	Oxide Layer Composition (at. %)	Leaching Medium	Immersion Time (days)	Nickel Conc. in Media (mg/L)	Nickel Release ($mg/L/cm^2$)	% Reduction from untreated	Ref.
Mechanical Polishing	Wet polished, 600 grit	N/A	Ti: 5.7 Ni: 1.4	Human endothelial cell medium	3	0.006	0.001	99.5%	[8]
Chemical Etching	$1HF + 4HNO_3$	1.5 nm	Ti: 15 Ni: 6.7	Human endothelial cell medium	3	0.011	0.003	99.2%	[8]
Chemical Etching	Proprietary Fort Wayne Metals solution	15 nm	Ti: 15.7 Ni: 1.3	Cell culture media	3	<0.005	<0.019	99.9%	[4]
Chemical Etching	Proprietary Fort Wayne Metals solution	15 nm	Ti: 15.7 Ni: 1.3	Cell culture media	~ 180	<0.005	<0.019	100%	[4]
Electropolishing	10% perchloric acid + 90% acetic acid, room temp, 20 V, 6 min	1.8 nm	Ti: 15 Ni: 2.5	Human endothelial cell medium	3	0.006	0.003	99.5%	[8]
Electropolishing	70% methanol + 30% nitric acid, -45°C, 20 V, 6 min.	1.8 nm	Ti: 13 Ni: 5.0	Human endothelial cell medium	3	0.007	0.001	99.5%	[8]
Electropolishing	Glacial acetic acid and perchloric acid (vol 5:100), 30 V, 2 min 15 s	6 nm	12.3 Ti/Ni ratio	Simulated body fluid	30	N/A	N/A	N/A	[16]
Thermal Oxidation	400°C, $3x10^{-2}$ mbar	63 nm	14 0 Ti/Ni ratio	Simulated body fluid	30	0.013	0.0862	86.2%	[17]
Nitriding	900°C nitrogen, 20 min	N/A	TiN surface layer	Artificial saliva	~83	~0.06	0.078	70%	[18]
Nitriding	Pulse-biased arc ion plating	2 μm	TiN surface layer	Artificial saliva	30	0.150	0.015	400% increase	[19]
Nitriding	Pulse-biased arc ion plating	2 μm	Ti/TiN multilayer	Artificial saliva	30	ND	ND	100%	[19]
DLC Coating	Ion beam plating	1 μm	N/A	Physiological saline	14	ND	N/A	100%	[20]
DLC Coating	Ion beam plating	1 μm	N/A	Physiological saline	60	0.150	N/A	83.9%	[20]

2.2 Nickel Release from Nitinol

When left untreated, nickel ion release has been shown to occur from the surface of Nitinol. In a 2011 study, Haider *et al.* [21] compared nickel ion release from bare Nitinol with surface treated Nitinol and Nitinol alloys. The surface treatments used in the experiment were electropolishing, magnetoelectropolishing, and water boiling and passivation. Electropolishing and magnetoelectropolishing were done by Electrobright® (Macungie, PA, USA). The water-boiled samples were boiled in distilled water at 132°C for 30 min, followed by immersion in 20% concentration HNO_3 at 80°C for 20 min. Each of these surface treatments was performed on NiTi, NiTiCu, NiTiTa, and NiTiCr. Following surface treatment, a corrosion test using the cyclic potentiodynamic polarization method was performed, followed immediately by measurement of the nickel concentration in solution. Using a saturated calomel electrode as the reference electrode, the test was performed at 37ºC in 70 mL PBS solution with a scan rate of 1 mV/s over a potential range of -0.5 V to 2.2 V. Haider observed a nickel concentration of 0.0699 mg/L in the phosphate buffered saline (PBS) solution in which the untreated Nitinol was immersed. Treatment of the Nitinol surface, whether by magnetoelectropolishing, electropolishing, or water boiling and passivation reduced the nickel concentration in the PBS solution to undetectable levels. The nickel concentration measurements were only taken once, immediately after the corrosion test was performed. If the samples had been exposed to the PBS solution for a longer period of time, higher nickel concentrations could have been observed over time.

In a 2008 study, Shabalovskaya *et al.* [8] also compared the nickel release characteristics of untreated Nitinol with Nitinol samples that had been chemically etched, wet polished, electropolished, or heat treated. Chemical etching was done in 1HF + $4HNO_3$. Some chemically etched samples were subsequently boiled in distilled water for 30 min. Wet polishing was performed using silicon carbide paper up to 600 grit and 1 μm finish. Electropolishing was done in one of two electrolytes. The first electrolyte contained 10% perchloric acid and 90% acetic acid, and the Nitinol electropolished at room temperature at 20 V for 6 min. The second electrolyte contained 70% methanol and 30% nitric acid, with electropolishing being done at -45°C for 6 min. Heat treatment was done in air at 520°C for 15 min. The Nitinol in this experiment was placed in a human microvascular endothelial cell medium for 72 h. The nickel concentration in the medium with pure, untreated Nitinol was 0.849 mg/L. The various surface treatments studied reduced the release rate of nickel from 100 to 1000 times. Wet polished Nitinol resulted in a nickel concentration of 0.0047 mg/L. The nickel concentration in the media exposed to electropolished Nitinol was 0.0047 mg/L for the first electrolyte and 0.0055 mg/L for the second electrolyte. Chemically etched Nitinol resulted in a nickel concentration of 0.0086 mg/L. This was reduced to 0 mg/L or 0.001 mg/L when subsequently water boiled or water boiled and heat treated, respectively.

In 2005, Kobayashi *et al.* [20] compared the nickel release, into physiological saline solution, of Nitinol coated with a diamond-like carbon (DLC) coating versus that of non-coated Nitinol. In the experiment, ion beam plating was used to deposit 1.0 μm thick DLC films on Nitinol archwires. High purity benzene gas at 2.3×10^{-5} Pa was used

for DLC deposition. An SiC interlayer was employed to improve the adherence of the DLC coating to the substrate. The Nitinol samples were immersed in physiological saline solution for 14 days at 80 °C and for 6 months at 37°C. In the 14 day test, the nickel ion release was undetectable for DLC-coated wire. The nickel ion concentration in the medium exposed to non-coated samples was 2.5×10^{-6} mg/L after 14 days. For the 6 month experiment, it was found that the nickel concentration in the solution exposed to non-coated Nitinol archwires was 0.933 mg/L. The solution containing the DLC-coated wire had a nickel concentration of 0.150 mg/L. In 2006, Clarke *et al.* [16] examined the nickel release of surface treated Nitinol in comparison to untreated Nitinol in cell culture medium. The surface treatments included combinations of etching, pickling, and mechanical polishing. Etching and pickling were done in proprietary Fort Wayne Metals solutions. Mechanical polishing was performed using a mechanical wire polishing machine with abrasive pads. The solution of one untreated sample was found to have a nickel concentration of 1 mg/L which increased to almost 2 mg/L over 6 months. The nickel concentrations in the solutions containing the two untreated samples increased from 0.005 mg/L to almost 0.0030 mg/L over the course of 6 months. No nickel was detected in the solutions containing treated Nitinol.

In a 2009 study, Shabalovskaya *et al.* [5] showed that a nickel-rich layer beneath the Nitinol surface layers could act as a reservoir for continuous nickel release. In this study, three types of Nitinol wires were immersed in 45 mL of 0.9 NaCl solution at 37°C. Two wires were drawn using synthetic polycrystalline diamond dies (Wires 1 and 2). The other wire was drawn with single crystal natural diamond (Wire 3). All three wires

had a 0.75 mm diameter and were left untreated. The solutions were analyzed by atomic absorption spectrometry over a period of 6 months. It was found that the Nitinol wires continued to release increasing amounts of nickel over the six month time period. The nickel concentration in the solution containing Wire 1 increased from an initial 1 mg/L to 1.8 mg/L. The other two Nitinol wire types exhibited nickel release rates that increased two to five-fold over six months, to about 0.025 mg/L. The increase in the release rate was attributed to the presence of a nickel-rich zone beneath the surface layer in concert with the dissolution of the external oxide layer. This nickel-rich zone served as a permanent reservoir that allowed for the long lasting nickel release exhibited by Wire 1. It was proposed that the thickness of the oxide layer of Wire 1 (up to 720 nm) led to the formation of both a nickel-rich Ni_3Ti intermetallic phase and a pure nickel phase at the interface between the surface and the substrate. In addition, liberation of nickel atoms after spontaneous formation of the titanium-based oxide layer on the Nitinol surface allowed for interstitial migration of those atoms through the surface oxide.

2.3 Nitinol Surface Treatments

Various methods for treating the surface of Nitinol to reduce or prevent nickel leaching have been developed and tested for their effectiveness. A summary of these treatment methods was presented in Table 1 and are described in greater detail in this section.

2.3.1 Mechanical Polishing

One method for treating Nitinol is by mechanically modifying the surface, such as through mechanical polishing. However, according to Shabalovskaya *et al.* [8], simply mechanically polishing Nitinol without additional surface treatment leads to inconsistent corrosion resistance properties. This is due to the cracks, inclusion particles, and residual plastic deformation incurred as a result of the grinding and polishing process. Despite this, mechanical polishing of Nitinol has been shown to be effective at reducing nickel leaching. It was shown by Shabalovskaya *et al.* in a nickel leaching test that the nickel concentration in media exposed to samples wet polished with 600 grit SiC paper was 0.006 mg/L compared to 1.080 mg/L for untreated samples. Cissé *et al.* [22] compared the nickel ion release of mechanically polished Nitinol with Nitinol with the following surface finishes: blue-colored oxide, straw-colored oxide, electropolished, and electropolished and chemically passivated. After immersing the samples in Hanks' solution at 37°C for 14 days, the nickel concentration in the solution containing the mechanically polished specimens reached 0.0002 mg/L, which, with the electropolished specimens, was the lowest nickel concentration in the test. The nickel concentrations in the solutions containing the blue oxide samples and chemically passivated samples reached about 0.0005 mg/L while the nickel concentration in the solution containing the straw-colored oxide was about 0.001 mg/L. Thus, if no other treatments are possible, wet mechanical polishing alone can still greatly reduce nickel leaching from Nitinol.

2.3.2 Chemical Etching

The Nitinol surface can also be treated chemically through chemical etching, commonly performed in a $1HF + 4HNO_3 + 5H_2O$ solution for about 4 min. The process cleans the surface, removes cracked, discontinuous surface layers, oxidizes the surface, and simultaneously removes nickel from the surface. The process may be accompanied by boiling the Nitinol sample for 20 to 30 min in 130°C distilled water, which further removes nickel from the oxide layer. Shabalovskaya *et al.* and Clarke *et al.* [8, 16] previously demonstrated the ability of chemical etching to reduce the amount of nickel ion release from Nitinol. In the Clarke *et al.* study, a proprietary Fort Wayne Metals solution was used to etch the Nitinol, specifically made to target the oxide layer only. The etching temperature was not specified. Short-term (72 hours) and long-term (6 months) analyses were performed.

In the short-term study, Nitinol samples were immersed in cell culture media for 24, 48, and 72 h at 37°C. In the long-term study, Nitinol wires were immersed in 0.9% NaCl at 37°C for various time periods up to six months. In both cases, the nickel released by the chemically etched Nitinol was below the detection limit of the analyzer. For the short-term study, a flame atomic absorption spectrometer with a detection limit of 0.200 mg/L was used. An inductively coupled plasma-optical emission spectrometer with a detection limit of 0.005 mg/L was used for the long-term study.

In 2008, Shabalovskaya *et al.* compared the nickel release profiles of chemically etched Nitinol with chemically etched Nitinol that had been water boiled afterwards for 30 minutes. One set of samples was etched in 10% HF + 40% HNO_3 + 50% H_2O

solution. Another set was etched and then boiled in distilled water for 30 minutes. Both sets of samples had reduced nickel release compared to untreated Nitinol. The nickel concentration observed in the medium exposed to the chemically etched sample was 0.011 mg/L, much lower than the 1.080 mg/L of the medium exposed to the untreated sample. The etched and water boiled samples did not release any detectable nickel.

2.3.3 Electropolishing

Electropolishing of Nitinol is another common surface treatment. The procedure for this treatment can vary greatly. Shabalovskaya *et al.* [8] used two methods to electropolish the Nitinol. The first sample was immersed in an electrolyte consisting of 10% perchloric acid and 90% acetic acid. This was done at room temperature at 20 volts for 6 minutes. The second sample was immersed in 70% methanol and 30% nitric acid. This was done for 6 minutes at 20 volts and -45°C when the Nitinol was in the martensite phase. Nickel release was reduced in both samples by about 99% when compared to untreated Nitinol. In a 2006 study, Michiardi *et al.* [17] used an electrolyte of glacial acetic acid and perchloric acid in a ratio of 5:100. The treatment was performed at 30 V for 2 min and 15 s. This treatment resulted in a surface Ti/Ni ratio of 12.3, which was three times higher than that of boiling in water (4.0 Ti/Ni ratio), 6 times higher than autoclave treatment (1.6), and 12 times higher than mechanical polishing (1.0) using silicon carbide papers up to 1200 grit. In addition, the resulting 6 nm oxide layer was twice as thick as the oxide layers of the other three treatments. Nickel leaching tests were not performed on the electropolished samples in this study.

2.3.4 Thermal Oxidation

Nitinol can be treated through thermal oxidation, as well. When exposed to oxygen, a stable TiO_2 layer forms on the surface of the Nitinol. This occurs because at room temperature the standard Gibbs free energy of formation for titanium oxide, -889 kJ/mol, is lower than that for nickel oxide, -212 kJ/mol [23, 24]. Surface nickel, however, may react with atmospheric oxygen to produce NiO. Increasing the temperature at which Nitinol is oxidized makes diffusion of oxygen into the Nitinol surface layer faster and also helps titanium readily migrate towards the surface. The oxidation temperature is a key factor in reducing the amount of nickel that is present in the Nitinol surface layer. When oxidizing in air at 300-500°C for 30 minutes, the surface layers were composed of TiO, pure nickel, and NiTi [25]. Oxidizing at 600°C resulted in TiO_2 and Ni_3Ti being observed in the surface layers, with visible traces of the Ni phase. However, the nickel concentration was much lower than when oxidizing at lower temperatures. Samples oxidized at 300°C exhibited a surface Ni concentration of 15 at. % while those oxidized at 800 °C had a surface Ni concentration of 0.3 at. % [26]. Oxidizing at higher temperatures also resulted in a thicker oxide layer. The samples oxidized at 600°C had an oxide layer thickness of about 0.53 μm while those oxidized at 400°C had an oxide layer thickness of about 0.028 μm. The thicker oxide layer, however, led to an accumulation of nickel at the interface between the bulk and the oxide layer, as a result of depletion of the titanium in the area. This nickel-rich zone is present even in untreated Nitinol because the spontaneous formation of titanium oxide on the surface liberates some nickel atoms beneath the oxide layer. The presence of the nickel-

rich zone can cause increased nickel ion release over time as well as reduced corrosion resistance, as verified by a potentiodynamic polarization study performed by Shabalovskaya *et al*. [5]. The wire samples were exposed for 1 hour to a 0.9 NaCl solution using a three electrode configuration. It was shown that the breakdown potential for untreated Nitinol wire was 200 mV compared to 1200 mV for wire chemically etched in $1HF + 4HNO_3 + 5H_2O$ solution.

In 2006, Michiardi *et al.* [17] tested an oxidation method that would create a nickel-free TiO_2 surface layer. The method involved oxidizing the Nitinol in an oxygen atmosphere at a pressure of 3×10^{-2} mbar at 400°C for 2 hours and 30 minutes. As demonstrated in a 1990 study by Chan *et al.* [27], oxidation of Nitinol using a low oxygen pressure (1.33×10^{-4} mbar) method at 400°C caused preferential oxidation of titanium over nickel. Some samples that underwent this thermal treatment were subsequently boiled in water for 1 hour. According to XPS depth profiles, the thermally treated samples had a nickel concentration of <3 at. % up to about 25 nm in depth. In comparison, the mechanically polished samples (120 to 1200 grit) had a Ni surface concentration of 15 at. % which increased to about 65 at. % at about 6 nm beneath the surface. It was found that the oxidized Nitinol reduced the nickel release compared to untreated Nitinol. Within the first hour of immersion in simulated body fluid, the nickel release from the oxidized Nitinol was decreased by 73% in comparison to the untreated Nitinol. Following that, the decrease averaged about 50%. Nickel release was measured by atomic absorption spectroscopy and was normalized by surface area. The samples treated then subsequently boiled in water showed an even greater decrease. Over one

month, the concentration of nickel in the SBF exposed to thermally oxidized and boiled Nitinol was 0.040 mg/L, compared to 0.130 mg/L and 0.290 mg/L for oxidized and untreated Nitinol, respectively. The oxide layer produced by thermal oxidation was a 63 nm thick TiO_2, which was the only species detected by x-ray photoelectron spectroscopy for the thermally oxidized Nitinol.

2.3.5 Surface Nitriding

One way to ensure a nickel-free surface layer is to nitride the Nitinol. Nickel does not form a nitride compound, so a TiN layer on the surface would be nickel-free [23, 24]. The formation of the TiN layer must be done under conditions that make its formation thermodynamically favorable to TiO_2. This can be done by removing oxygen from the system, or at least reducing the partial pressure of the oxygen in the system such that the Gibbs free energy of formation for TiN is lower than that of TiO_2.

One method to reduce the oxygen in the system was employed by Starosvetsky *et al.* [28]. A powder immersion reaction assisted coating (PIRAC) method was employed in which the Nitinol was nitrided in sealed containers of stainless steel foil. This foil contained large amounts of chromium, which reacted with the oxygen, preventing it from reacting with the Nitinol. The foil also allowed for nitrogen atoms to diffuse through the walls of the container, creating a nitrogen-rich layer on the Nitinol surface. The Nitinol was then nitrided at either 900 or 1000 °C for 1.5 hours and 1 hour, respectively. This produced a thin (0.1 μm at 900°C, 0.4 μm at 1000°C) TiN coating on the surface and a thick (0.6 μm at 900°C, 1 μm at 1000°C) Ti_2Ni layer beneath it.

Gil *et al.* [18] used high purity nitrogen to nitride the Nitinol samples. For each experiment, a fixed temperature of 800, 900, or 1000°C was used. The nitriding times used were 5, 7, 10, 15, 20, 25, and 30 minutes. Leaching tests in artificial saliva were performed on the untreated and nitrided samples. Samples from the solution were removed periodically over 560 hours. Over the course of the experiment, the nitrided samples released 3 to 4 times less nickel than the untreated Nitinol. In addition, the optimum treatment time was determined to be 900°C for 20 minutes due to the nitride layer's homogeneity and good adherence properties.

In a study of corrosion resistance of Nitinol orthodontic plates and brackets, Liu *et al.* [19] generated both single-layered TiN and multilayered Ti/TiN coatings on the surfaces of the Nitinol using a pulse-biased arc ion plating system. The single-layered TiN was created by introducing argon and nitrogen to the vacuum chamber containing the samples. For the multilayered Ti/TiN coatings, Ti was deposited using an argon plasma and the TiN layers were deposited with an argon and nitrogen mixture. The partial pressure of nitrogen was 0.34 Pa and the argon partial pressure was 0.5 Pa. The multilayered Ti/TiN coating was made up of 22 Ti layers and 22 TiN layers. The thickness of both the single and multilayered coatings was about 2 μm. Coated and uncoated samples were immersed in 100 mL of artificial saliva at 37°C for 720 h. The Ti/TiN coated samples did not release detectable amounts of nickel into the solution. The detection limit of the atomic absorption spectrometer used in this study was not given. The uncoated samples released about 2.5×10^{-4} mg/cm^2/day of nickel into solution. The TiN coated samples released the most nickel into solution: ~1.5 μg/cm^2/day. The higher

nickel release was attributed to poor corrosion resistance by TiN layers, in addition to a columnar microstructure, micro-particles, and pinholes in the coatings. These results agreed with a prior study by Kao *et al.* [29] in which 3 out of 4 TiN-plated stainless steel bracket types were shown to have greater nickel ion release into artificial saliva at 37°C than non-TiN-plated brackets, over a 12 week period. Reasons for the disparity included nonuniform coating of the substrate and galvanic corrosion between the TiN coating and the bracket.

2.3.6 Ion Implantation

Ion implantation is another method employed to passivate the Nitinol surface. For the most part, the method used to introduce the ions to the samples was plasma-immersion ion implantation. The particular ions used for implantation varied widely. Cheng *et al.* [30] used tantalum immersion ion implantation to treat the Nitinol, chosen because of its biocompatibility and high mass absorption coefficient. A plasma immersion ion implanter with a 13.56 MHz, 2 kW RF plasma source was used to produce RF plasmas while four sets of MEVVA plasma sources introduced ions into the plasma. The ion doses were about 3.1×10^{17} ions/cm^2. An XPS depth profile of the treated Nitinol samples confirmed that no nickel was detected after 12 minutes of sputtering, indicating the presence of a nickel-free surface layer. Maitz *et al.* [31] used oxygen and helium implantation techniques to produce a nickel-depleted TiO_x surface. The helium-ion implantation was performed only for the purpose of a scientific model because of the nanoporous surface that is produced as a result of the treatment. For the oxygen implantation, 2×10^6 high voltage negative pulses with -25 kV amplitude and a frequency

of 300 Hz were applied to the samples at 160°C. For the helium implantation, 4 x 10^6 pulses at 20 kV and 150 Hz frequency were applied to the samples at 95°C. The surface nickel concentrations for the oxygen and helium implanted samples were 1.6 and 7 at. %, respectively. These ion implantation techniques reduced the concentration of nickel at the Nitinol surface, but the surface layers were not completely nickel-free. Other ions used in the plasma immersion ion implantation process included nitrogen [32-34], argon [32], and boron [34].

2.3.7 Nitriding and Oxidation

In his 2011 M.S. thesis, Bazochaharbakhsh [24] described a method that produced a nickel-free oxide layer on the surface of Nitinol. The method involved nitriding Nitinol samples in 96% N_2 + 4% H_2 at 1000°C for 20 minutes, followed by oxidation in air at 700°C for 60 minutes. X-ray diffraction and X-ray photoelectron spectroscopy both confirmed that the nickel concentration in the resulting surface oxide layer contained only undetectable amounts of nickel. Performing the nitriding step first allowed for the formation of a nickel-free TiN layer on the surface. Since nickel does not form a nitride, only the titanium reacted with the nitrogen in the system to form the TiN and, as a result, no nickel was present in the nitride layer. Oxidation of this TiN layer created a nickel-free titanium oxide layer. Nickel leaching tests were not performed on the samples in this study.

2.4 Surface Layer Thickness

The thickness of the surface layer can impact whether nickel leaches to the surface, or not. Presumably, a sufficiently thick surface layer would prevent any nickel

from diffusing through to the surface, barring any defects in the layer. However, as demonstrated by Shabalovskaya *et al.* and Firstov *et al.* [5, 25], a thicker oxide layer leads to the formation of nickel-rich Ni_3Ti intermetallics at the interface of the surface layer and the bulk as titanium is depleted during oxidation. This nickel-rich zone causes poor corrosion resistance, which may lead to increasing nickel release over time.

The surface layer thicknesses that were generated experimentally varied based on the treatment method and even the measurement technique. Shabalovskaya *et al.* [5] measured the original oxide layer thicknesses, shown in Table 2, of Nitinol wires. The variations in thickness measurements in Table 2 show the disparities among the methods and the site of measurement. Because Wire 1 exhibited some cracking, the variance in measurement was large. The oxide layer for Wire 3 was thinner than that of Wire 2, which contributed to its higher nickel release rate over the 6 month period.

Table 2. Original oxide layer thickness of Nitinol wires (nm).

Sample	Auger 1 μm^2 raster	Auger 50 μm^2 raster	TEM thinned samples
Wire 1	80; 440	720	160-190
Wire 2	120; 300	220	50-100
Wire 3	36; 72	84	25-50

The effect of different treatment methods on oxide layer thickness can be seen in the 2008 Shabalovskaya *et al.* study [8]. Auger depth profiles for chemically etched and electropolished Nitinol revealed oxide layer thicknesses that ranged from 1.5 to 1.8 nm. For mechanically polished/heat treated and chemically etched/water boiled/heat treated samples, the range was between 100 and 150 nm. This difference was also explored in

the Michiardi *et al.* study [17]. The thinnest oxide layer came from the autoclave treatment, in which the Nitinol was autoclaved at 121 °C for 30 minutes. This resulted in a 2.4 nm oxide layer. The oxide layer thickness from the mechanically polished and water boiled samples were slightly thicker, at 3 nm each. The electropolished Nitinol had an oxide layer thickness of 6 nm. The thickest oxide layer came from the thermally treated Nitinol at 63 nm.

Oxide layer thickness has been shown to be sensitive to the oxidation temperature. Milosev *et al.* [35] compared the thickness of the oxide layers created as a result of oxidation at different temperatures and between polished and ground surfaces. It was shown that the thickness of the oxide layer increased dramatically as the temperature increased. The change was most dramatic when moving from 500 °C to 600 °C, where the difference in oxide layer thickness increased by 5.8 times for the polished surface (180 nm to 1050 nm) and by 4.7 times for the ground surface (180 nm to 850 nm). The increase in thickness of the oxide was mostly a result of the increase in thickness of TiO_2, in comparison to that of NiO. This is because of the greater oxygen affinity of titanium ($\Delta G_f^o{}_{,TiO2,298}$ = -957 kJ/mol) as compared to nickel ($\Delta G_f^o{}_{,NiO,298}$ = -241 kJ/mol).

2.5 Nickel Leaching Test Parameters

The general strategy for determining biocompatibility of biomaterials *in vitro* is to immerse the sample in simulated body fluid, and then incubate the immersed samples at 37°C over a period of time. The fluid is then analyzed periodically using either atomic absorption spectrometry or inductively-coupled mass spectrometry. This procedure has been employed in studies by Jiang *et al.*, Liu *et al.*, and Poon *et al.* [36-38], among

others. The key differences among the studies lie in the sample surface area to solution volume ratio and the immersion time.

The volume of solution in which the samples are immersed is important for leaching tests. If the volume of the solution is too small, then the solution can saturate, preventing any meaningful results from being acquired. If the volume is too large, the resulting concentrations over time may be difficult to measure. The appropriate ratio, then, must be determined for the experiment. One guideline to follow is described in the study by Nakamura *et al.* [39] which was adopted as the ASTM STP 1173 standard. The study describes using a ratio of 1 cm^2 sample surface area to 10 mL of fluid. Specifically, the samples used were cylinders with a surface area of 1.51 cm^2 and were immersed in 15 mL of solution. This same ratio of surface area to solution volume has been used by Jiang *et al.* [36] (8.8 cm^2 to 90 mL), Liu *et al.* [37] (16 cm^2 to 1.6 mL), Liu *et al.* [19] (10 cm^2 to 100 mL), and Chu *et al.* [40] (240 cm^2 to 25 mL). The problem with these ratios is that there is a risk of saturation over a long period of time. Since these experiments did not exceed 50 days in duration, the risk of saturation was lower than if the studies had been done over several months. One study done by Shabalovskaya *et al.* [5] was performed over the course of six months. The ratio used in the experiment was 2.65 cm^2 to 45 mL. This is almost twice the amount of fluid called for by ASTM STP 1173. This ratio makes sense considering the longer time period over which the leaching tests were performed.

There was very little variation in the ionic composition of the simulated body fluid in which the Nitinol samples were immersed. Jiang *et al.* and Poon *et al.* [36, 38]

used simulated body fluid consisting of sodium, potassium, calcium, magnesium, bicarbonate, chloride, hydrogen phosphate, and sulfate ions. The simulated body fluid used by Jiang also included glucose as part of the solution. As shown in Table 3, the ion concentration for the simulated body fluid (SBF) used by Poon *et al.* [38] closely matched that of blood plasma. The greatest discrepancy between the simulated body fluid and the actual blood plasma concentrations was with the bicarbonate concentration and the chloride concentration. In the SBF the chloride concentration was 148.5 mMol while in blood it was 103.0 mMol. In the SBF, the bicarbonate concentration was 4.2 mMol, while in the SBF, it was 27.0 mMol. These differences in ion concentration help to stabilize SBF for long-term testing. A common alternative to simulated body fluid is physiological saline solution (0.9 NaCl solution), as used in studies by Shabalovskaya *et al.*, Kobayashi *et al.*, and Clarke *et al.* [5, 17, 18].

Table 3. Comparison of ion concentration in simulated body fluid and blood plasma (mMol).

	Na^+	K^+	Ca^{2+}	Mg^{2+}	HCO_3^-	Cl^-	HPO_4^{2-}	SO_4^{2-}
SBF	142.0	5.0	2.5	1.5	4.2	148.5	1.0	0.5
Blood Plasma	142.0	5.0	2.5	1.5	27.0	103.0	1.0	0.5

2.6 Summary of Literature Survey

Nickel release from untreated Nitinol can be a problem, even with the existence of a naturally forming oxide layer. Defects in the layer could allow access to the nickel-rich reservoir beneath the surface layers, which in turn can lead to increased nickel ion release over time. Surface treatments such as chemical etching, oxidation, and nitriding can help

to reduce nickel ion release from the bulk by preventing outward diffusion of nickel and reducing the defect density of the surface layers. These treatments have a large impact on the thickness and quality of the surface layers that are created.

Although mechanical polishing may have negative effects on the corrosion resistance properties of Nitinol, it has been shown to be an effective method for reducing nickel leaching. Chemical etching is another effective Nitinol surface treatment method which has the ability to remove oxide layers with defects, oxidize the surface, and remove nickel from the surface. Electropolishing of Nitinol has produced samples with a 99% reduction in nickel leaching and thick oxide layers with high Ti/Ni surface ratios. Thermal oxidation is a simple surface treatment method that produces a protective oxide layer on the surface of Nitinol, although nickel and nickel oxide present in these layers can lead to nickel leaching. Nitriding produces a nickel-free TiN layer on the Nitinol surface, but nickel leaching tests with these nitrided samples have resulted in higher nickel release rates from Nitinol samples as compared to untreated Nitinol samples. Ion implantation has also been successfully used to treat the Nitinol surface, but nickel leaching tests with these samples have not been performed. The nitriding and oxidation method described by Bazochaharbakhsh [24] produced nickel-free oxide layers, but also requires testing for nickel leaching. The thickness of the surface layers produced by these methods varies widely, ranging from around 1 nm to 1 μm.

Any surface treatment used to make Nitinol safer for implantation must be tested to ensure that the nickel ion release has been reduced, preferably to zero. Although the exact methodology for these tests may differ among researchers, the basic principles

remain the same for all the tests. Ideally, these tests should be performed over the course of several months in conditions that closely simulate the conditions inside the human body. Simulated body fluid and physiological saline solution are common fluids used for these tests because they simulate the ionic content of human plasma. The ratio of sample surface area to solution volume used in the test is also important since saturation may occur when using smaller volumes of solution, while larger volumes may make it difficult to detect small amounts of nickel release. By performing these nickel leaching tests, the safety of long-term Nitinol implantation can be improved.

CHAPTER THREE

RESEARCH OBJECTIVES

The purpose of this research was to characterize nickel leaching from surface-treated Nitinol. Specifically, the treatment methods tested for nickel leaching were untreated (mechanical polishing only), oxidation, and the nitriding and oxidation method introduced by Bazochaharbakhsh [24]. The samples produced by Bazochaharbakhsh were not subjected to any tests designed to measure nickel leaching. The focus of this research was to quantify the nickel released by these samples into phosphate-buffered saline solution at 37°C over a 91-day period. In addition, samples were prepared at varying nitriding temperatures to obtain different nitride layer thicknesses. The effect of the differing nitride layer thicknesses on nickel leaching could then be determined to find if there was a critical thickness that would prevent nickel leaching.

A secondary objective was to develop the method for determining the nickel release rates from Nitinol at SJSU. This method can be used for Nitinol in almost any form and can serve as early biocompatibility testing for new Nitinol treatment methods. This method was based on the ASTM 1173 standard for elucidating the biocompatibility of biomaterials but modified for use with the equipment available at SJSU. This testing method may also be employed for determining the concentration of a variety of other ions in aqueous solutions.

CHAPTER FOUR

MATERIALS AND METHODS

4.1 Overview

Thirty-five Nitinol specimens were cut from a 1.54 mm thick sheet into 10 mm x 20 mm pieces. The composition of the Nitinol was 51.78 at. % Ni and 48.22 at. % Ti, as verified by energy dispersive spectroscopy and presented in Chapter 5. One hole, 1 mm in diameter was drilled into the top two corners of each Nitinol specimen, such that the specimens could be suspended with wire. Each specimen was mechanically polished on all sides to a mirror finish, ultrasonically cleaned, and dried. The mechanical polishing of the specimens was performed using silicon carbide papers of progressively finer grit size: 240, 320, 400, and 600 grit. The mirror finish was achieved by polishing the samples using 1 μm Al_2O_3 paste. The group names and respective treatment method for each specimen are shown in Table 4.

Table 4. Experimental design matrix for all specimens.

Specimen Group (N=5)	Nitriding Temperature (°C)	Nitriding Time (min)	Oxidation temperature (°C)	Oxidation time (min)
Untreated	N/A	N/A	N/A	N/A
800-N-700-O	800	20	700	60
850-N-700-O	850	20	700	60
900-N-700-O	900	20	700	60
950-N-700-O	950	20	700	60
1000-N-700-O	1000	20	700	60
700-O	N/A	N/A	700	60

Immediately following surface preparation, five specimens were nitrided in 96% N_2 + 4% H_2 for 20 min at each of the following temperatures: 800°C, 850°C, 900°C, 950°C, and 1000°C. The presence of a titanium nitride layer on the surface of the specimens was verified visually by the golden color of the specimen. The specimen group names shown in Table 4 correspond to the respective treatment methods. For example, the specimens nitrided at 800°C and oxidized at 700°C were named 800-N-700-O. The individual samples within this group were named 800-01, 800-02, 800-03, 800-04, and 800-05, as shown in Table 5.

Table 5. Nomenclature for individual specimens.

Specimen Group	Specimen Names				
Untreated	Unt 01	Unt 02	Unt 03	Unt 04	Unt 05
800-N-700-O	800-01	800-02	800-03	800-04	800-05
850-N-700-O	850-01	850-02	850-03	850-04	850-05
900-N-700-O	900-01	900-02	900-03	900-04	900-05
950-N-700-O	950-01	950-02	950-03	950-04	950-05
1000-N-700-O	1000-01	1000-02	1000-03	1000-04	1000-05
700-O	700-O-01	700-O-02	700-O-03	700-O-04	700-O-05

After nitriding, the specimens were oxidized in air for 60 min at 700°C. A titanium oxide layer was formed on the specimens after oxidation; this was verified visually by the presence of a gray-colored surface layer. Untreated specimens were not subjected to any form of heat treatment. Another group of specimens underwent the oxidation heat treatment without going through a nitriding step.

All 35 specimens were then immersed in 1X phosphate buffered saline solution at 37°C for 91 days. Over the first week of the nickel leaching experiment, the nickel

concentration in the solution was measured daily, using an atomic absorption spectrometer (AAS). Following the first week of measurements the nickel concentration was measured twice a week.

The chemical composition of the specimen surfaces was obtained using EDS. Images of specimens were obtained using scanning electron microscopy (SEM) and optical microscopy.

4.2 Specimen Preparation

A 1.54 mm thick Nitinol sheet was cut into 10 mm x 20 mm pieces. A hole was drilled into each of the top two corners of each specimen, allowing for the passage of a copper wire, as shown in Figure 2.

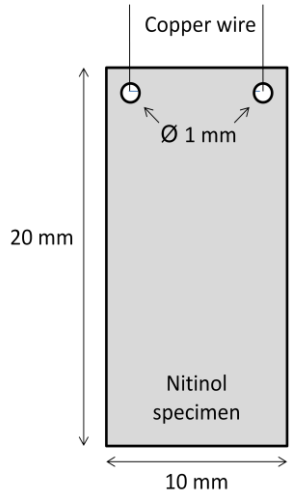

Figure 2. Diagram of Nitinol specimen

To remove the native oxide layer and prepare the surface of the specimens, each Nitinol piece was mechanically ground on all sides using silicon carbide papers of progressively finer grit, ranging from 240 grit to 600 grit. The specimens were then mechanically polished using 1 μm Al_2O_3 paste to obtain a mirror finish on all sides. Each

specimen was then rinsed and ultrasonically cleaned in deionized (DI) water, then air-dried.

4.3 Tube Furnace and Gas Delivery System Setup

Nitriding and oxidation of the Nitinol samples were performed in a Lindberg 55035 tube furnace with a 1 in. diameter quartz tube. The maximum temperature capability of the tube furnace was 1100°C. An R-type thermocouple was placed at the center of the tube and connected directly to the temperature controller of the furnace. The temperature profile of the tube furnace was obtained by means of a separate thermocouple to verify temperatures along the length of the tube. As shown in Figure 3, the temperature within the tube furnace varied only by about 5°C within 1 inch, longitudinally, on either side of the thermocouple. The Nitinol specimens were heat treated within this range to keep the treatment temperature constant among runs. The heat treatment setup is shown in Figure 4.

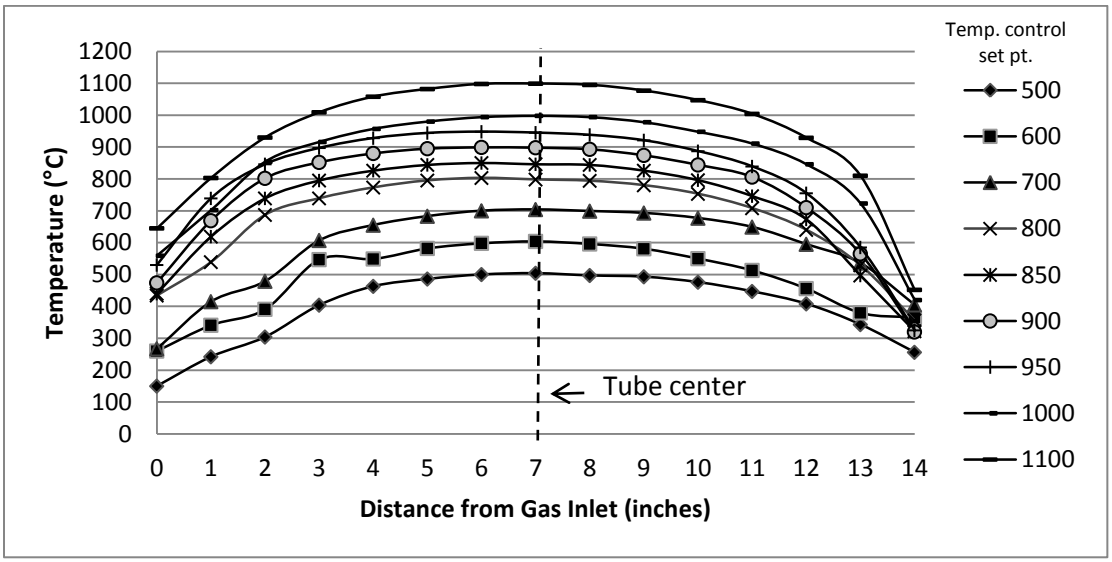

Figure 3. Tube furnace temperature profile. The thermocouple extended from 0 to 6 inches.

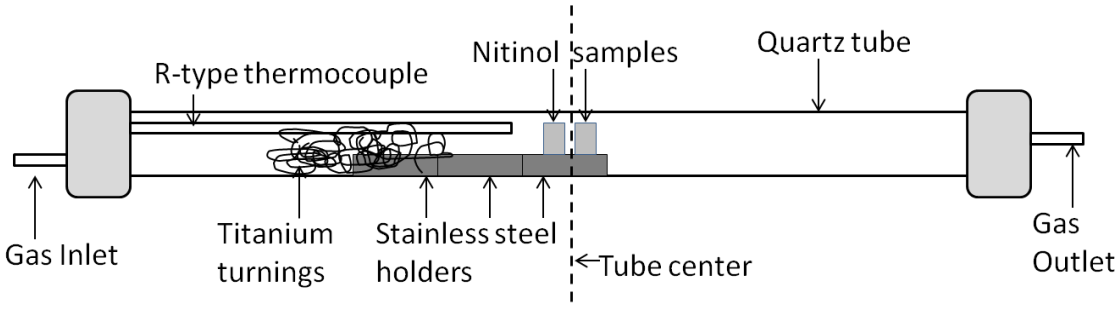

Figure 4. Schematic of the quartz tube and heat treatment setup.

The quartz tube was sealed at both ends with airtight Teflon fittings which allowed only for the passage of the gas of interest through the tube. The inlet Teflon fitting also allowed for the placement of the R-type thermocouple for temperature control. During heat treatment, two Nitinol specimens were placed vertically in the tube, close to the tip of the thermocouple. The specimens were held up, with the hole side down, by a custom-made stainless steel holder that allowed for even gas flow across both sides of the specimen. Two other holders were placed upstream of the specimen holder to promote even flow of gas over the specimens. Titanium turnings were placed even further upstream, of all three holders, to react with any residual oxygen entering the system. A schematic of the tube furnace system is shown in Figure 5.

During heating and cooling of the furnace, ultra high purity argon was flowed through the tube furnace system. For the nitriding processes, a gaseous 96% N_2 + 4% H_2 mix was introduced to the tube inlet. For oxidation, ambient air was pumped into the tube using an Elite 802 aquarium pump. Inlet and outlet flow rates were adjusted such that the flow of the gas was nominally equal to 0.5 SCFH. In order to remove moisture and oxygen from the nitrogen mixture and the argon, oxygen and moisture traps were installed. For the argon and nitrogen lines, a BOT-4 oxygen trap from Agilent

Technologies was used. The capacity of the trap was 3 L O_2 (3,200 mg) and it lowered oxygen concentrations to less than 1 ppb. A moisture trap was also used on the argon and nitrogen lines. A refillable in-line moisture trap from Alltech was used in series with the oxygen trap. The capacity of the trap was 31 mL, and it reduced moisture concentrations to below 1 ppm. Titanium turnings placed in the inlet of the tube furnace's quartz tube reacted with any residual oxygen that may have been present in the gases after passing through the oxygen and moisture traps. A separate BMT-2 moisture trap from Agilent Technologies was used for the air line. The capacity of the trap was 130 g H_2O, and it reduced water content to below 5 ppb.

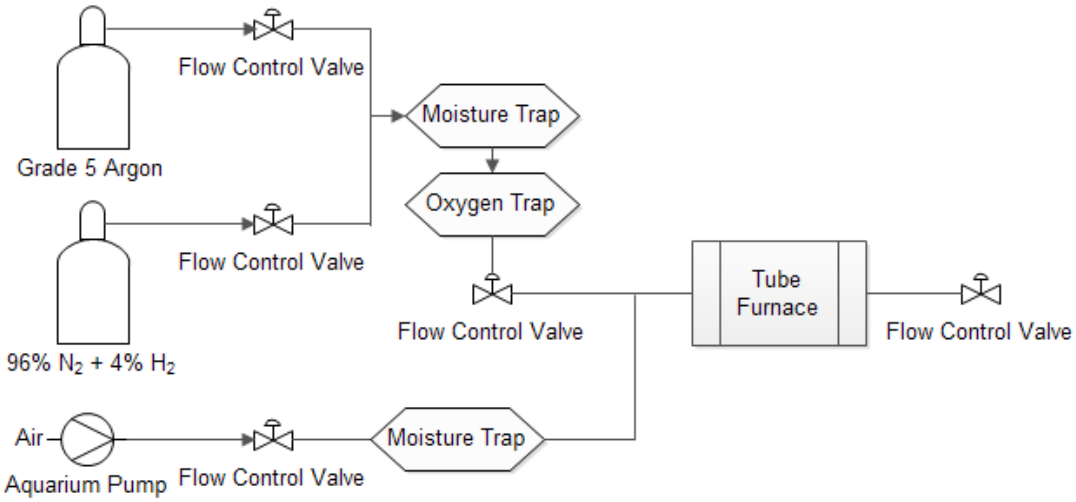

Figure 5. Schematic of gas delivery system used for all heat treatments.

4.4 Nitriding and Oxidation

The Nitinol samples in this experiment were nitrided at specific temperatures between 800 °C and 1000 °C for 20 minutes in 96% N_2 + 4% H_2, as was shown in Table 4. For each specimen number in the experimental matrix, there were 5 specimens tested. The specimens nitrided at 1000 °C followed the protocol explained in

Bazochaharbakhsh's M.S. thesis [24], with stainless steel holders keeping the specimens in place as opposed to the quartz boat used in his research. This change was made to ensure even flow of gas along both sides of the specimens. The presence of titanium nitride on the surface of the specimens was confirmed visually by the golden color of the surface. Successfully nitrided specimens were then oxidized in air at 700 °C for 1 hour. During the heating and cooling of the furnace, argon was flowed through the system to prevent any reaction with the gases in the system.

4.5 Nickel Leaching Test

Five specimens from each specimen number were used for the nickel leaching test. 1X phosphate buffered saline (PBS) solution was prepared to serve as the leaching solution in the experiment. The PBS tablets used were Amresco E404 biotechnology grade tablets in which one tablet would yield 100 mL 1X solution. The nominal composition of the PBS solution that results from dissolution of these tablets is 10 mM phosphate buffer, 137 mM sodium chloride, and 2.7 mM potassium chloride, with a pH between 7.3 and 7.5. The tablets were dissolved in deionized water.

Forty mL of PBS solution was poured into each BD Falcon 50 mL centrifuge tube. A pushpin was used to poke two holes in the middle of the cap of the centrifuge tube. The distance between the holes matched the distance between the holes in the Nitinol specimens. Coated copper wire was passed through the holes in the specimens and the ends of the wire were passed through the holes in the centrifuge tube cap. The specimens were lowered into the solution such that 18 mm of the 20 mm length was immersed in solution, as seen in Figure 6.

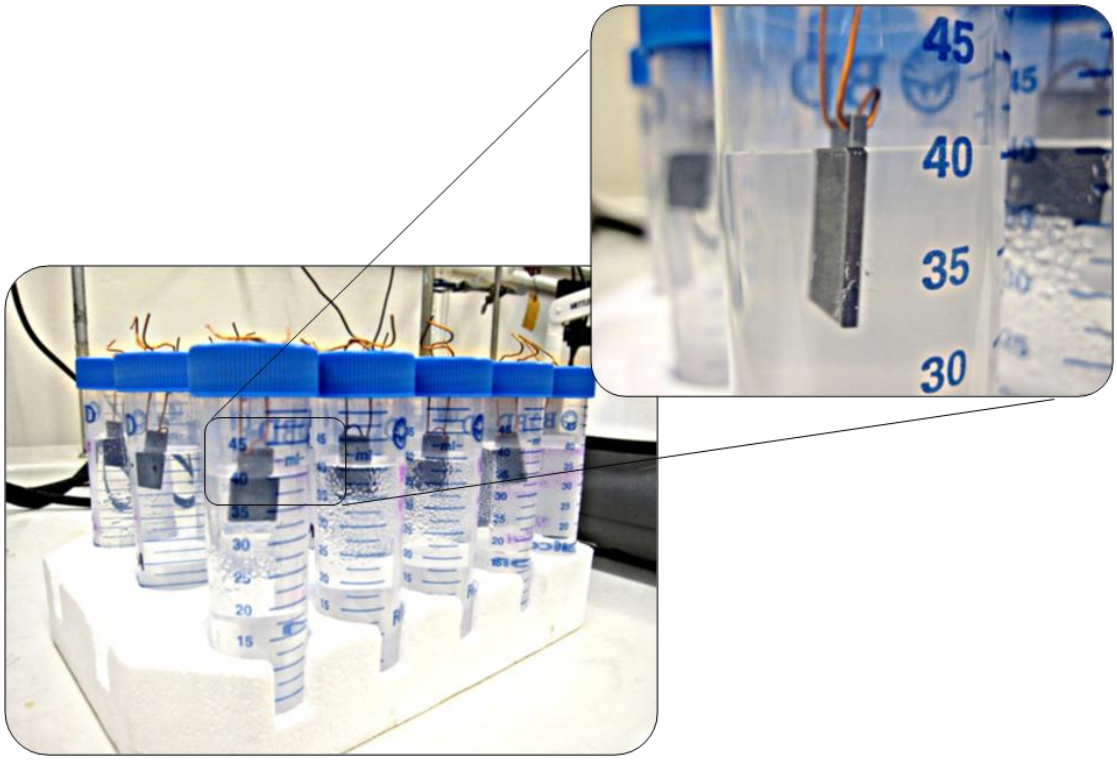

Figure 6. Nitinol samples in centrifuge tubes, immersed in PBS.

The immersed area of the Nitinol specimens corresponded to the upper portions of the specimens which were exposed to the nitrogen and air during heat treatment. The bottom portions of the specimens, where the holes were present, were not exposed to the PBS solution as these areas were held within the stainless steel holders during heat treatment. After heat treatment, a line formed between the exposed and unexposed portions of the Nitinol specimens, which indicated how deep the specimen should be immersed. Since the dimensions of the specimens and the holders were the same, the immersed area of the specimens was the same: 4.06 cm^2. The centrifuge tubes were then placed in a Styrofoam holder and kept in a Heraeus incubator at 37 °C over a 91 day period.

4.6 Nickel Concentration Measurement

Nickel concentration in the PBS solution was measured using a Varian SpectrAA 220FS atomic absorption spectrometer. The detection limit for the atomic absorption spectrometer was 0.1 mg/L. For the optimum working range of 0.1 – 20 mg/L, the wavelength used was 232.0 nm and the slit width was 0.2 nm. The nickel stock solution was prepared by dissolving 1 g 99.99% pure nickel wire in 1:1 nitric acid, then diluting to 1 L to yield 1000 mg/L nickel. The standard solutions were prepared to conform to Table 6, by diluting the stock solution with DI water to the desired concentration. Using these standard solutions, a calibration curve was generated, shown in Figure 7 and Table 7. The equation of the curve, as generated by the SpectrAA software, was:

$$C = (A + 0.00027) / 0.00243 \qquad \text{Equation 1}$$

where C is the concentration and A is the absorbance. This equation was used to calculate nickel concentration of samples with concentrations higher than the range of the calibration curve. In order to test the validity of the calibration curve, samples with known nickel concentration were created from the nickel stock solution and tested. Based on the data shown in Table 8, nickel concentration measurements taken from the AAS have an error less than ± 0.1 mg/L.

Table 6. Preparation of nickel standard solutions.

Concentration (mg/L)	Ni Stock Solution (mL)	Total Volume (mL)
1	0.04	40
2	0.08	40
3	0.12	40
4	0.16	40
5	0.20	40

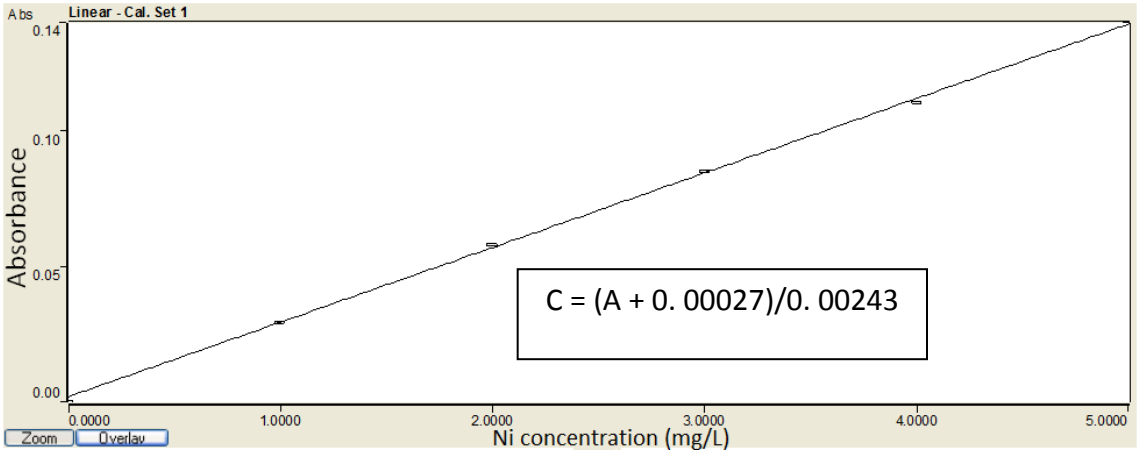

Figure 7. Nickel concentration calibration curve.

Table 7. Calibration standards used to generate the calibration curve.

Standard	Concentration (mg/L)	Absorbance	Precision
Calibration zero	0.00	0.0020	11.7%
Standard 1	1.00	0.0292	1.0%
Standard 2	2.00	0.0581	1.0%
Standard 3	3.00	0.0850	0.9%
Standard 4	4.00	0.1105	0.8%
Standard 5	5.00	0.1401	0.6%

Table 8. Nickel concentration measurements for samples of known concentration.

Concentration of Sample (mg/L)	Conc. Reading 1 (mg/L)	Conc. Reading 2 (mg/L)	Conc. Reading 3 (mg/L)	Conc. Reading 4 (mg/L)	Conc. Reading 5 (mg/L)	Std. Dev.	Mean Abs. Error
0.5	0.4876	0.4876	0.4876	0.4966	0.4916	0.0040	0.0098
1	1.0095	1 064	0.9492	1.0157	1.0012	0.041	0.028
1.5	1.5005	1.4933	1.5535	1.5121	1.5363	0.025	0.022
2.5	2.4824	2.5749	2.5653	2.4767	2.5289	0.046	0.042
3.5	3.5620	3.5047	3.5293	3.4966	3.5112	0.026	0.022

Nickel concentration measurements were taken frequently over a 91 day period. For the first week, measurements were taken daily. Following that, measurements were taken every 3 or 4 days, alternating. The amount of solution removed from the centrifuge tubes for each measurement was 0.750 mL, which was immediately replaced by 0.750 mL of fresh PBS solution. Concentration measurements were tabulated and, based on a constant PBS solution volume of 40 mL, the amount of nickel in the solution was calculated at each time point. The difference in nickel amount in the solution was then divided by the surface area of Nitinol exposed to the solution, resulting in nickel release per square cm of Nitinol. These data were plotted over the duration of the leaching test to determine nickel release rates. Release rates calculated in this manner, which resulted in a negative value or a value below the detection limit of the AAS, were assumed to have no nickel release over that time period. The 0.1 mg/L detection limit of the AAS corresponded to 0.004 mg Ni per 40 mL solution. Dividing the 0.004 mg Ni by the 4.06 cm^2 surface area exposed to the PBS resulted in a minimum detectable nickel release rate of 0.00099 $mg/cm^2/day$.

4.7 Surface Characterization

Samples treated identically to those used for the nickel leaching test were imaged using optical microscopy and scanning electron microscopy (SEM) and characterized using energy dispersive X-ray spectroscopy (EDS) and X-ray diffraction (XRD). Optical microscopy images were taken at 400x magnification. The SEM images were taken with the backscatter electron detector to more easily detect changes in phase. XRD was performed at a glancing angle of 0.5°. EDS analysis was performed at 20 kV. In order to

obtain images of the cross sections of the treated samples, two samples treated at the same temperature were joined face-to-face with epoxy. The joined samples were then stood upright on the long edge and supported by a SamplKlip support clip. The sample and clip were then mounted in epoxy resin. Once hardened, the cylindrical mount was ground and polished until the edge of the sample had a mirror finish. Images were taken from the edges of the sample that were joined with epoxy. Thickness measurements were obtained using Motic Images Plus 2.0 (Motic®) software.

CHAPTER FIVE

RESULTS

5.1 Overview

The characterization of the Nitinol specimens and the results of the nickel leaching test are described in this chapter. The surfaces of Nitinol specimens used for the nickel leaching test were characterized to verify the composition of the surfaces. The techniques used to study the surfaces included SEM and XRD. Surface layer thicknesses were measured from images of the cross-sections of treated samples. Nickel release rates were calculated based on the nickel concentration measurements that were taken.

5.2 Characterization of Untreated Nitinol

The surface of a mechanically polished Nitinol specimen was characterized using X-ray diffraction at a glancing angle of 0.5°. Figure 8 shows that the only phase that was present on the surface of the untreated, mechanically-polished Nitinol was NiTi, as expected. The energy dispersive spectroscopy results shown in Figure 9 also confirmed the presence of nickel and titanium on the surface of the untreated specimens. The ratio of nickel to titanium on the surface was 1.07. The titanium concentration is lower than the nickel concentration since after mechanical polishing, the native titanium oxide layer was removed.

5.3 Characterization of Treated Nitinol

The treated Nitinol specimens were characterized by XRD, SEM, EDS, and optical microscopy to determine surface composition and the thickness and composition of the layer formed during the treatment.

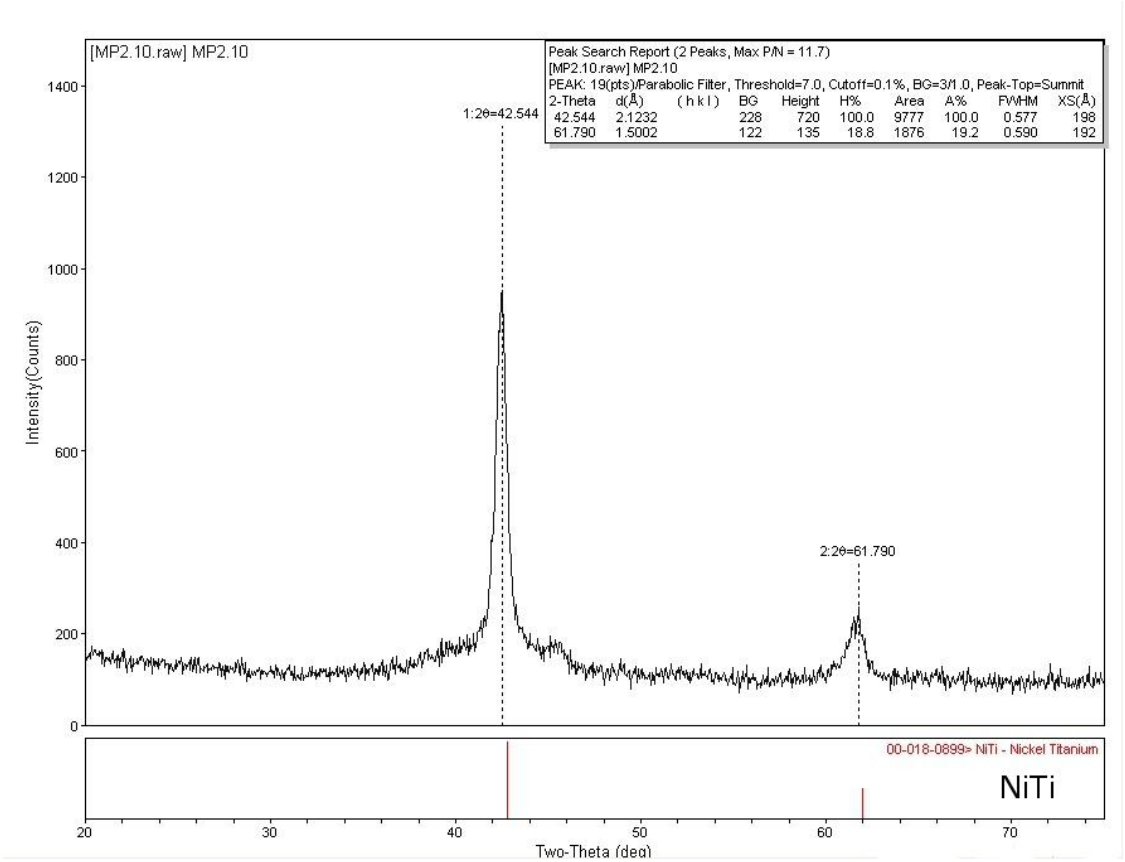

Figure 8. X-ray diffraction spectrum for mechanically polished NiTi.

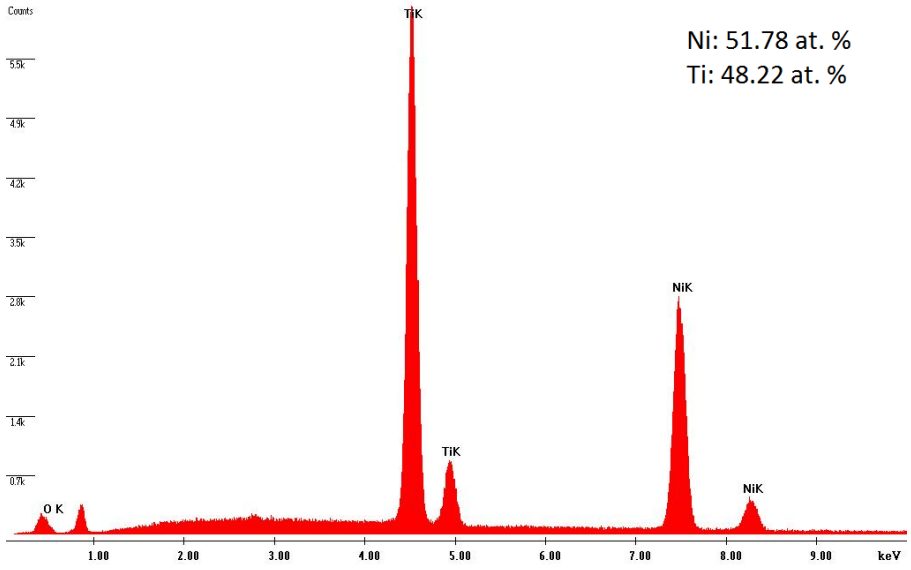

Figure 9. Energy-dispersive X-ray spectroscopy spectrum for untreated Nitinol.

5.3.1 Analysis of Nitrided Specimens

XRD was used to determine the composition of the gold-colored film present on the surface of the Nitinol samples after nitriding. A sample nitrided in 96% N_2 + 4% H_2 at 1000°C was studied. As shown in Figure 10, the phases detected were TiN and Ti_2Ni. The presence of a Ti_2Ni intermetallic beneath the surface has been reported in previous studies by Bazochaharbakhsh and Starosvetsky [24, 41]. The thickness of the nitride layer was measured in multiple areas along the surface of specimens nitrided at 800°C, 850°C, 900°C, 950°C, and 1000°C. The range of nitride layer thicknesses is shown in Figure 11. The specimens nitrided at 950°C and 1000°C had median thicknesses of 6.8 and 6.5 microns, respectively. The thicknesses for the nitride layers of these specimens ranged from 3 microns to 9.7 microns.

Cross sections of some of the Nitinol nitrided at 850°C and 900°C also revealed the presence of nickel-rich regions directly beneath the nitride layer, as shown in Figure 12. Finger-like projections of this layer into the surface layer were also present. According to an EDS analysis of the specimen nitrided at 900°C, these nickel-rich regions consisted of nickel and titanium in a 2:1 ratio, as shown in Table 9. The higher nickel content in the intermediate layers suggests that the phase is not Ti_2Ni, which was found in the XRD analysis. Based on the Ni-Ti phase diagram, the intermediate layer is most likely a Ni_3Ti intermetallic with the surrounding NiTi phase being detected as a result of the approximately 1.4 μm interaction volume of the electrons at 20 kV.

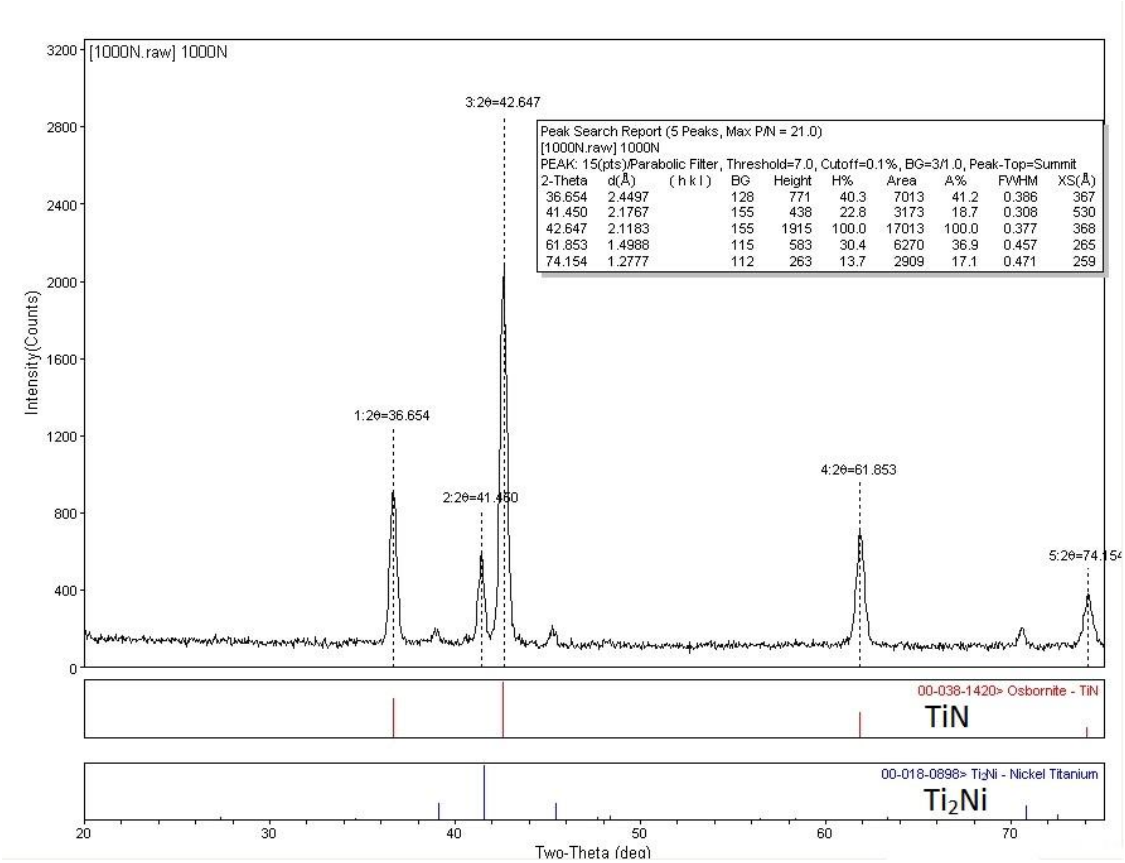

Figure 10. X-ray diffraction spectrum for NiTi sample nitrided at 1000°C.

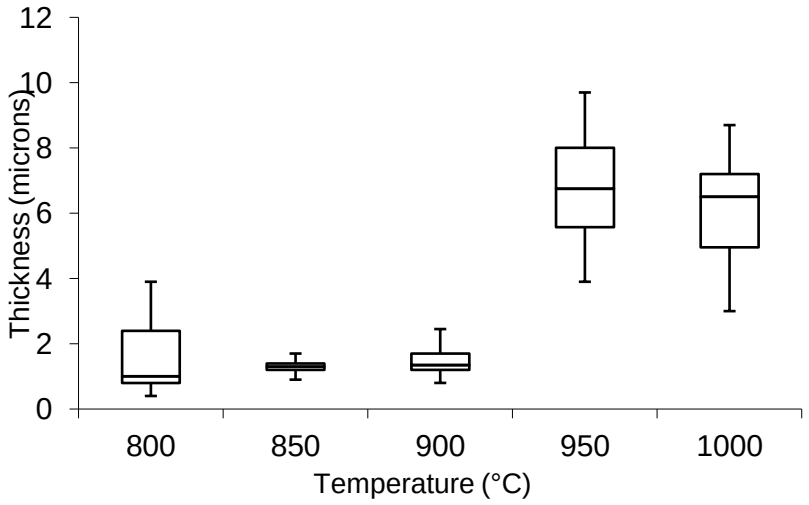

Figure 11. Nitride layer thickness (μm) as a function of temperature (°C). Median thickness is displayed within each box.

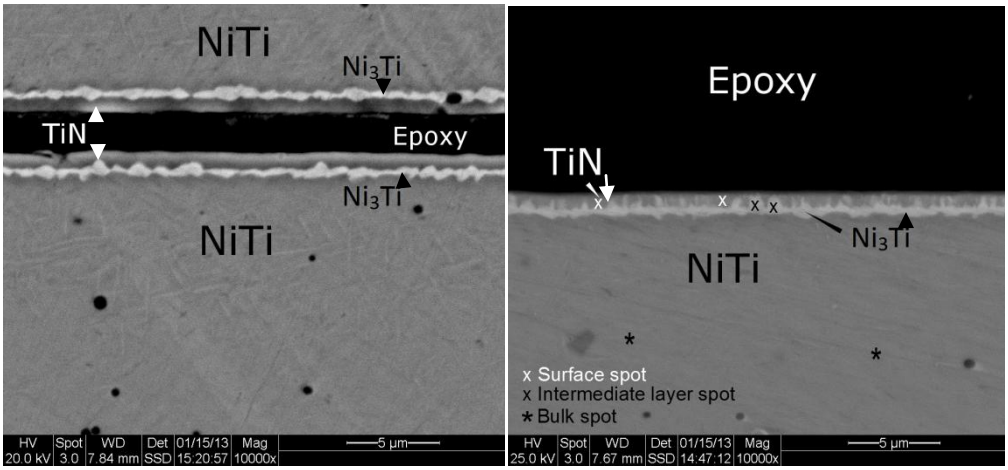

Figure 12. Back-scatter electron image of nitrided Nitinol cross sections. *Left*: Specimen nitrided at 850°C. *Right:* Specimen nitrided at 900°C

Table 9. EDS analysis of spots in TiN sample nitrided at 900°C. Spot locations indicated in Figure 12

Spot location	Ni (at. %)	Ti (at. %)	O (at. %)	N (at. %)
Bulk spot 1	55.10	44.90	-	-
Bulk spot 2	50.62	42.35	2.72	4.31
Intermediate layer spot 1	61.82	28.95	3.37	5.86
Intermediate layer spot 2	59.78	30.63	3.82	5.77
Surface spot 1	39.52	39.07	12.64	8.77
Surface spot 2	42.90	40.17	9.62	7.32

5.3.2 Characterization of Nitrided and Oxidized Specimens

The specimens treated with the nitriding and oxidation treatment were characterized to determine their surface composition. XRD was used to characterize the phases present on the surface and EDS was used to determine surface nickel content. For the XRD analysis, samples treated using the 800-N-700-O, 900-N-700-O, and 1000-N-700-O modalities were examined. The presence of only the rutile form of TiO_2 on the treated Nitinol surface was confirmed by XRD as shown in Figures 13-15.

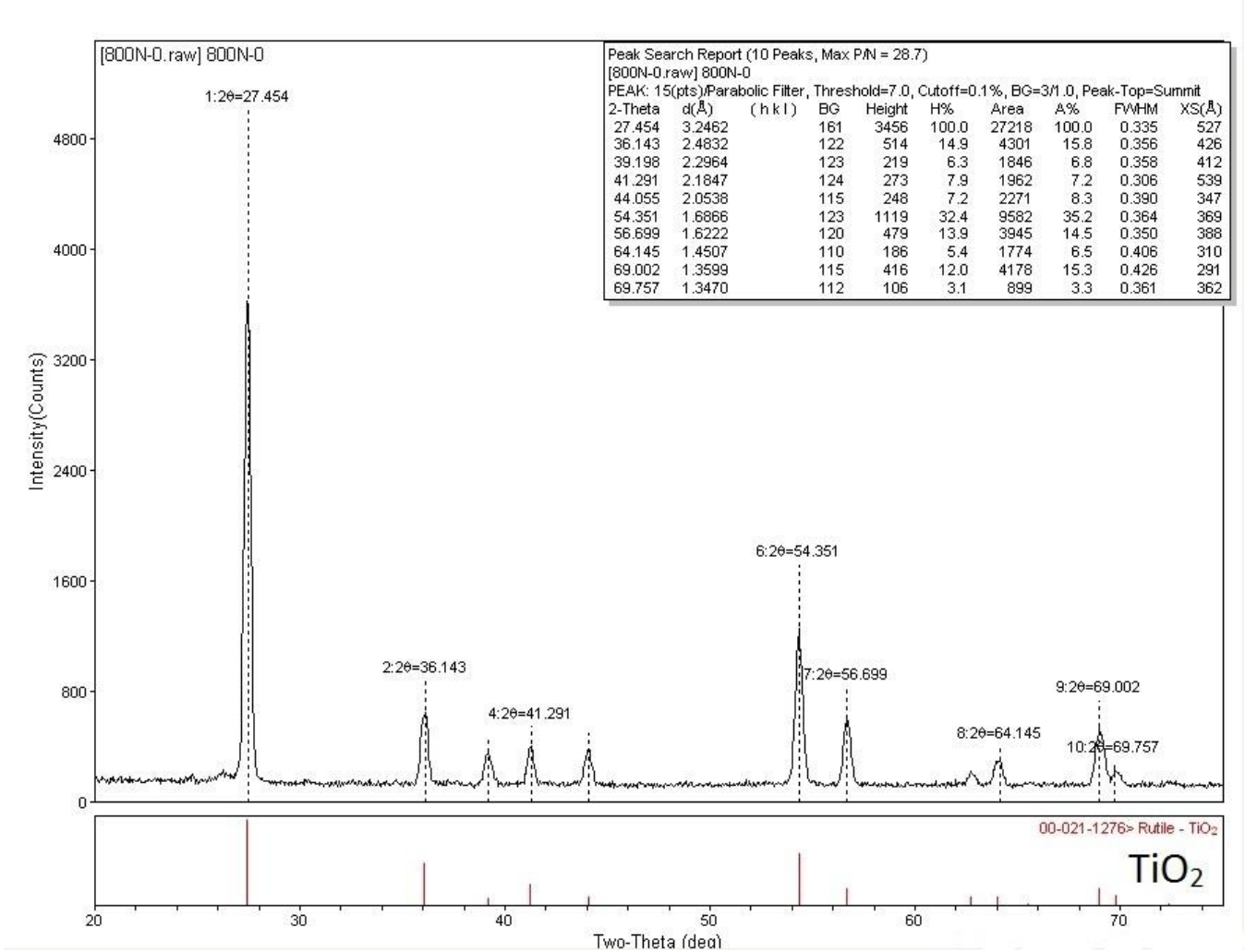

Figure 13. X-ray diffraction spectrum for an 800-N-700-O sample.

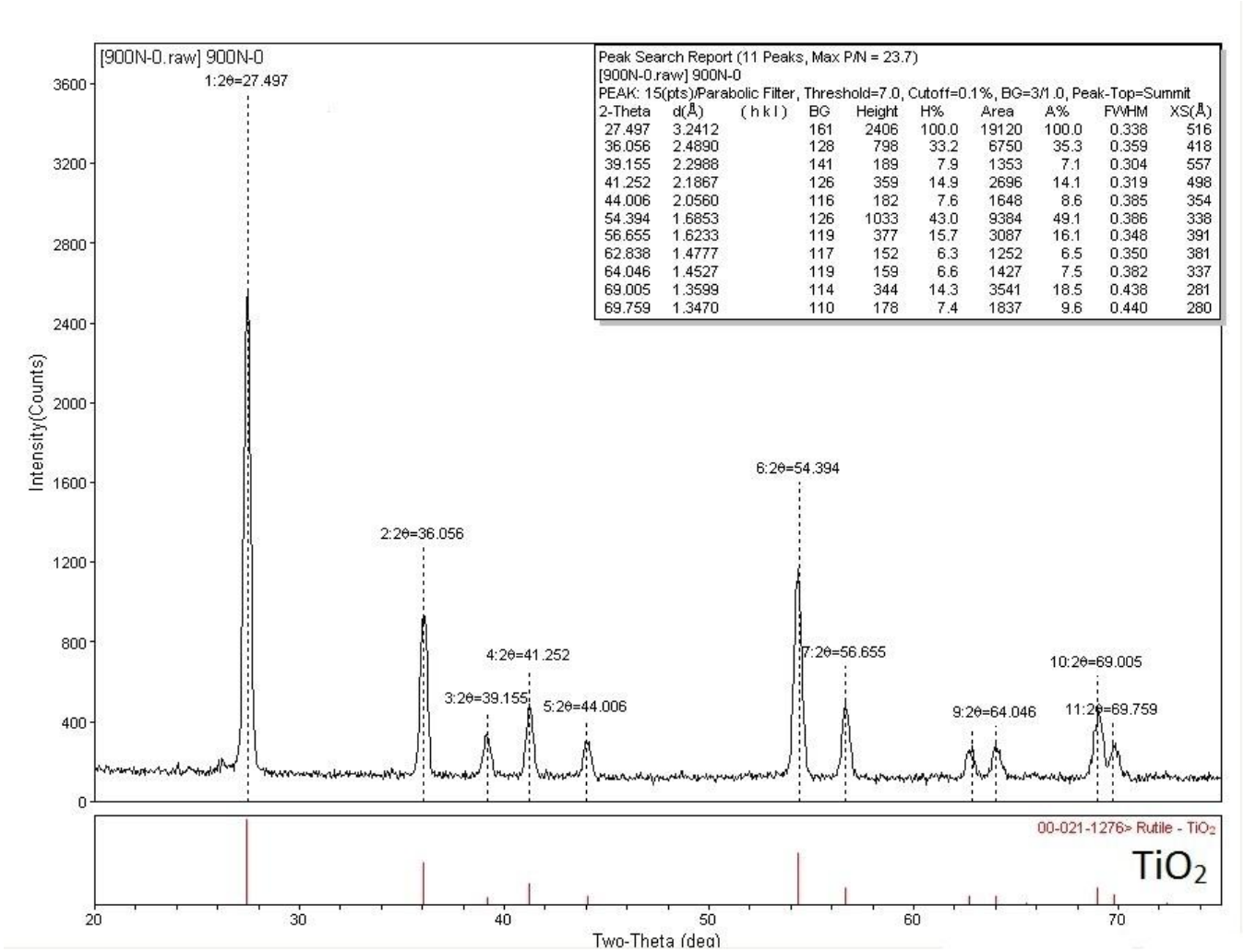

Figure 14. X-ray diffraction spectrum for a 900-N-700-O sample.

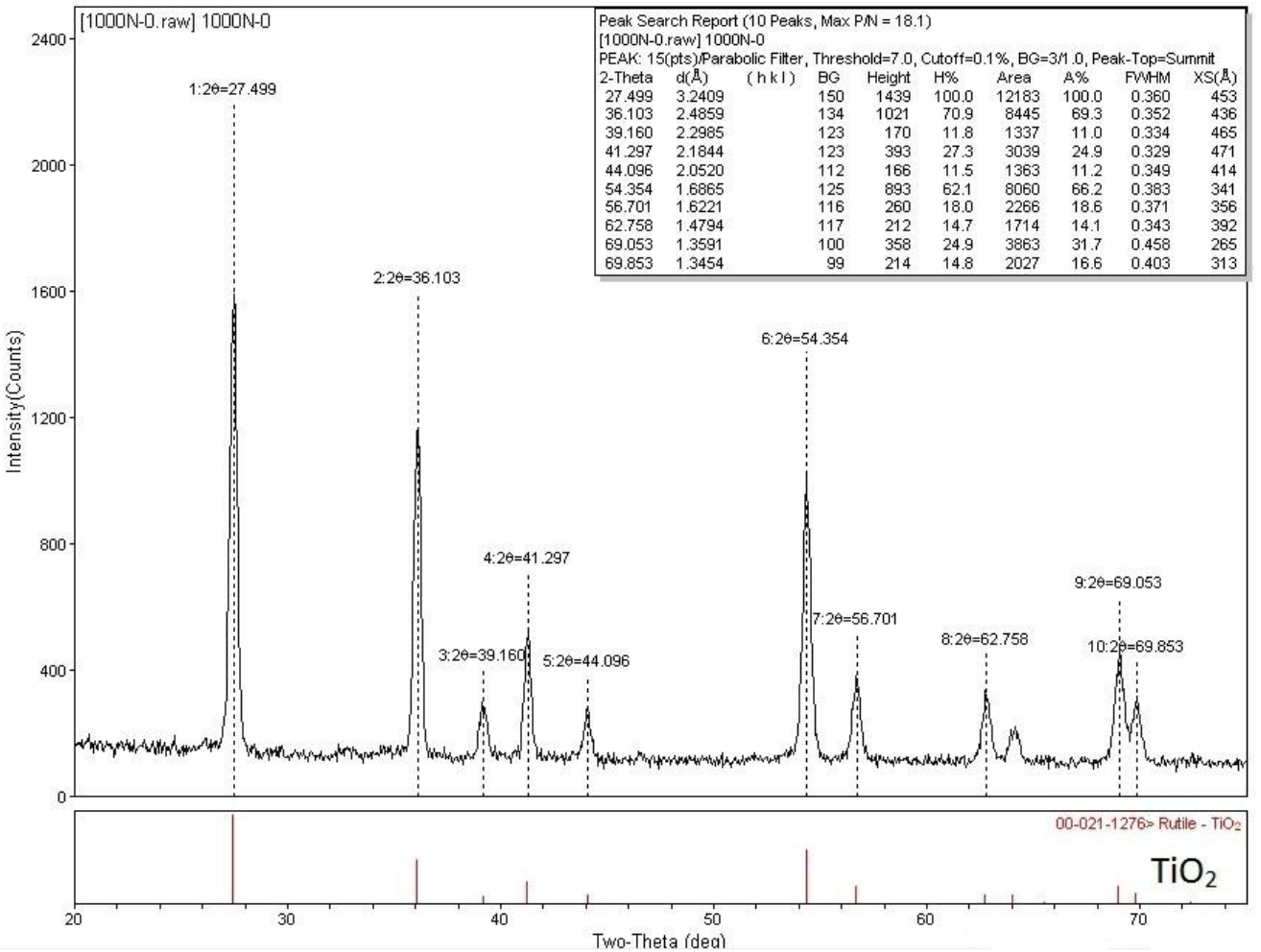

Figure 15. X-ray diffraction spectrum for a 1000-N-700-O sample.

For each of these samples, the only peaks that were present corresponded to the rutile form of TiO_2; no other phases were detected on the surface of these samples. The same samples were analyzed by EDS for their surface nickel content. The spectra are shown in Figures 16-18. The accompanying atomic concentrations are shown in Tables 10-12.

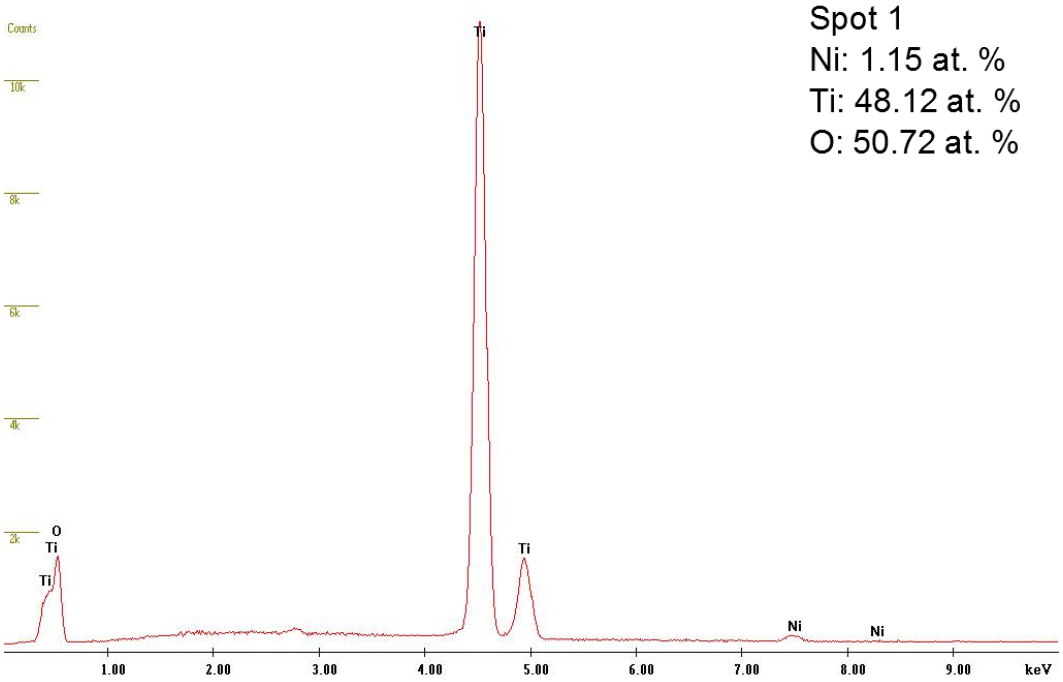

Figure 16. Energy dispersive X-ray spectroscopy spectrum from an 800-N-700-O sample.

Table 10. Elemental surface composition of an 800-N-700-O sample.

Spot	Ni (at. %)	Ti (at. %)	O (at. %)
1	1.15	48.12	50.72
2	1.13	48.52	50.34
3	1.16	48.27	50.57

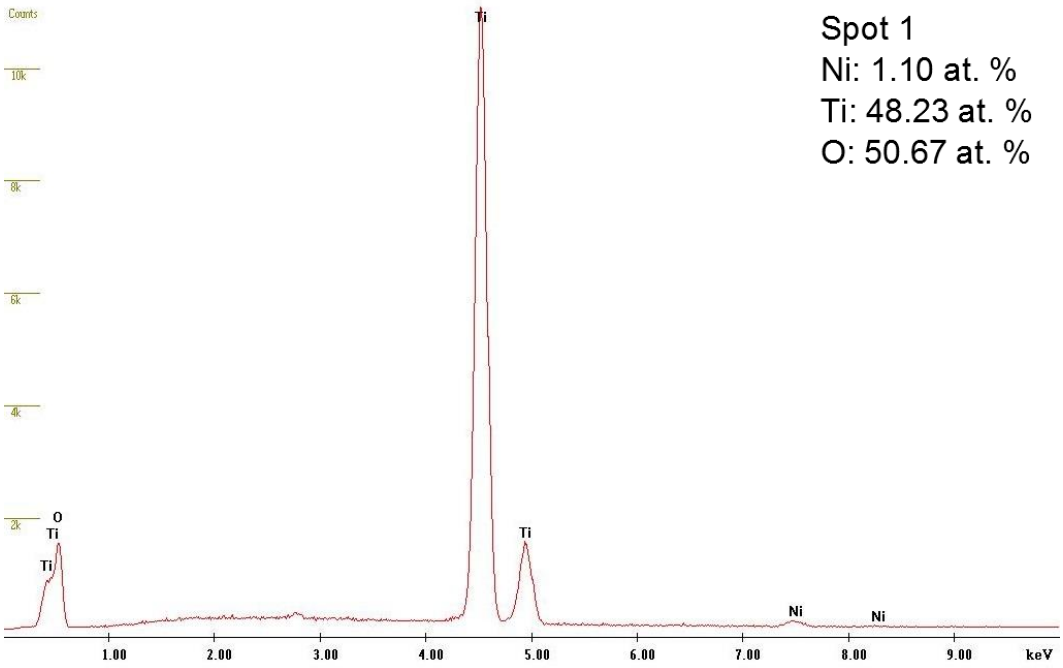

Figure 17. Energy dispersive X-ray spectroscopy spectrum from a 900-N-700-O sample.

Table 11. Elemental surface composition of a 900-N-700-O sample.

Spot	Ni (at. %)	Ti (at. %)	O (at. %)
1	1.10	48.23	50.67
2	1.01	48.84	50.15
3	1.11	48.74	50.16

The average nickel concentration on the surface of the 800-N-700-O sample was 1.15 at. %. For the 900-N-700-O sample, the average nickel concentration was 1.07 at. %. For the 1000-N-700-O sample, the average nickel concentration was 1.76 at. %.

Images of the cross sections of other nitrided and oxidized samples were also obtained using optical microscopy at 400x magnification, and SEM at 10,000x and 20,000x magnification. The optical microscopy images are shown in Figures 19-21. The optical microscopy images were used to measure the thickness of the oxide layers

obtained after the 1 hour oxidation treatment at 700°C. The thickness measurements are shown in Figure 22.

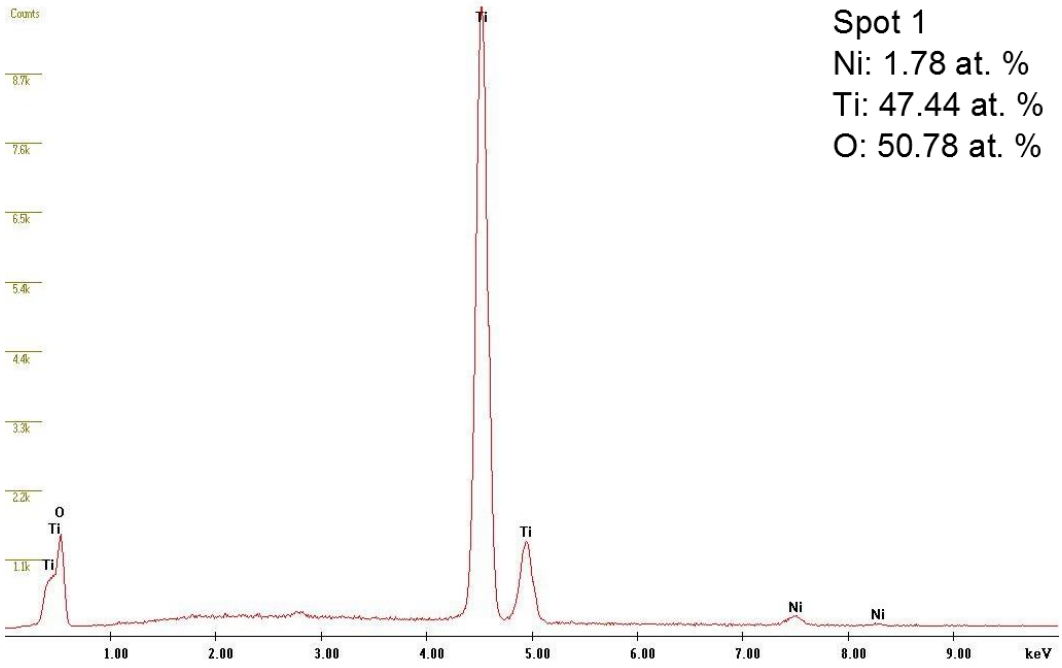

Figure 18. Energy dispersive X-ray spectroscopy spectrum from a 1000-N-700-O sample.

Table 12. Elemental surface composition of a 1000-N-700-O sample.

Spot	Ni (at. %)	Ti (at. %)	O (at. %)
1	1.78	47.44	50.78
2	1.82	48.75	49.43
3	1.67	48.04	50.29

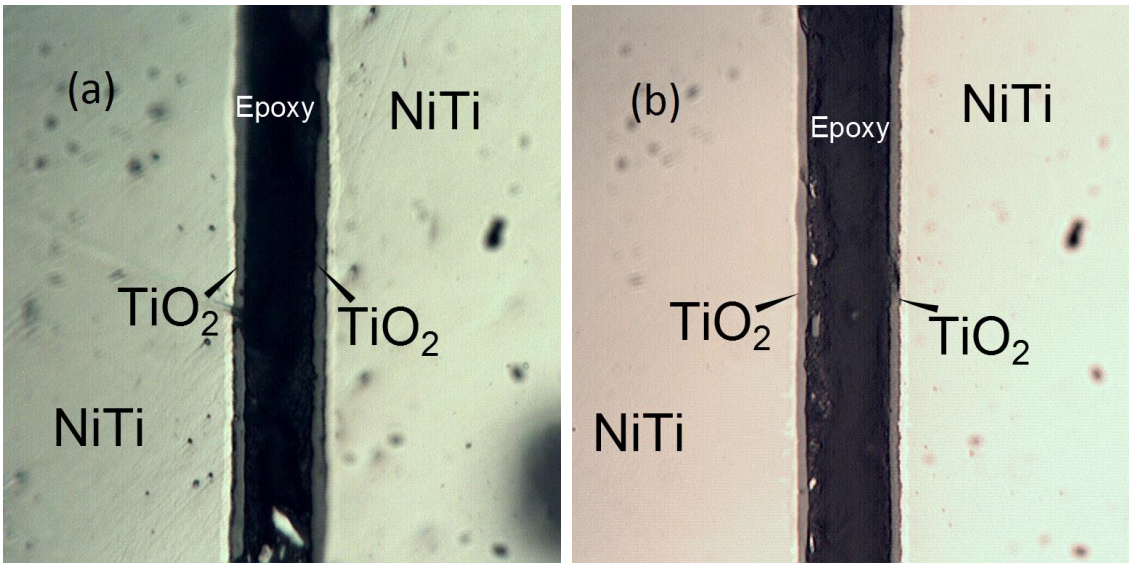

Figure 19. Optical microscopy images (400x) of the cross sections of (a) 800-N-700-O (b) 850-N-700-O samples.

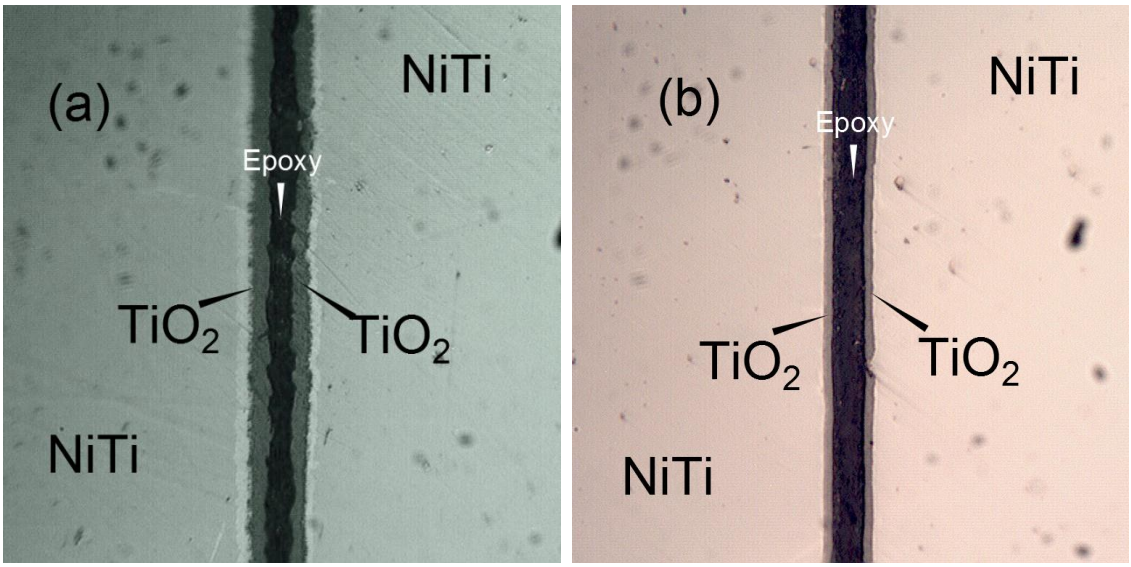

Figure 20. Optical microscopy images (400x) of the cross sections of (a) 900-N-700-O (b) 950-N-700-O samples.

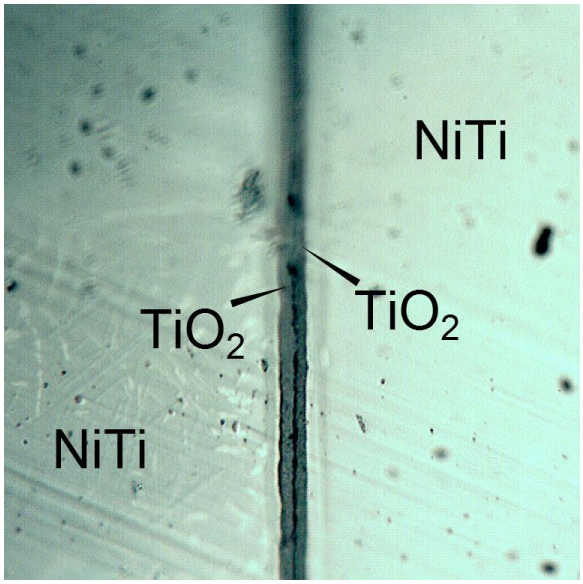

Figure 21. Optical microscopy images (400x) of the cross sections of 1000-N-700-O samples.

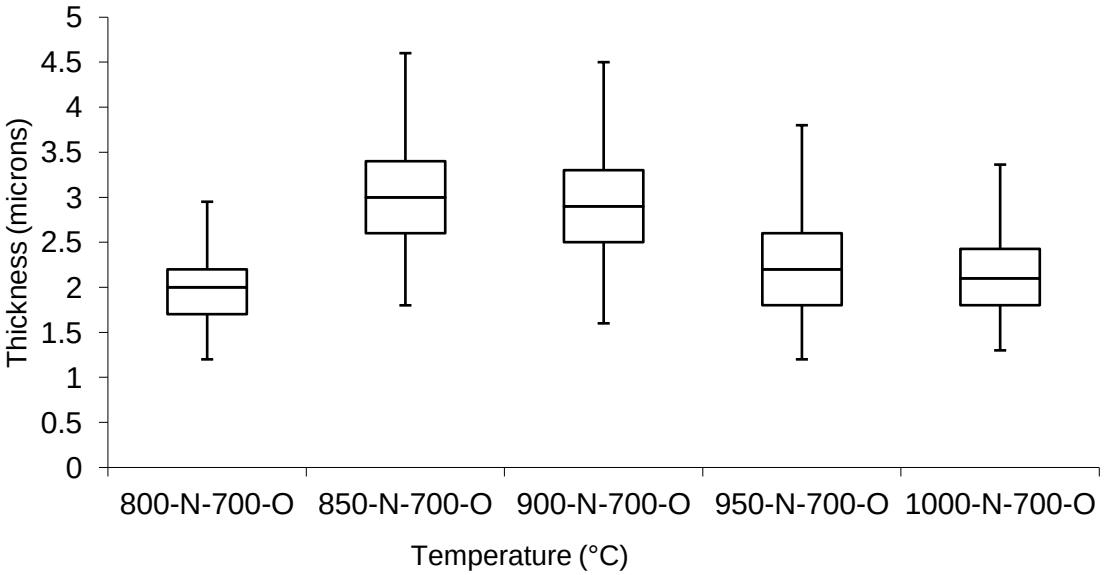

Figure 22. Oxide layer thickness for each set of nitrided and oxidized samples. Median thicknesses are shown within the boxes.

A one-way ANOVA test for all 5 groups returned an F-ratio of 42.9 with a p-value of 2.31×10^{-29} ($\alpha = 0.05$) which suggests that the variance among the groups was

statistically significant. The η^2 value was 0.33, meaning that 33% of the variance in thickness was due to the difference in treatment method. However, the temperature and time for the oxidation step was the same for all samples, so the variance in thickness was due to differences in flow patterns across the surface of the samples during treatment.

The optical microscopy images also revealed the presence of buried sublayers beneath the oxide layer on the surface, which can be seen adjacent to the TiO_2 layers in Figures 17-19. Samples were then analyzed with SEM and EDS in order to determine the nickel content of the sublayers. EDS analysis of these intermediate layers revealed that they contained nickel at higher concentrations than the adjacent TiO_2 layers. EDS analysis of a spot in the sublayer shown in Figure 23 showed that the nickel concentration was about 66 at. % compared to a nickel concentration of 1.58 at. % in the oxide layer. The results of the EDS analysis are shown in Figures 24-26. The EDS elemental composition results for these samples are shown in Tables 13 and 14.

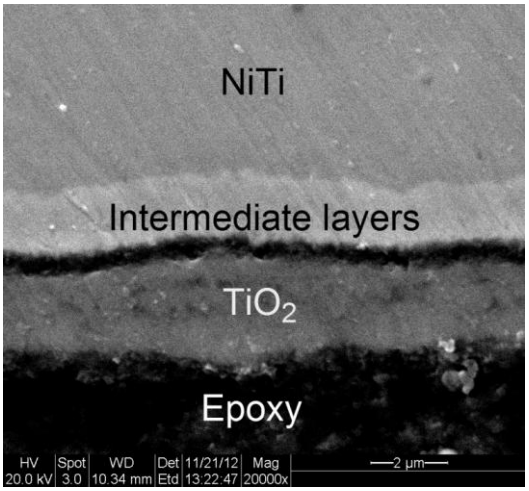

Figure 23. 20,000x magnification SEM image of the cross section of a Nitinol sample nitrided at 800°C and oxidized at 700°C.

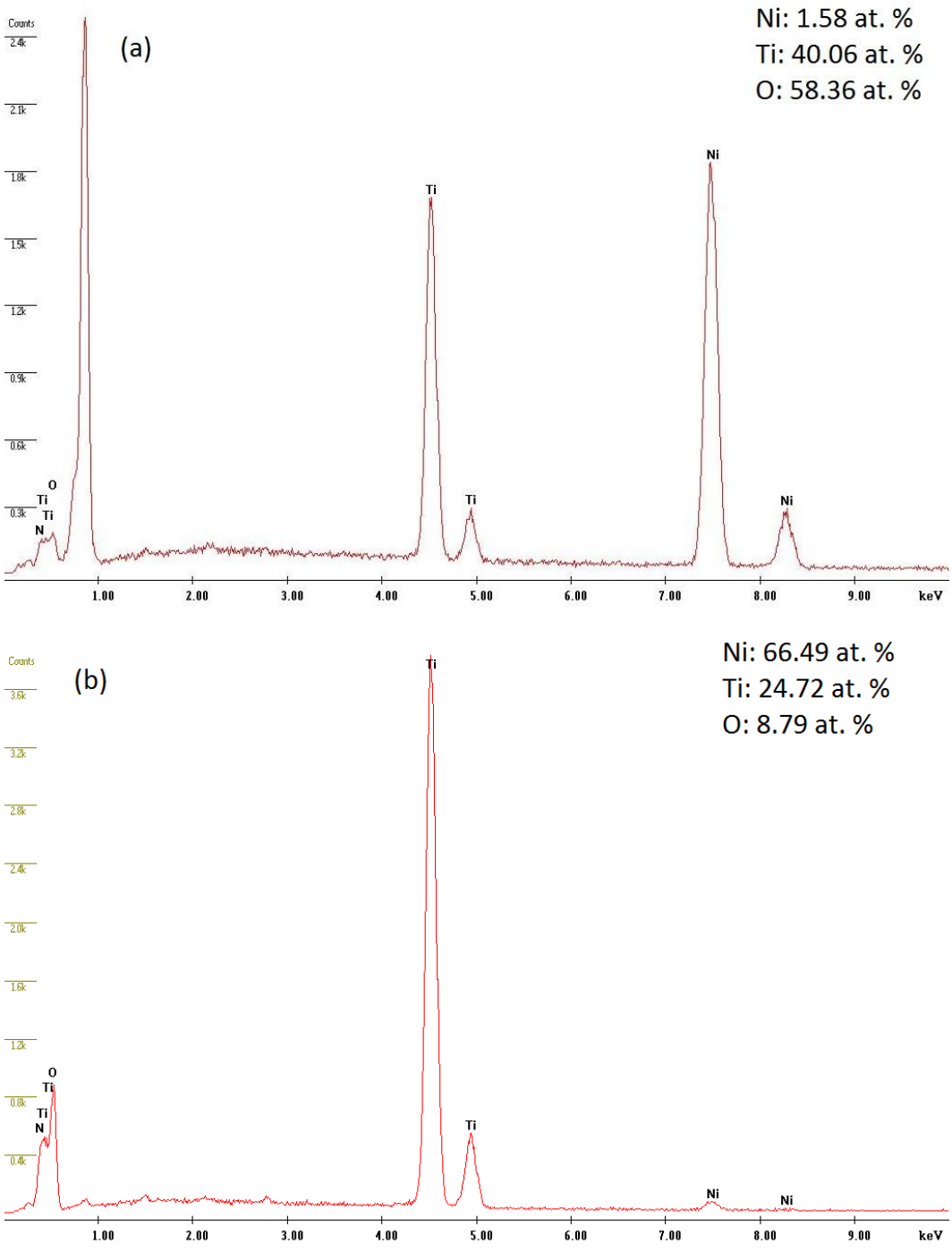

Figure 24. Energy dispersive X-ray spectroscopy spectrum from the (a) oxide layer and (b) intermediate layer of an 800-N-700-O sample.

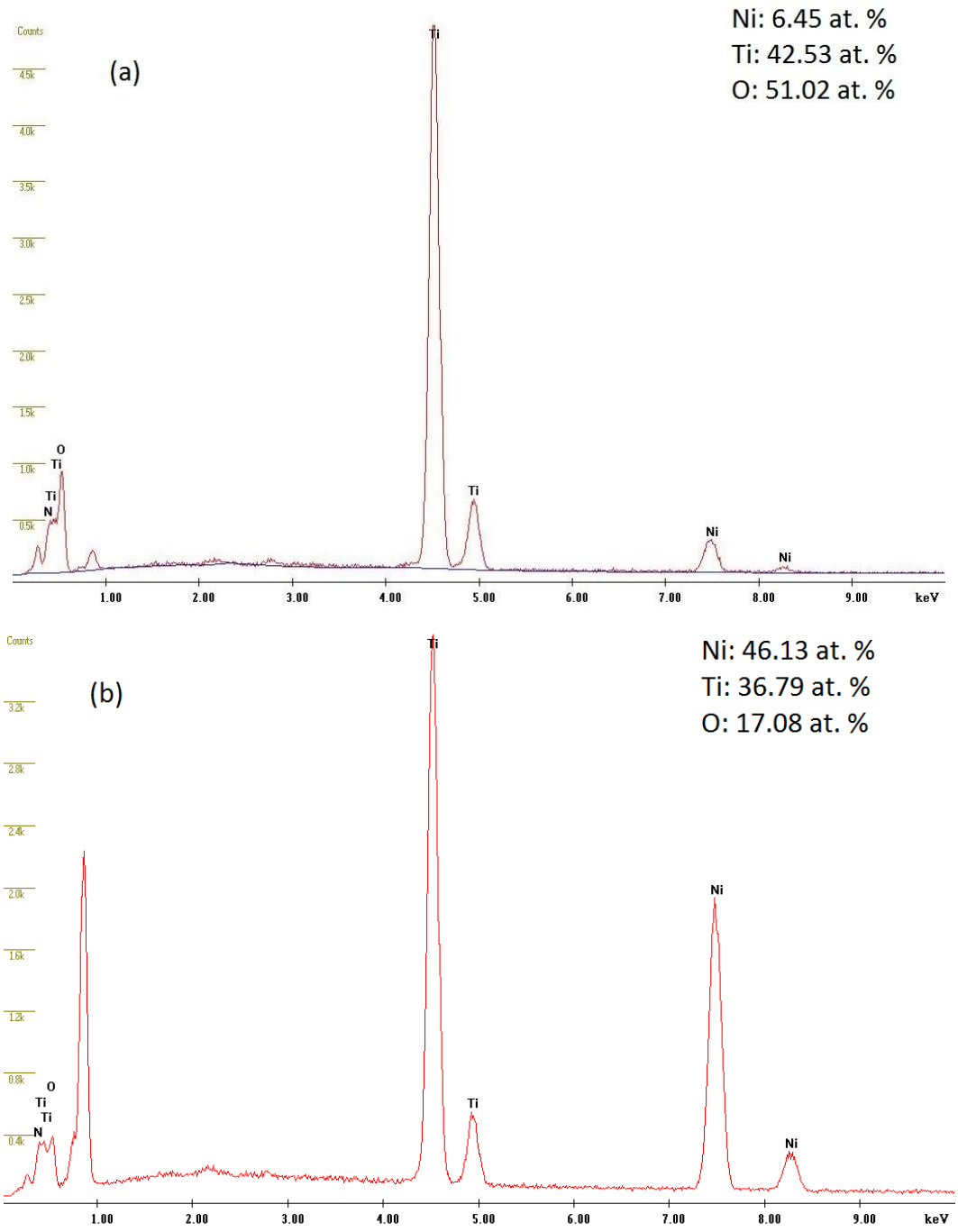

Figure 25. Energy dispersive X-ray spectroscopy spectrum from the (a) oxide layer and (b) intermediate layer of a 950-N-700-O sample.

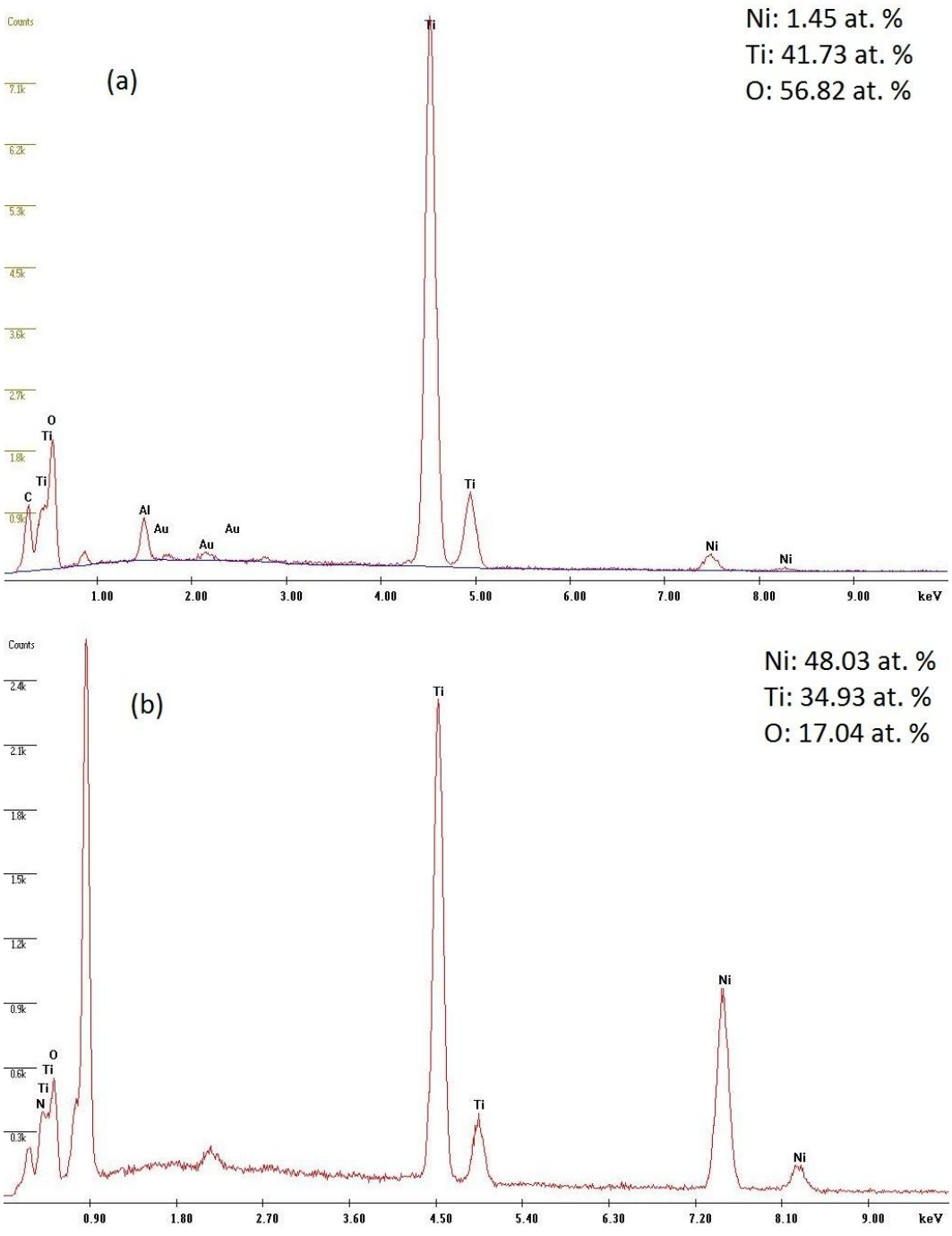

Figure 26. Energy dispersive X-ray spectroscopy spectrum from the (a) oxide layer and (b) intermediate layer of a 1000-N-700-O sample.

Table 13. Elemental surface composition for nitrided and oxidized samples.

Sample	Ni (at. %)	Ti (at. %)	O (at. %)
800-N-700-O oxide layer	1.58	40.06	58.36
950-N-700-O oxide layer	6.45	42.53	51.02
1000-N-700-O oxide layer	1.45	41.73	56.82

Table 14. Elemental composition in the sublayer for nitrided and oxidized samples.

Sample	Ni (at. %)	Ti (at. %)	O (at. %)
800-N-700-O intermediate layer	66.49	24.72	8.79
950-N-700-O intermediate layer	46.13	36.79	17.08
1000-N-700-O intermediate layer	48.03	34.93	17.04

All of these samples had nickel concentrations in the intermediate layer that were much higher than in the oxide layer. The intermediate layer in the 950-N-700-O sample had a nickel concentration of 46.13 at. % while the oxide layer nickel concentration was about 6.45 at. %. In the case of the 1000-N-700-O sample, the nickel concentration in the sublayer was about 48 at. % compared to a 1.45 at. % nickel concentration in the oxide layer. Given the interaction volume of about 1.4 microns for the 20 kV EDS analysis and the thin geometry of the features in the cross section, it is difficult to identify the phases for certain from elemental concentrations. However, based on the Ti/Ni ratios in the intermediate layer, the Ni-Ti phase diagram, and previous studies on NiTi intermetallics [42, 43], a good estimation of the composition is a mixture of Ni_3Ti and $NiTi_2$. These are

the only intermetallics that form at these temperatures in the binary Ni-Ti system. These intermetallics, along with detection of the bulk NiTi, lead to the results shown in the EDS analysis.

5.4 Nickel Leaching Test

The nickel concentration readings from the PBS for each sample are presented in this section, grouped by treatment method. Based on these readings, nickel release rates were determined for each sample, as described in Chapter 4.

5.4.1 Untreated Samples

The untreated samples reached peak nickel concentrations around Days 4 and 5 of the leaching test, after which the concentrations stabilized, as seen in Figure 27. The maximum concentration reached by the untreated samples was 0.54 mg/L. The standard deviation of the nickel concentrations over the duration of the leaching test was only 0.05 mg/L, less than the 0.1 mg/L detection limit of the AAS and within the mean absolute error of the measurements, which shows that the concentration values did not differ much from day to day. This suggests that the surface properties of all of the untreated samples were very similar.

The nickel released from the samples at each measurement point is shown in Figure 28. The highest nickel release occurred in the first 4 or 5 days of the leaching test, at which point the solutions reached their maximum concentrations. The release rates for the untreated samples were, on average, only detectable for the first 7 days of the immersion test, as shown in Table 15. After the first 7 days, the nickel release was negligible.

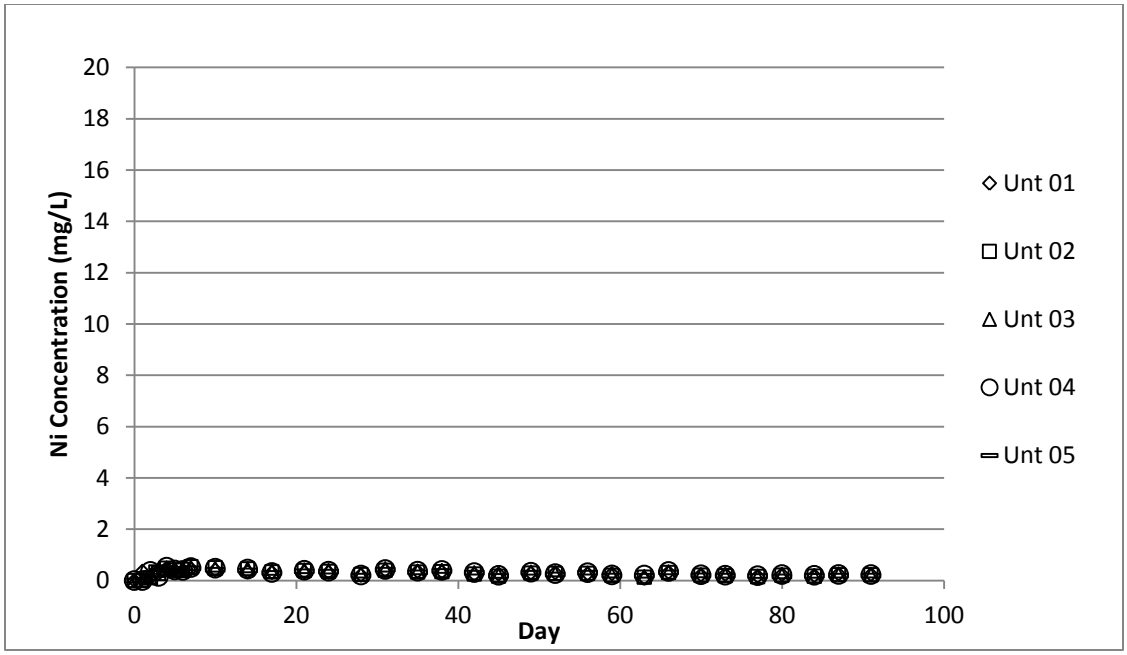

Figure 27. Nickel concentration in PBS for untreated samples.

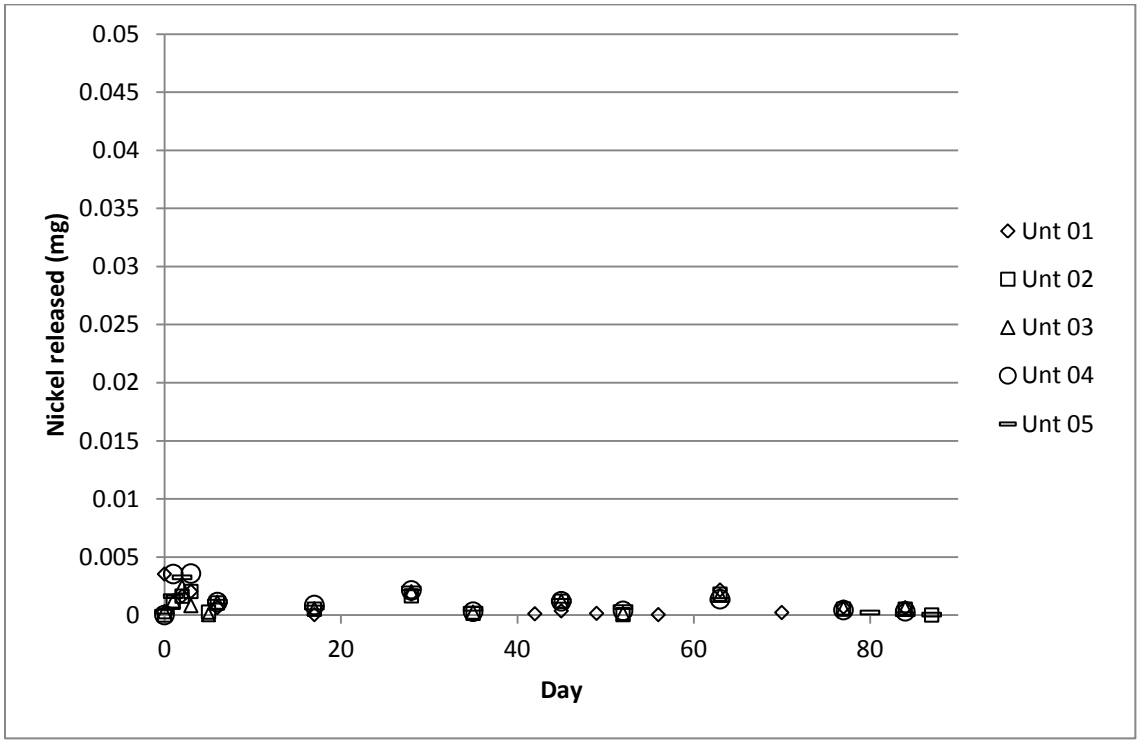

Figure 28. Nickel release from untreated samples.

Table 15. Release rates (mg/cm^2/day) for untreated samples.

Sample	Day 1-7	Day 8-35	Day 35-63	Day 64-91
Untreated 01	0.001	0.000	0.000	0.000
Untreated 02	0.001	0.000	0.000	0.000
Untreated 03	0.001	0.000	0.000	0.000
Untreated 04	0.001	0.000	0.000	0.000
Untreated 05	0.001	0.000	0.000	0.000
Untreated avg	0.001	0.000	0.000	0.000

5.4.2 Oxidation-Only Samples

The samples which were oxidized at 700°C for one hour released more nickel into the PBS solution than the untreated samples (Unt avg) over the immersion period, as seen in Figure 29. There was a wider spread of nickel concentrations among the 5 oxidized samples as compared to the untreated samples, as evidenced by the standard deviation of 1.33 mg/L for the oxidized samples, compared to the standard deviation of 0.05 mg/L for the untreated samples. In addition, the 700-O-04 sample reached a much higher nickel concentration than the other samples. The nickel release rate of this sample was also higher during the first 35 days of immersion, tapering off during the latter part of the test, as seen in Figure 30 and Table 16.

The 700-O-04 sample was one of the samples with an oxide layer that delaminated, losing 6% of the entire surface oxide. This was the likely cause of the increased nickel release rate for this sample. The sample reached a maximum concentration of 7.6 mg/L on Day 56 of the leaching test.

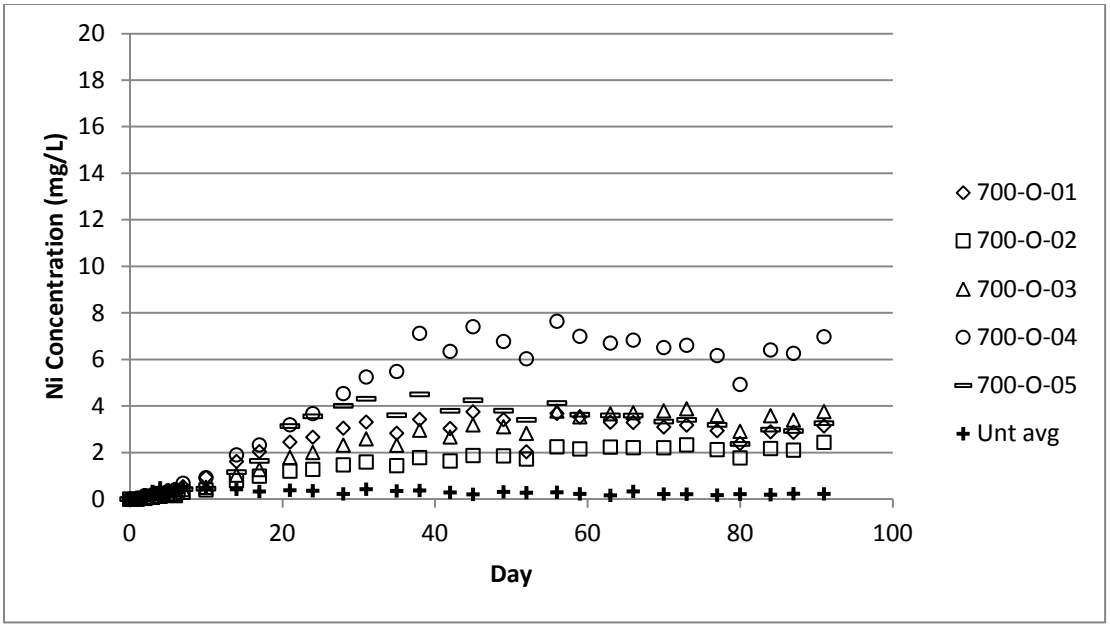

Figure 29. Nickel concentration in PBS for oxidation-only samples.

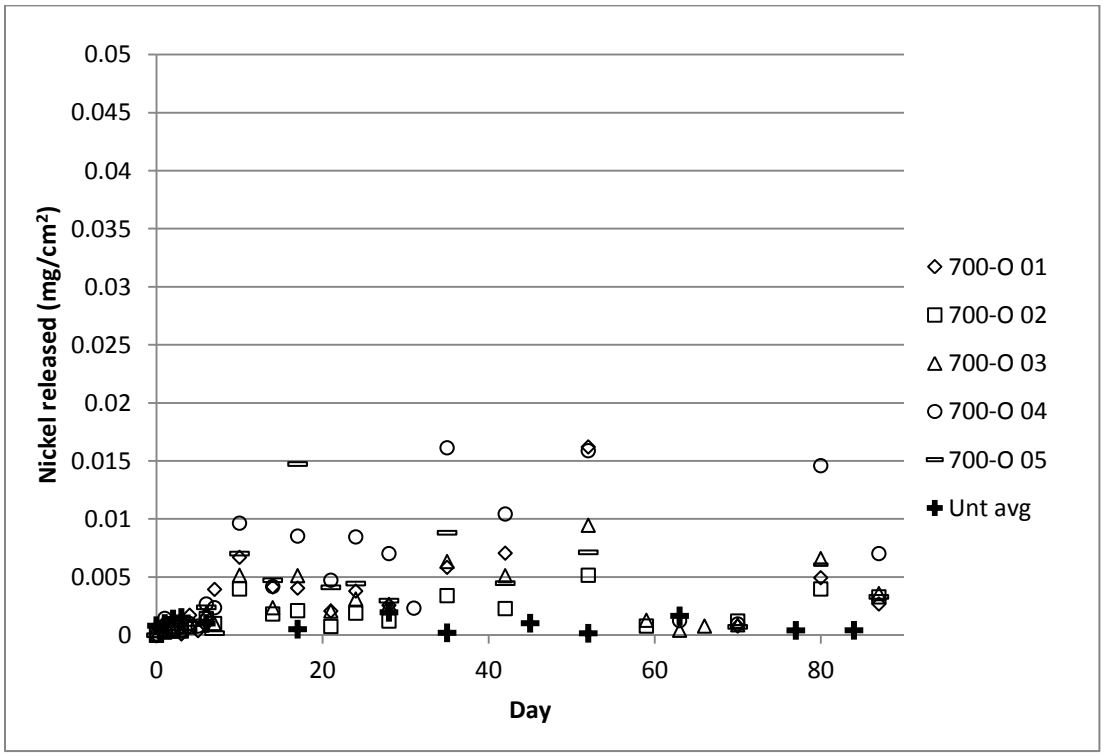

Figure 30. Nickel release from samples oxidized at 700°C for 1 hour.

Table 16. Release rates (mg/cm^2/day) for samples oxidized at 700°C for 1 hour.

Sample	Day 1-7	Day 8-35	Day 35-63	Day 64-91
700-O-01	0.001	0.008	0.002	0.000
700-O-02	0.000	0.004	0.003	0.001
700-O-03	0.001	0.007	0.005	0.000
700-O-04	0.001	0.017	0.004	0.001
700-O-05	0.001	0.011	0.000	0.000
Untreated avg	0.001	0.000	0.000	0.000

5.4 3 Nitrided and Oxidized Samples

Almost all of the samples subjected to the nitriding and oxidation treatment released more nickel into the PBS than the untreated samples. The highest concentrations and nickel release rates belonged to the 800-N-700-O group of Nitinol samples and, surprisingly, two of the five 1000-N-700-O samples. On the first day of immersion, 29 of the 30 treated samples did not release any nickel into the PBS, while three of the five untreated samples did, as shown in Table 17. On the third day of the leaching test, only one of the 15 samples nitrided at 800°C, 850°C, or 900°C leached any nickel into the PBS.

After about two weeks of immersion in the PBS, several samples began showing signs of delamination of the gray titanium oxide layer, revealing a black layer underneath. The 800-05 sample lost 78% of the oxide layer due to delamination, as shown in Figure 31. XRD analysis of the black layer confirmed the presence of the Ni_3Ti phase on the surface, just beneath the rutile titanium oxide layer, as shown in Figure 32.

Table 17. Nickel concentration (mg/L) in PBS solution, Days 0-3.

Sample Name	Day 0	Day 1	Day 2	Day 3
800-N-01	0	0	0	0
800-N-02	0	0	0	0
800-N-03	0	0	0	0
800-N-04	0	0	0	0
800-N-05	0	0	0	0
850-N-01	0	0	0	0
850-N-02	0	0	0	0
850-N-03	0	0	0	<0.1
850-N-04	0	0	0	0
850-N-05	0	0	0	0
900-N-01	0	0	0	0
900-N-02	0	0	0	0
900-N-03	0	0	0	0
900-N-04	0	0	0	0
900-N-05	0	0	0	0
950-N-01	0	0	0	<0.1
950-N-02	0	0	0	0.3
950-N-03	0	0	0	<0.1
950-N-04	0	0	<0.1	0.2
950-N-05	0	0	0.3	0.9
1000-N-01	0	0	0.1	0.2
1000-N-02	0	0	<0.1	0.4
1000-N-03	0	<0.1	0.3	0.6
1000-N-04	0	0	0.2	0.5
1000-N-05	0	0	0	0.2
700-O-01	0	0	0.1	0.2
700-O-02	0	0	<0.1	<0.1
700-O-03	0	0	<0.1	<0.1
700-O-04	0	0	0.1	0.2
700-O-05	0	0	<0.1	0.1
Untreated 01	0	0.4	0.1	0.3
Untreated 02	0	0	0.1	0.3
Untreated 03	0	<0.1	0.2	0.4
Untreated 04	0	0	0.4	0.2
Untreated 05	0	<0.1	0.2	0.5

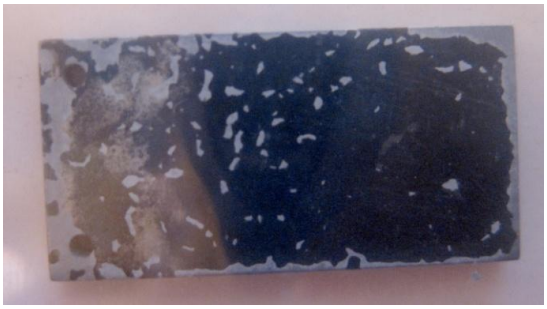

Figure 31. Delamination of the oxide layer for the 800-05 sample, revealing the black intermediate layer beneath.

The Nitinol samples in the 800-N-700-O group had the highest average nickel concentration at the end of the immersion period as well as the highest average maximum concentration. The 800-05 sample almost reached 20 mg/L before the concentration decreased dramatically over the last 45 days of the test, as seen in Figure 33. The other four samples released nickel at high rates in the first 5 weeks, followed by a reduced nickel release rate, as seen in Figure 34 and Table 18.

All of these samples began to delaminate after 2-3 weeks and exhibited a much greater extent of delamination than the other samples, as evidenced by the data in Table 19. The percentage of delamination was calculated by dividing the area of the removed oxide layer by the total area of the Nitinol surface.

The samples nitrided at 850°C and oxidized at 700°C had similar nickel release profiles during the immersion test, with the exception of the 850-03 sample. The standard deviation for the other four samples in the group was 0.44 mg/L; for all five samples, it was 0.93 mg/L. As shown in Figure 35, Figure 36, and Table 20 the 850-03 sample released nickel at a higher rate than the other four samples in the group over the first 35 days of the test.

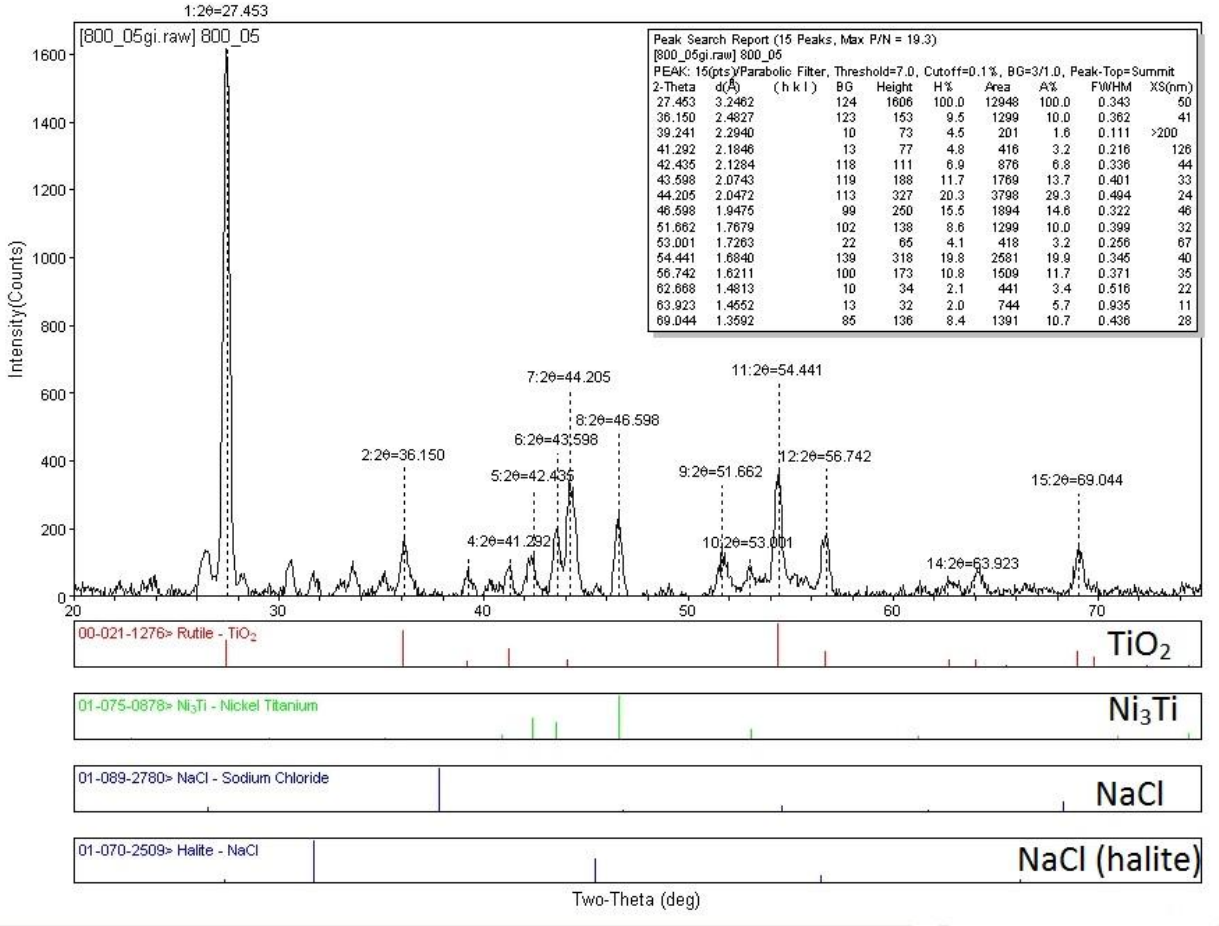

Figure 32. XRD spectrum for the black layer beneath the TiO_2 layer in the 800-N-700-O-05 sample.

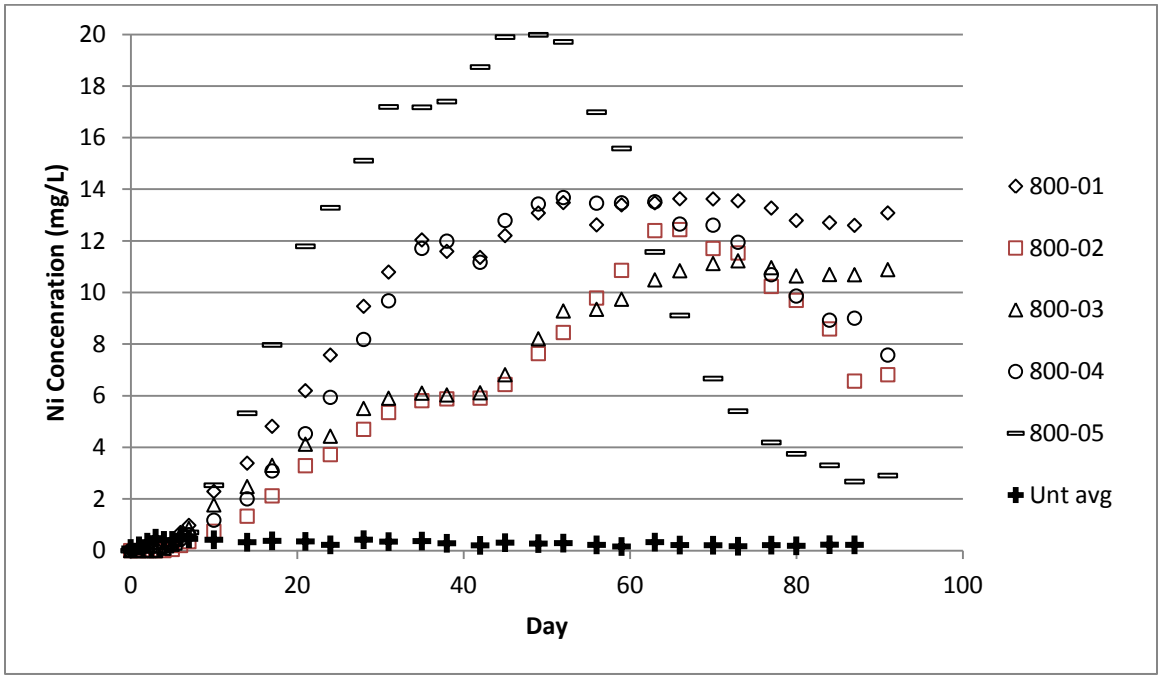

Figure 33. Nickel concentration in PBS for samples nitrided at 800°C and oxidized at 700°C.

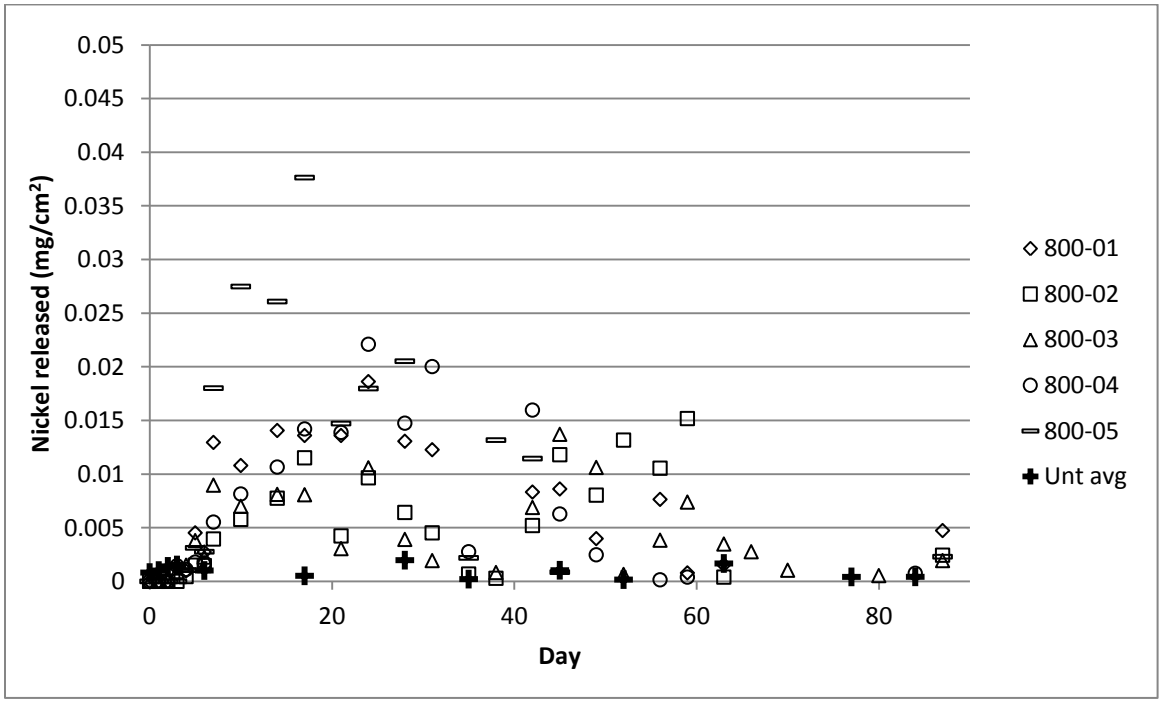

Figure 34. Nickel release from Nitinol nitrided at 800°C and oxidized at 700°C.

Table 18. Release rates (mg/cm^2/day) for 800-N-700-O samples.

Sample	Day 1-7	Day 8-35	Day 35-63	Day 64-91
800-N-01	0.001	0.039	0.005	0.000
800-N-02	0.000	0.019	0.023	0.000
800-N-03	0.001	0.018	0.015	0.001
800-N-04	0.001	0.039	0.006	0.000
800-N-05	0.001	0.058	0.000	0.000
Untreated avg	0.001	0.000	0.000	0.000

Table 19. Delamination of oxide layer from Nitinol samples, measured after 91 days

Sample	Percentage of Delamination	Maximum concentration (mg/L)	Maximum release rate (mg/cm^2/day)
800-01	12	13.6	0.005
800-02	18	12.4	0.004
800-03	28	11.3	0.003
800-04	44	13.7	0.005
800-05	78	20.0	0.009
850-01	7	7.1	0.002
850-02	7	8.2	0.002
850-03	5	8.2	0.003
850-04	6	8.2	0.002
850-05	27	7.5	0.002
900-04	9	9.26	0.002
950-05	26	16.3	0.004
1000-02	10	17.6	0.005
1000-03	14	9.1	0.004
1000-04	3	18.0	0.004
700-01	1	3.7	0.002
700-04	6	7.6	0.002

All the samples in this group reached their respective maximum concentrations near the end of the leaching test, ranging from 7.11 mg/L for the 850-01 sample to 8.23 mg/L for the 850-04 sample. Each of the samples in this group also exhibited delamination of the surface oxide layer, although at a lesser extent than the 800-N-700-O

group, as seen in Table 19. The sample with the highest percentage of delamination, 850-05, was not responsible for the highest nickel release rate in the group. The highest release rate was found for the 850-03 sample exhibited only 5% delamination, compared to 27% delamination from the 850-05 sample.

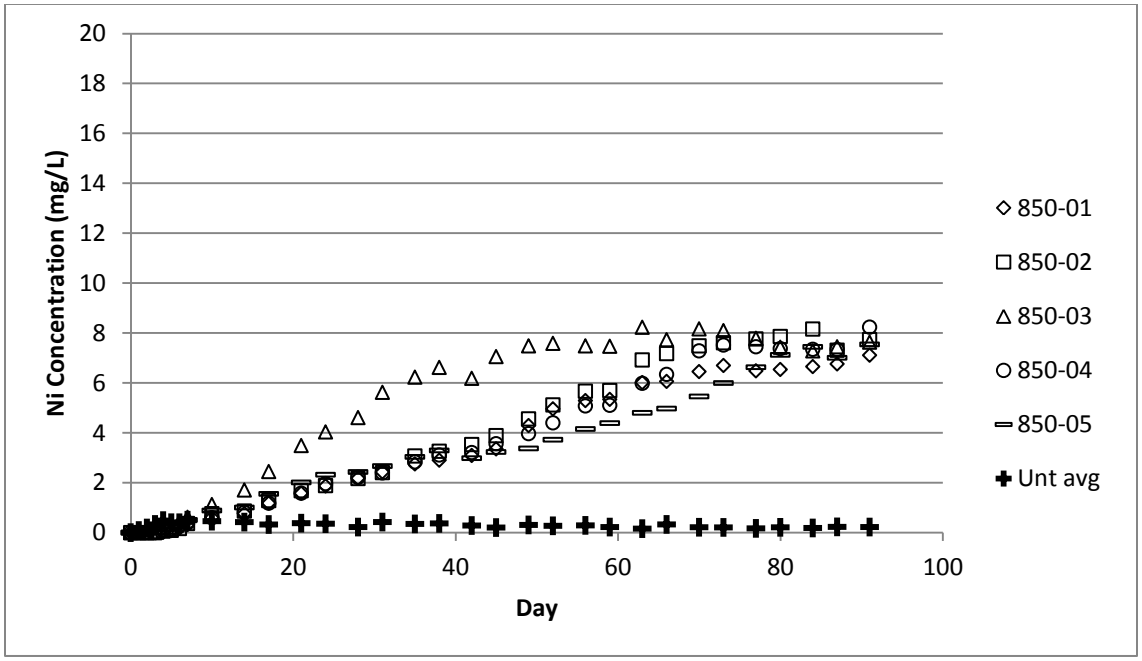

Figure 35. Nickel concentration in PBS for samples nitrided at 850°C and oxidized at 700°C.

The nickel concentrations obtained from the samples in the 900-N-700-O group varied much more than the samples nitrided at 850°C. The standard deviation for these samples over the duration of the test was 1.89 mg/L. As shown in Figure 37, the maximum concentration for the 900-04 sample was about 9 mg/L, while the nickel concentration for the 900-02 sample did not exceed 2 mg/L. The 900-04 sample was also the only sample in the group that exhibited any delamination, as shown in Table 19. The

other three samples, 900-01, 900-03, and 900-05, had very similar release profiles over the first 35 days of immersion, with a standard deviation of 1.06 mg/L during that time, but then diverged afterwards as seen in Figure 37, Figure 38, and Table 21.

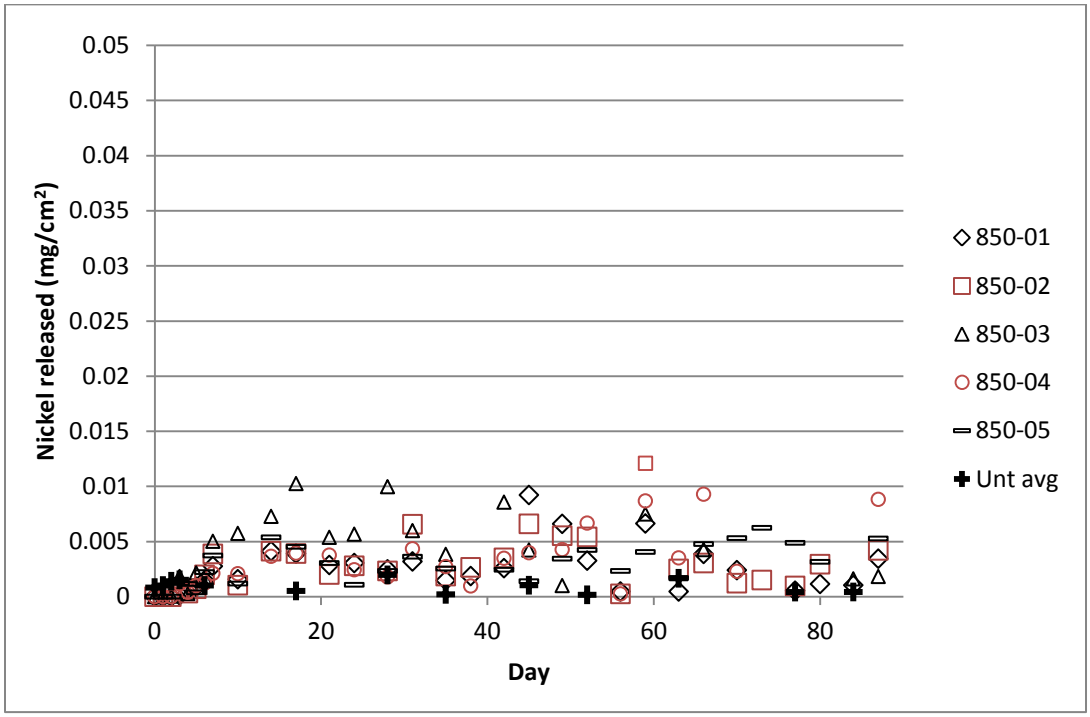

Figure 36. Nickel release from Nitinol nitrided at 850°C and oxidized at 700°C.

Table 20. Release rates (mg/cm^2/day) for 850-N-700-O samples.

Sample	Day 1-7	Day 8-35	Day 35-63	Day 64-91
850-N-01	0.000	0.009	0.011	0.004
850-N-02	0.001	0.010	0.014	0.003
850-N-03	0.001	0.020	0.007	0.000
850-N-04	0.001	0.009	0.011	0.008
850-N-05	0.001	0.009	0.006	0.010
Untreated avg	0.001	0.000	0.000	0.000

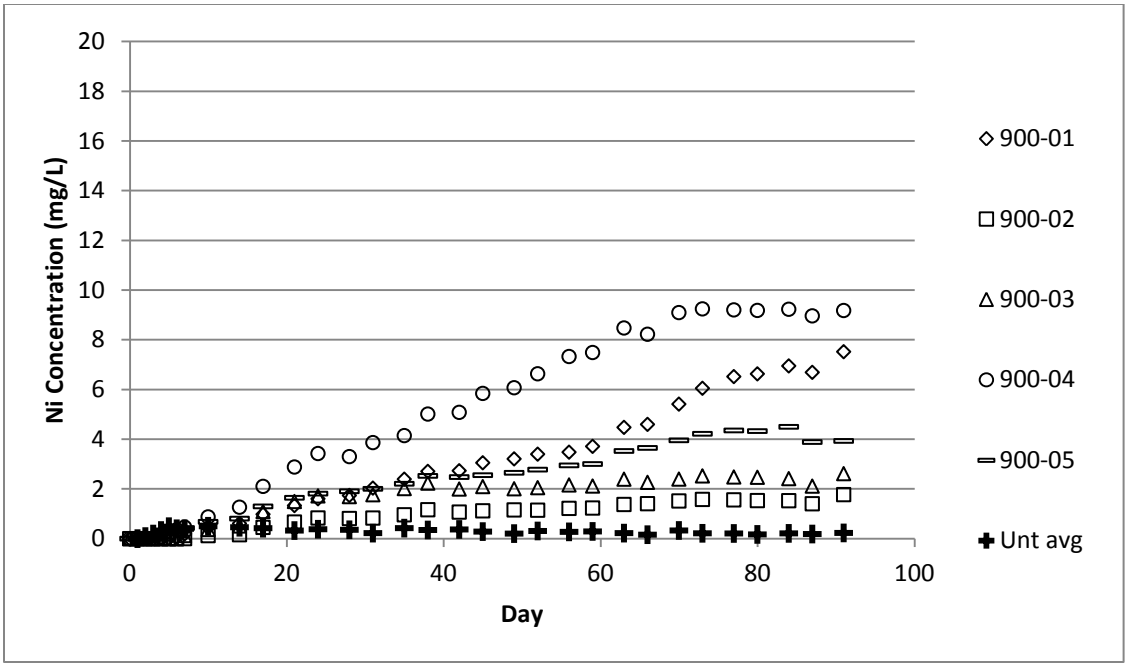

Figure 37. Nickel concentration in PBS for samples nitrided at 900°C and oxidized at 700°C.

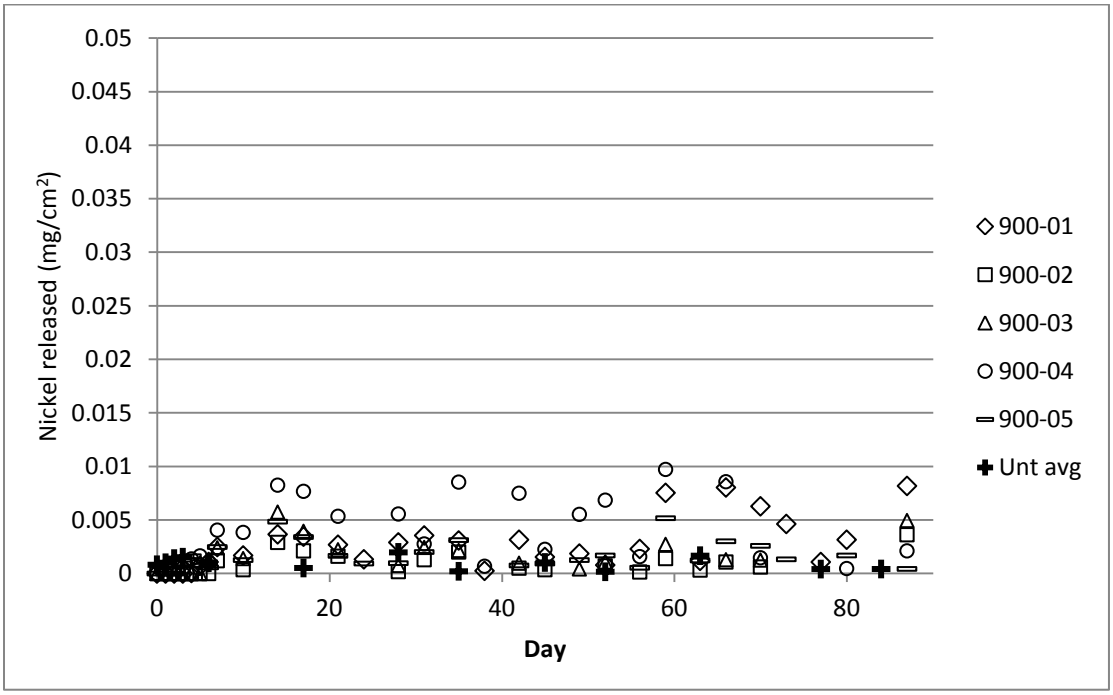

Figure 38. Nickel release from Nitinol nitrided at 900°C and oxidized at 700°C.

Table 21. Release rates (mg/cm^2/day) for 900-N-700-O samples.

Sample	Day 1-7	Day 8-35	Day 35-63	Day 64-91
900-N-01	0.000	0.008	0.007	0.011
900-N-02	0.000	0.003	0.001	0.001
900-N-03	0.000	0.007	0.001	0.001
900-N-04	0.001	0.013	0.015	0.002
900-N-05	0.001	0.006	0.005	0.001
Untreated avg	0.001	0.000	0.000	0.000

The results of the nickel leaching test for the first four samples in the 950-N-700-O group were fairly consistent, with a standard deviation of 1.10 mg/L, while the 950-05 sample reached much higher nickel concentrations, as seen in Figure 39. According to Table 19, this sample was also the only one of the samples treated at 950°C to exhibit any delamination of the oxide layer. The 950-02 sample had slightly higher nickel release rates over the course of the immersion test, as shown in Figure 40 and Table 22, but no signs of oxide layer delamination were detected.

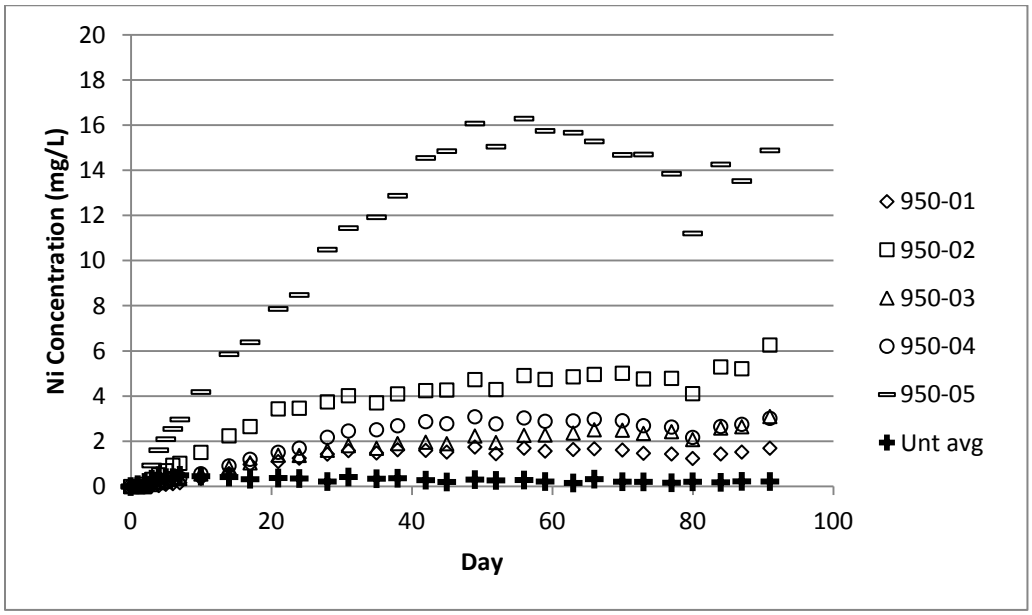

Figure 39. Nickel concentration in PBS for samples nitrided at 950°C and oxidized at 700°C.

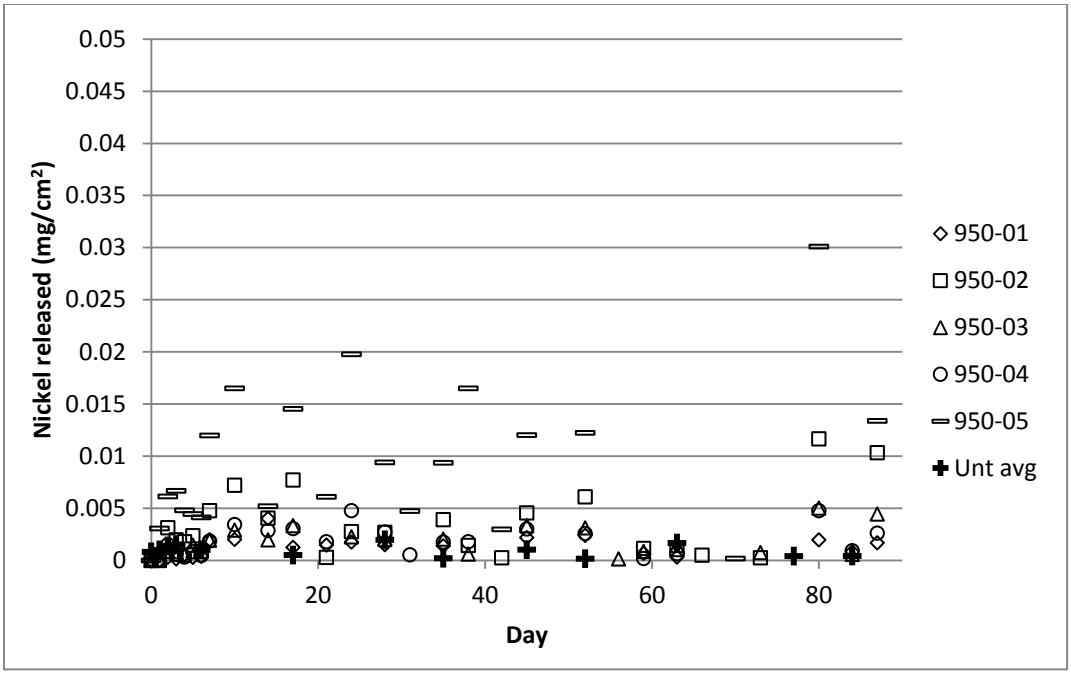

Figure 40. Nickel release from Nitinol nitrided at 950°C and oxidized at 700°C.

Table 22. Release rates (mg/cm^2/day) for 950-N-700-O samples.

Sample	Day 1-7	Day 8-35	Day 35-63	Day 64-91
950-N-01	0.000	0.005	0.001	0.000
950-N-02	0.001	0.009	0.004	0.005
950-N-03	0.001	0.005	0.002	0.003
950-N-04	0.001	0.008	0.001	0.000
950-N-05	0.004	0.032	0.013	0.000
Untreated avg	0.001	0.000	0.000	0.000

The 1000-N-700-O group had samples with a variety of different nickel release profiles. Most notably, the 1000-01 sample exhibited very low nickel release rates, resulting in much lower nickel concentrations than the rest of the samples in the group, as seen in Figure 41. The nickel concentrations were also lower than that of the untreated group, as shown in Figure 42. The nickel release rate from this sample was lower than

that of the untreated samples, as shown in Figure 43 and Table 23, resulting in a maximum concentration of 0.33 mg/L. In contrast, the untreated samples reached maximum concentrations ranging from 0.48 mg/L to 0.54 mg/L. The 1000-02 sample released nickel at a similar rate to that of the 800-05 sample, almost reaching a nickel concentration of 18 mg/L, before the concentration began to reduce over the last month of the test. In contrast, the 1000-04 sample continued to release nickel into the PBS solution over the duration of the immersion test, almost reaching 18 mg/L on the final day. These two samples, in addition to the 1000-03 sample, exhibited oxide layer delamination, as shown in Table 19.

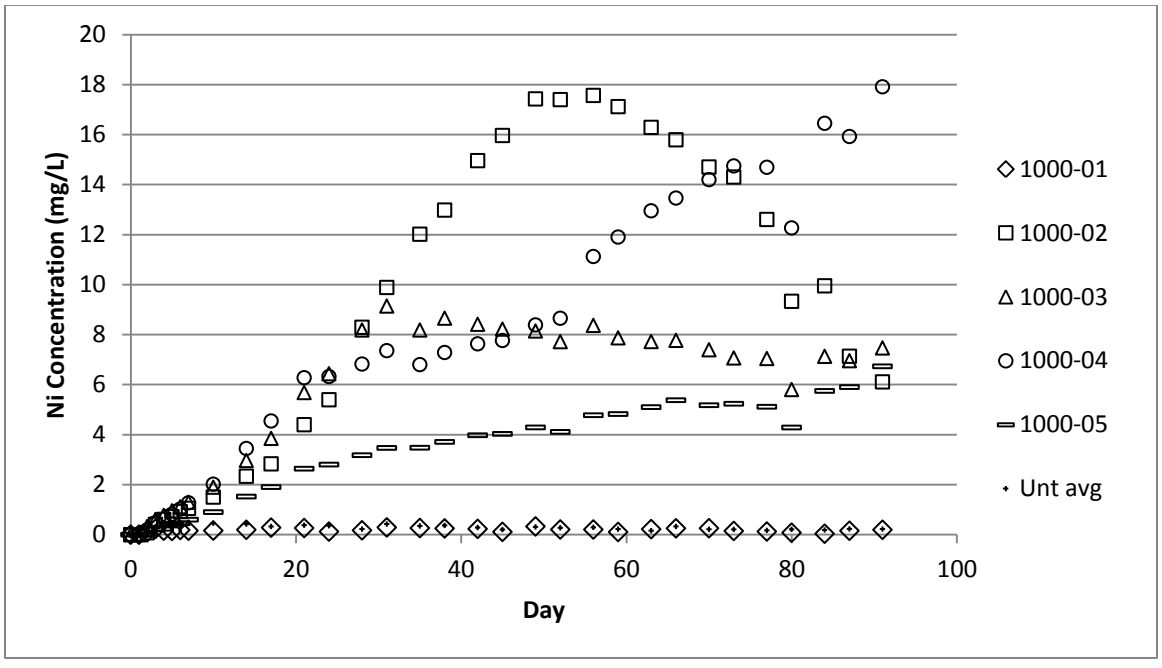

Figure 41. Nickel concentration in PBS for samples nitrided at 1000°C and oxidized at 700°C.

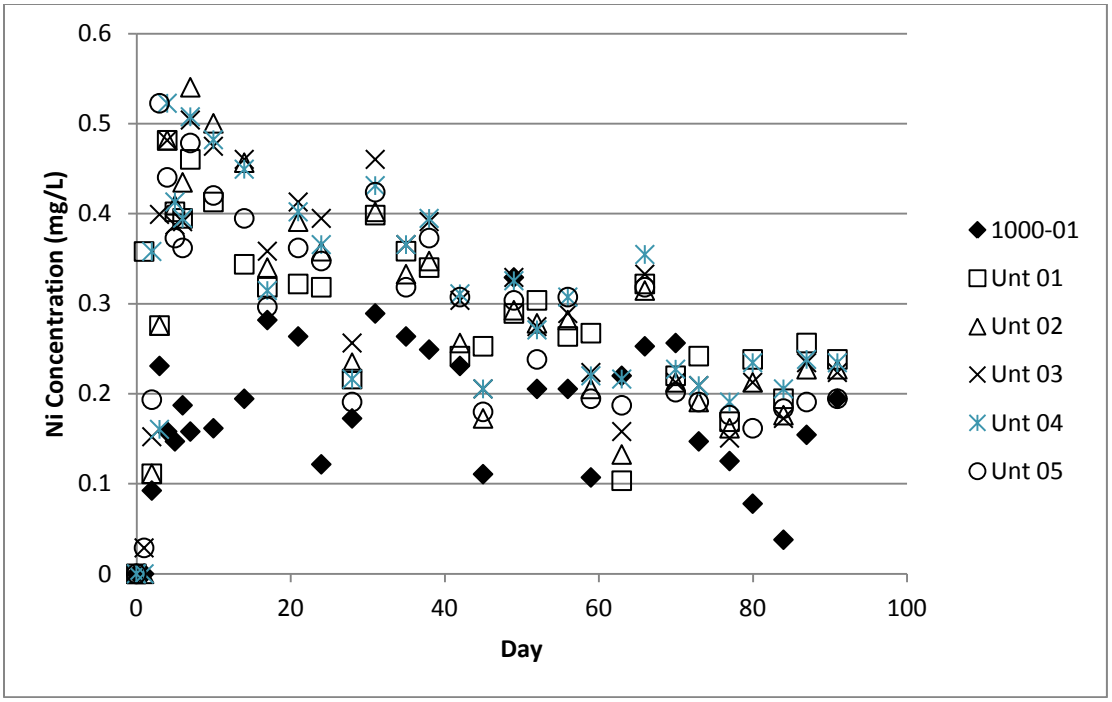

Figure 42. Nickel concentration in PBS for 1000-01 and untreated samples.

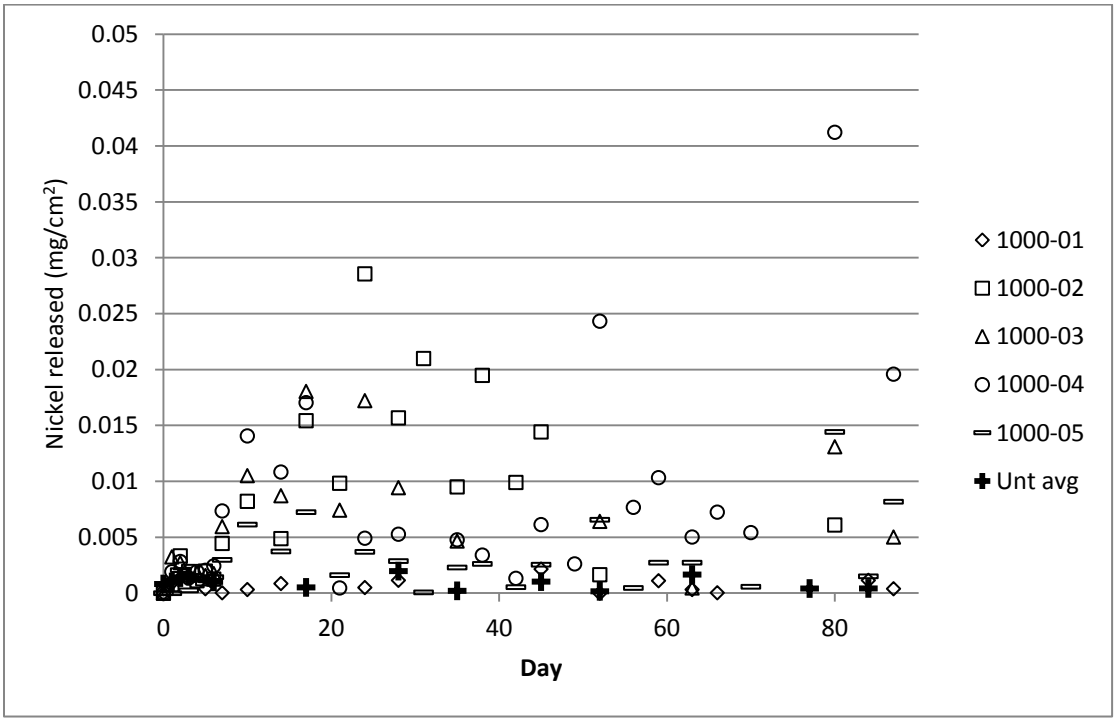

Figure 43. Nickel release from Nitinol nitrided at 1000°C and oxidized at 700°C.

Table 23. Release rates (mg/cm^2/day) for 1000-N-700-O samples.

Sample	Day 1-7	Day 8-35	Day 35-63	Day 64-91
1000-N-01	0.000	0.000	0.000	0.000
1000-N-02	0.001	0.039	0.015	0.000
1000-N-03	0.002	0.024	0.000	0.000
1000-N-04	0.002	0.019	0.022	0.017
1000-N-05	0.001	0.010	0.006	0.006
Untreated avg	0.001	0.000	0.000	0.000

5.4.4 Overview of All Samples

A comparison of the median concentrations for each of the specimen groups over the first 7 days is shown in Figure 44. It can be seen that over the first 7 days of the leaching test, several of the treated samples did not leach any nickel into the PBS until around the fourth day of immersion, while the untreated samples began to leach nickel on the first day. The median nickel concentration for the 1000-N-700-O group surpassed the median concentration of the untreated group by the third day of immersion.

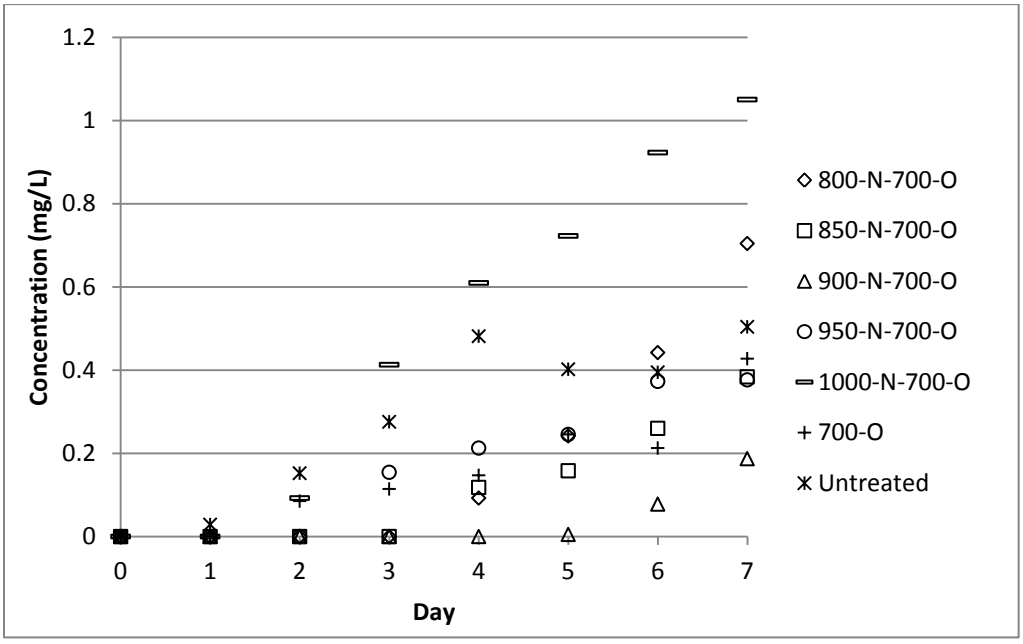

Figure 44. Median nickel concentration in PBS for all samples over the first 7 days.

Over the course of the course of the nickel leaching test, the nickel concentrations for the treated samples increased far beyond the nickel concentrations for the untreated samples, as shown in Figure 45. The exception was the 1000-01 sample, which reached a maximum concentration of 0.33 mg/L, compared to the lowest maximum concentration of the untreated samples of 0.4815 mg/L. The median release rates shown in Table 24 reflect the steady nickel concentration of the untreated samples over the duration of the test and the high release rates of the treated samples.

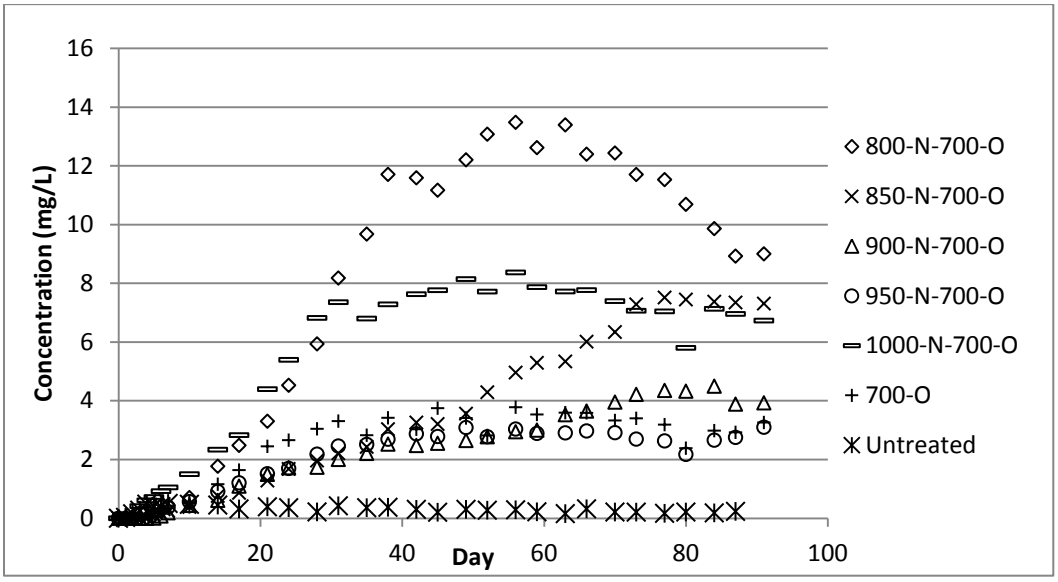

Figure 45. Median nickel concentration in PBS for all samples over 91 days.

Table 24. Median nickel release rates (mg/cm^2/day) for all samples over 91 days.

Specimen Group	Day 1-7	Day 8-35	Day 35-63	Day 64-91
800-N-700-O	0.002	0.075	0.012	0.000
850-N-700-O	0.001	0.017	0.021	0.007
900-N-700-O	0.001	0.013	0.009	0.003
950-N-700-O	0.001	0.015	0.005	0.001
1000-N-700-O	0.003	0.038	0.011	0.000
700-O	0.001	0.016	0.005	0.001
Untreated	0.001	0.000	0.000	0.000

5.5 Surface Comparison of Select Samples

Select samples were chosen from among the immersed samples for SEM analysis of the surface. The SEM images are shown in Figure 46. The Unt 01 (mechanically polished, untreated) sample was chosen as the baseline for surface roughness comparisons. The SEM image of the surface of this sample, as seen in Figure 46(a), shows the smooth surface that was obtained after mechanical polishing. A representative sample from the oxidation only group, 700-O-04 (700°C oxidation, 1 hr) was imaged to analyze surface features of the oxide layer. The features on the surface of this sample are quite large (~1 μm), and the surface of the sample appears much rougher than the polished sample, as shown in Figure 46(b). The 1000-01 sample (1000°C nitriding, 20 min; 700°C oxidation, 1 hr) was chosen because of its low nickel release rate. As seen in Figure 46(c), the surface features are much smaller than in the oxide layer of the oxidation only sample and the overall surface appears smoother. These results can be compared to a sample that was nitrided at 800°C for 20 min and oxidized at 700°C for 1 hour. This sample was not included in the nickel leaching test. As shown in Figure 46(d), this sample also had large features and the appearance of a rough surface. The EDS results of the treated samples from the immersion test are shown in Figures 47-49, including the 800-05 sample.

The 1000-01 sample had a surface nickel concentration of only 0.74 at. %, much lower than the samples in Figures 14-16, which exceeded 1 at. %. The nickel concentration on the surface of the 800-05 samples was almost 43 at. %, attributed to the

presence of the Ni_3Ti intermetallic on the surface. The nickel concentration on the surface of the 700-O-05 sample was similar to that of the samples in Figures 14-16.

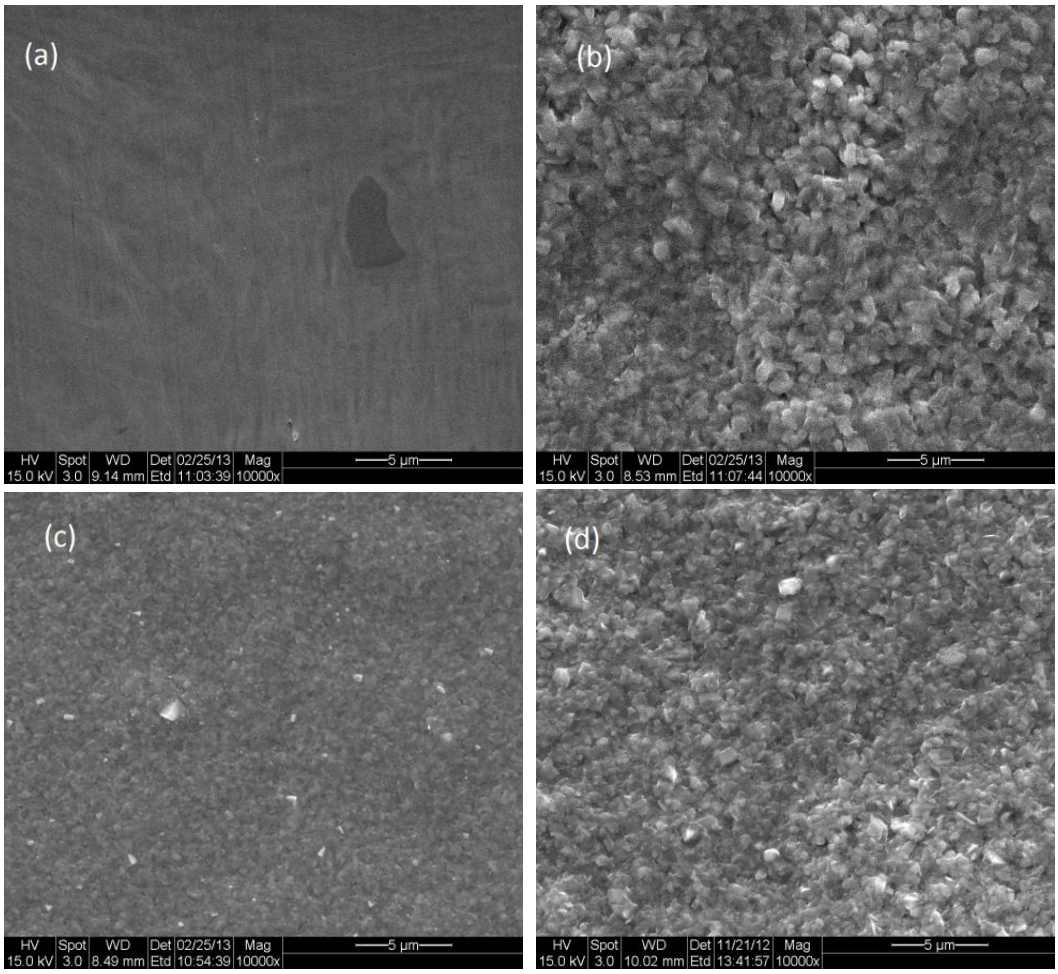

Figure 46. 10000x SEM surface images of samples (a) Unt 01 (b) 700-04 (c) 1000-N-01. (d) 800-N-700-O, not part of the immersion test.

5.6 Oxide Layer Defects

Some nitrided and oxidized samples used for oxide layer thickness measurement had defects in the oxide layer, as shown in Figure 50. The presence of these defects was localized and was not indicative of the quality of the rest of the oxide layers of the

samples. Also, defects in one sample did not necessarily correspond to defects in the other sample, despite the fact that they were treated at the same time under the same conditions.

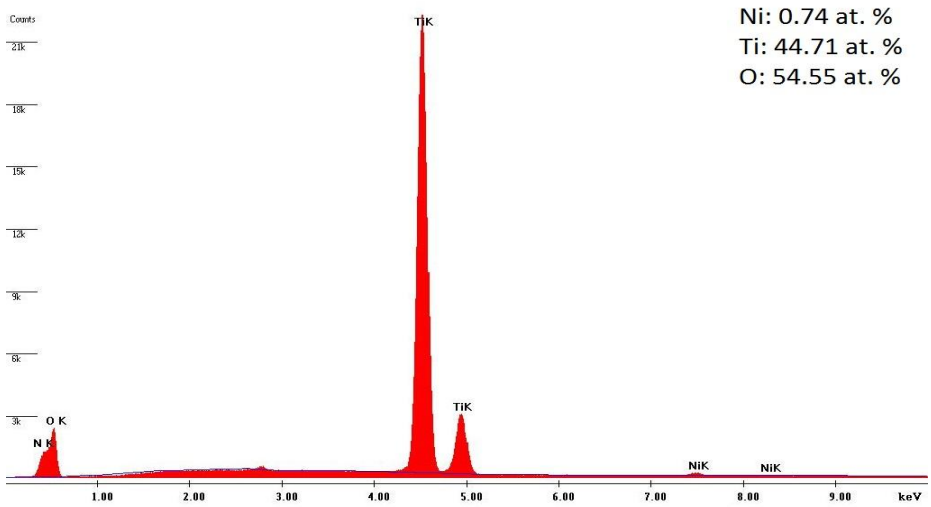

Figure 47. Energy dispersive X-ray spectroscopy spectrum from the surface of the 1000-01 sample.

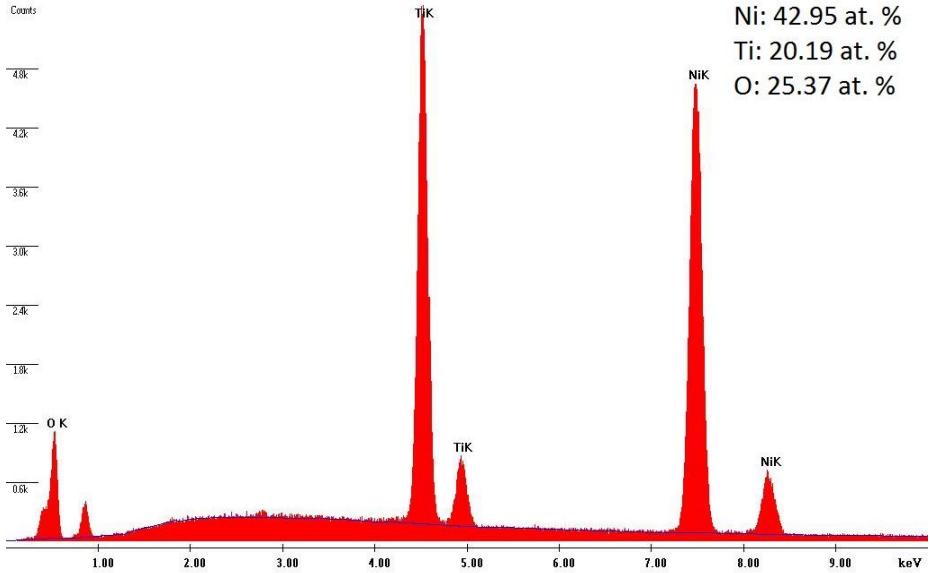

Figure 48. Energy dispersive X-ray spectroscopy spectrum from the surface of the 800-05 sample.

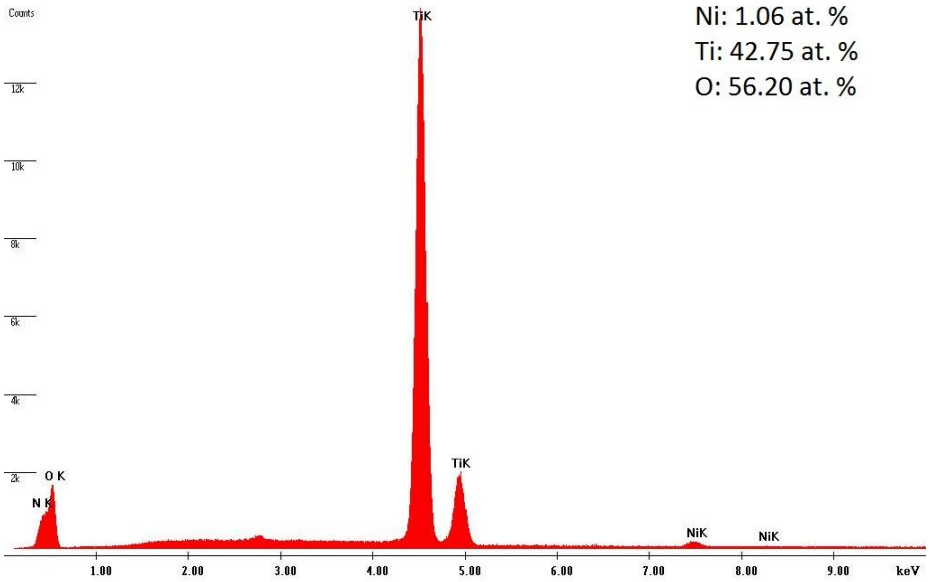

Figure 49. Energy dispersive X-ray spectroscopy spectrum from the surface of the 700-O-04 sample.

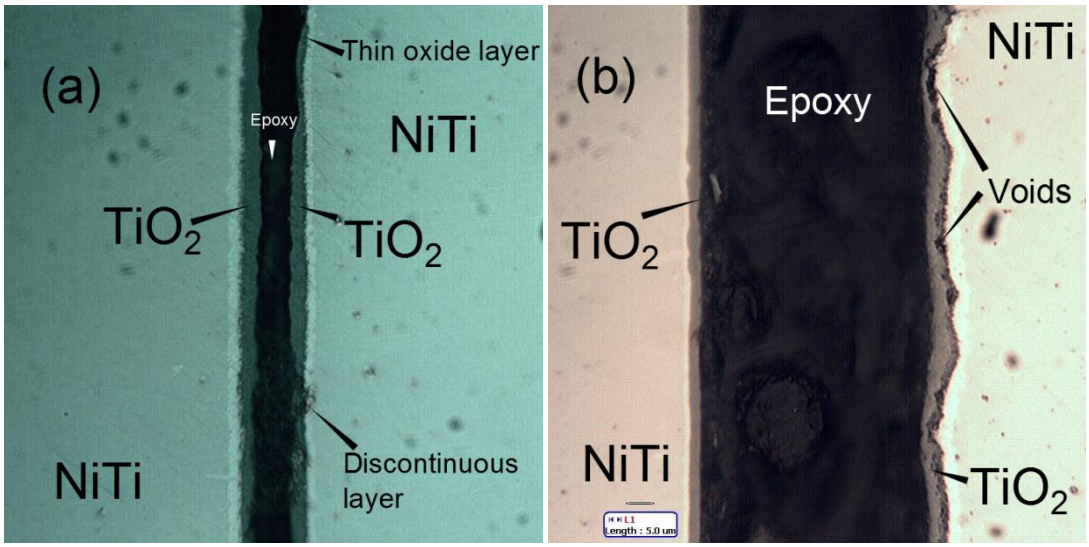

Figure 50. Defects in the oxide layer of samples in the (a) 900-N-700-O and (b) 850-N-700-O group

CHAPTER SIX

DISCUSSION

6.1 Results of Nitinol Heat Treatments

The heat treatments performed on the Nitinol samples were able to reduce the surface nickel content to levels on par with that of many of the other surface treatments described in Table 1. Although the phases detected on the surface by XRD reflected only the desired crystalline phase of TiO_2, interstitial nickel and nickel-rich intermetallic sublayers were present after treatment, as evidenced by the EDS analysis of the cross sections of treated samples, shown in Figures 22-24. Thickness measurements of the oxide layer showed that the oxidation treatment at 700°C for 1 hour produced thicknesses ranging from 1 to 4.5 microns, with median thicknesses ranging from 2 to 3 microns. The thicknesses for the nitride layers produced by heat treatments at 950°C and 1000°C produced nitride layers thicker than the oxide layers, ranging from 3 to 9.7 microns. Although the median nitride layer thicknesses produced by the treatments at these temperatures was larger than the median oxide layer thicknesses, it is certainly possible that the oxidation process extended beyond the nitride layer in areas where the nitride layer was thinnest. In addition, the nickel-rich intermediate layers in Figure 11 extended almost to the surface in several areas, owing to the finger-like projections present. Oxidation of a nitride layer such as this would result in nickel presence in the titanium oxide layer. In Tables 9-11, it was shown by EDS analysis of the surface of treated samples that nickel was in fact present in the oxide layer in small amounts. An oxide

layer thickness between 0.1 and 10 microns has also been linked to decreased corrosion resistance [44]. This lowering of the breakdown potential has been attributed to voids in the oxide layer and pits in the nickel-rich layer, created during the oxidation process. An example of these voids is shown in Figure 50(b). The outward diffusion of titanium during oxidation can produce these vacancies in the oxide layer, which have been shown to lead to pitting corrosion [45]. A discontinuous oxide layer, such as the one shown in Figure 50(a), exposes the nickel-rich layer to the surrounding medium, allowing for ions to enter the pits and thus initiating corrosion.

The presence of nickel-rich intermetallic layers beneath the surface oxide layer in the study was confirmed both by EDS and by XRD. One problem with these layers is that if the layer is exposed to the environment, whether through cracks, delamination, or other defects, it may become a persistent source of nickel, increasing nickel concentrations to potentially toxic levels if implanted in the body. Also, as shown in Figure 11, the nickel-rich sublayers had finger-like projections that extended into the nickel-free surface layer. After oxidation, the nickel from these sublayers would have been closer to the surface, allowing for faster diffusion into the surrounding medium. In addition, the nickel-rich layer has been shown to be a site for the initiation of localized pitting corrosion due to the pits that form at the interface between the oxide and nickel-rich layer during oxidation [44].

6.2 Results of Nickel Leaching Test

Almost all of the treated samples exhibited higher nickel leaching than those samples which were simply mechanically polished and not subjected to any heat

treatment. None of the samples released more nickel in a single day than what is normally ingested as part of everyday exposure. The maximum amount of nickel released by a sample in a single day was about 0.042 mg, while the average daily intake is about 0.1 to 0.3 mg.

6.2.1 Delamination of Oxide Layer

The samples that exhibited abnormally high nickel release in comparison to similarly treated samples were associated with delamination of the surface oxide layer. This exposed the nickel-rich sublayers to the PBS and allowed for heightened nickel release rates. It was not immediately apparent that the delamination would occur. Most of the delaminated samples first experienced flaking of the oxide layer after about two weeks of immersion. Failure at the interface between the coating and the substrate has been reported as a reason for oxide layer delamination [46]. Pores or vacancies developed at the interface between the nickel-rich layer and the titanium oxide layer, such as those seen in Figure 50, as a result of the Kirkendall effect, wherein the depletion of Ti from the bulk NiTi formed vacancies. The collection of these vacancies resulted in the voids seen at the interface. This phenomenon has been reported previously by Zhu *et al.* [45]. These voids, in concert with discontinuous areas in the oxide layer as shown in Figure 50, allowed the ions, namely Cl^-, in the PBS to access the interface between the oxide and nickel rich layer. This led to pitting corrosion between the layers. Continued delamination and immersion in the PBS allowed for delamination to continue over time.

Also, differences in thermal expansion coefficients among the different layers contributed to the development of microcracks during the cooling phase of the heat

treatment. Cracking of the oxide layer during cooling did occur in test runs of the heat treatment method when the Nitinol samples were removed too quickly from the furnace. The poor adhesion of the oxide layer was due to residual stress in the layers, a phenomenon reported by Abdolldhi *et al.* [47]. This problem was remedied in this study by the implementation of a longer in-furnace cool-down period, reducing the residual stress.

6.2 2 Diffusion of Nickel through the Oxide Layer

Many of the treated samples showed no signs of delamination, but still released nickel at higher rates than the untreated samples. This was most likely a result of outward diffusion of nickel through the oxide layer due to the nickel concentration difference between the nickel-rich layer and the relatively nickel-free oxide layer. Defects such as voids or vacancies provide pathways for nickel to diffuse from the nickel-rich layer to the PBS. It was shown by Firstov *et al.* [25] that oxidation of Nitinol at high temperatures (600°C to 800°C) leads to the formation of a rough and porous oxide layer and that the rutile layer begins to crack as it grows thicker. The porosity of the oxide layer was explained by the change in NiTi oxidation behavior at temperatures above 600°C, in which the deep penetration of oxygen led to rapid depletion of Ti from the bulk. As a result, vacancies formed within the layer. The rough surface of the oxidation-only sample in Figure 46(b), the nitrided and oxidized sample in Figure 46(d), and the defects shown in Figure 50 are an indication of a defective, porous oxide layer that promoted outward nickel diffusion. The phenomenon of outward nickel diffusion following the oxidation of Nitinol has been reported previously [26, 49]. The presence of

nickel on the outer surface of the heat-treated Nitinol in this study, as confirmed by EDS, was further evidence of nickel diffusion through the oxide layer. The surface nickel was detected because the outward projections of the nickel-rich Ni_3Ti sublayer shown in Figure 12 brought nickel closer to the surface of the sample, simultaneously decreasing the diffusion distance.

6.2.3 Untreated Samples

Over the first 5 days of the immersion test, 25 of the 30 treated samples released nickel at lower rates compared to all of the mechanically polished Nitinol samples. However, over the duration of the test, almost all the samples continued to release nickel into the PBS, resulting in higher nickel concentrations than those caused by nickel release from the untreated samples. A theory to explain this seemingly inverse result is found in the 2007 study by Schroeder [50]. In that study, mechanically polished Nitinol was immersed in PBS solution and kept at 37°C. It was found that, over a 6 day immersion period, the thin (2.6 nm) passive titanium oxide film on the surface of the Nitinol became about 73% thicker and was relatively defect-free. In the present research, the leaching rate of the untreated Nitinol was positive over the first week of immersion but then showed a general downward trend over the rest of the immersion period. This indicates that over the first week of immersion, the passive film was initially thin and defective, allowing for high nickel release rates, but gradually became thicker and more defect-free, preventing further outward nickel diffusion. This phenomenon did not occur for the treated samples since the Ti exposed to the solution was already oxidized.

6.3 Nickel Leaching Test Protocol

The method developed for performing Nitinol nickel leaching tests at SJSU was effective and can be easily replicated for small Nitinol samples such as wires or stents. The basic equipment needed for the experiment, the atomic absorption spectrometer and incubator, are already working and available. The other equipment needed, including centrifuge tubes, PBS solution, and deionized water, are readily available or can be acquired at a low cost. The parameters chosen for nickel concentration readings in the present study were designed for nickel concentrations ranging from 0.1 to 20 mg/L. However, they can be adjusted to accommodate expected nickel concentrations of 1-100 mg/L or even up to 8000 mg/L.

As evidenced by the results of the nickel leaching test, the methods for measuring nickel release from Nitinol are fairly sound. If the Nitinol samples to be tested are uniformly treated on all sides, then suspending the samples as was done in the present study would not be necessary. This method could easily be employed for small implantable medical devices such as stents, vena cava filters, or wire. The biggest problem would be determining the surface area of irregularly shaped items in order to determine the appropriate surface area to volume ratio for the test as well as the nickel release per square centimeter. The method may also be used for other biomaterials of interest such as stainless steel or cobalt chrome, while focusing on the leaching of nickel or other elements.

6.4 Sources of Error and Limitations of Study

During heat treatment, care was taken to make sure that the conditions of each treatment run were the same. The samples were positioned in the same place for each run, but minor variations in the placement could have affected the actual temperature of the specimens. The actual processing temperature for the heat treated samples varied since the samples were not placed directly beneath the thermocouple tip, but rather 5 mm beyond the tip. The accuracy of the thermocouple (±0.25%) means that the actual temperature could have varied by as much as 2.5°C for 1000°C treatments. The amount, shape, and positioning of titanium turnings placed in the quartz tube resulted in variable gas flow across the sample surface. The times for the heat treatment periods varied by as much as 1 min based on changes in heating and cooling rates due to the surrounding environment and human error.

The temperature of the samples when immersed in the PBS varied based on their physical location in the incubator by as much as 0.5ºC. The amount of PBS in the centrifuge tubes differed among the samples by as much as 1 mL due to these variations in temperature and evaporation rates. This caused some samples to have a smaller surface area exposed to the PBS between readings. Reducing the depth of the sample in solution by 1cm results in a 6% reduction in surface area. A reduction of this size could reduce the nickel leaching in a day by about 0.003 mg. The nickel concentration readings varied day to day based on the calibration and the actual 750 mL aliquot of PBS that was removed from the solution. The mean absolute error for the nickel concentration measurements was less than ±0.1 mg/L. This was remedied by taking concentration

measurements of samples with known nickel concentration before proceeding. The measurements also varied based on the calibration curve set at the beginning of the immersion test. It was assumed that the equation for the nickel concentration calibration curve was linear. This assumption is valid for concentrations up to about 10 mg/L, but higher concentrations of around 20 mg/L could be off by as much as 4 mg/L. The detection limit for the AAS was 0.1 mg/L, so some samples with calculated release rates of 0.000 mg/cm^2/day actually released small amounts (<0.001 mg/cm^2/day) of nickel into solution.

The thickness measurements from the optical microscope were a source of error because the software returned readings only in increments of 0.2 microns. For this reason, at least 30 measurements were taken for each sample. The EDS results are sensitive to the spots chosen for analysis and the interaction volume of the electrons hitting the sample. As a result, EDS measurements for features smaller than a 1.4 micron diameter of the interaction volume were influenced by the surrounding features. Also, as seen in the results from one sample analyzed with XRD, impurities from immersion in the PBS added unwanted peaks that were difficult to identify.

CHAPTER SEVEN

CONCLUSIONS

Nickel leaching from Nitinol medical devices remains a serious problem, especially to those individuals who experience nickel hypersensitivity. A significant amount of research has been done to help reduce the amount of nickel that is released from Nitinol, including research performed at San José State University. These include surface treatments such as thermal oxidation and the nitriding and oxidation method developed by Bazochaharbakhsh [24].

As a result of this research, it was found that:

- Mechanical polishing of Nitinol can prevent long term nickel release when a thin, defect-free oxide layer grows on the surface.
- Surface nitriding and/or oxidation of Nitinol results in the formation of a nickel-rich Ni_3Ti layer beneath the surface.
- Exposure of the nickel-rich region due to delamination or porous surface layers leads to high amounts of nickel leaching.
- Voids can form at the oxide-substrate interface when oxidizing at high temperatures as a result of the Kirkendall effect.
- Delamination of oxide layers occurs as a result of pitting corrosion when the oxide-substrate interface is exposed to an ionic environment, such as in PBS, or by differential thermal contraction between the surface oxide and the layer beneath it.

CHAPTER EIGHT

RECOMMENDATIONS FOR FUTURE WORK

The nitriding and oxidation heat treatment method should be revised to improve the quality of the oxide layer. Testing of various oxidation methods of the nitrided surface should be performed. For example, lower oxidation temperatures and dwell times could be compared to determine their ability to produce a homogeneous, nickel-free oxide layer. Corrosion resistance and surface roughness characteristics of these samples should be determined to ensure that the treated surfaces can resist failure in corrosive environments.

The mechanical properties of the treated Nitinol should also be examined, with a focus on the effect of surface treatment on strain recovery and the stress-strain curve. Since titanium oxide is brittle, it affects the superelasticity of Nitinol. Fatigue testing on Nitinol wire with various oxide thicknesses would be helpful for determining parameters for treatment methods.

REFERENCES

[1] G. Kauffman and I Mayo, *"The story of Nitinol: The serendipitous discovery of the memory metal and its applications,"* The Chemical Educator, **2(2)**, 1-21, (1996).

[2] S.A. Thompson, *"An overview of nickel-titanium alloys used in dentistry,"* International Endontic Journal, **33**, 297-310, (2000).

[3] N.B. Morgan, *"Medical shape memory alloy applications – the market and its products,"* Materials Science and Engineering, **A 378**, 16-23, (2004).

[4] B. Clarke, W. Carroll, Y. Rochev, M. Hynes, D. Bradley and D. Plumley, *"Influence of Nitinol Wire Surface Treatment on Oxide Thickness and Composition and its Subsequent Effect on Corrosion Resistance and Nickel Ion Release,"* J. Biomed. Mater. Res., **A**, 61-70, (2006).

[5] S.A. Shabalovskaya, H. Tian, J.W. Anderegg, D.U. Schryvers, W.U. Carroll and J.V. Humbeeck, "*The influence of surface oxides on the distribution and release of nickel from Nitinol wires*," Biomaterials, **30**, 468-477, (2009).

[6] K. Cameron, V. Buchner and P. Tchounwou, *"Exploring the molecular mechanisms of nickel-induced genotoxicity and carcinogenicity: a literature review. "* Rev. Env. Health, **26(2)**, 81-92, (2011).

[7] C. Chen, Y. Wang, W. Huang and Y. Huang, *"Nickel induces oxidative stress and genotoxicity in human lymphocytes,"* Tox. App. Pharm., **189**, 153–159. (2003).

[8] S. Shabalovskaya, J. Anderegg and J. Van Humbeeck, "*Comparative* in vitro *performances of bare Nitinol surfaces*," Bio-Med. Mat. And Engr., **18**, 1-14 (2008).

[9] E. Denkhaus and K. Salnikow, "*Nickel essentiality, toxicity, and carcinogenicity,"* Crit Revs in Oncology/Hematology, ***42*(1)**, 35–56, (2002).

[10] D. Schaumlöffel, *"Nickel species: analysis and toxic effects,"* J. of Trace Elements in Medi. and Bio., **26**, 1–6, (2012).

[11] F. Sunderman, M. Cristostomo, M. Reid, S. Hopfer and S. Namoto, "*Rapid analysis of Ni in serum and whole blood by electrothermal atomic absorption spectrometry,"* Ann. Clin. Lab. Sci, **14**, 232-240, (1984).

[12] K. Das and V. Buchner, *"Effect of nickel exposure on peripheral tissues: role of oxidative stress in toxicity and possible protection by ascorbic acid,"* Rev. Env. Health, **22(2)**, 157-73, (2007).

[13] U.S. Environmental Protection Agency (2012). *Nickel, soluble salts (CASRN Various)* [Online]. Available at http://www.epa.gov/iris/subst/0271.htm (accessed 8 Nov 2012). WWW Article.

[14] P. Boscolo, M. Di Gioacchino, P. Conti, R.C. Barbacane, M. Andreassi, F. Di Giacomo and E. Sabbioni, *"Expression of lymphocyte subpopulations, cytokine serum levels and blood and urine trace elements in nickel sensitised women,"* Life Sci., **63(16)**, 1417-22, (1998).

[15] J. Hostynek, *"Sensitization to nickel: etiology, epidemiology, immune reactions, prevention and therapy,"* Rev. Env. Health, **21(4)**, 253-80, (2006).

[16] B. Clarke, W. Carroll, Y. Rochev, M. Hynes, D. Bradley and D. Plumley, *"Influence of Nitinol Wire Surface Treatment on Oxide Thickness and Composition and its Subsequent Effect on Corrosion Resistance and Nickel Ion Release,"* J. Biomed. Mater. Res., **A**, 61-70, (2006).

[17] A. Michiardi, C. Aparicio, J.A. Planell and F.J. Gil, *"New oxidation treatment of NiTi shape memory alloys to obtain Ni-free surfaces and improve biocompatibility,"* J. Biomed. Mat. Res., **77B**, 249-256, (2005).

[18] F.J. Gil, E. Solano, A. Campos, F. Boccio, I. Sáez, M.V. Alfonso and J.A. Planell. "*Improvement of the Friction Behaviour of NiTi Orthodontic Archwires by Nitrogen Diffusion,*" Biomed. Mater. Eng., **8**, 335, (1998).

[19] C. Liu, P. Chu, G. Lin, D. Yang, *"Effects of Ti/TiN Multilayer on Corrosion Resistance of Nickel-Titanium Orthodontic Brackets in Artificial Saliva,"* Corr. Sci., **49,** 3783-3796, (2007).

[20] S. Kobayashi, Y. Ohgoe, K. Ozeki, K. Sato, T. Sumiya, K.K. Hirakuri and H. Aoki, *"Diamond-like carbon coatings on orthodontic archwires,"* Diamond Rel. Mat. , **14**, 1094-1097 (2005).

[21] W. Haider and N. Munroe, *"Assessment of Corrosion Resistance and Metal Ion Leaching of Nitinol Alloys,"* J. Mat. Eng. Perf. , **20**, 812-815 (2011).

[22] O. Cissé, O. Savadogo, M. Wu and L'H. Yahia, *"Effect of surface treatment of NiTi alloy on its corrosion behavior in Hank's solution,"* J. Biomed. Mater. Res., **61(3),** 339-345, (2002).

[23] O. Kubaschewski and E.L. Evans, Metallurgical Thermochemistry, 2nd ed. (Pergamon Press. London, England, 1958).

[24] E. Bazochaharbakhsh, Surface Nitriding and Oxidation of Nitinol, Master's Thesis, San José State University, San José, California (2010).

[25] G.S. Firstov, R.G. Vitchev, H. Kumar, B. Blanpain and J. Van Humbeeck, "*Surface Oxidation of NiTi Shape Memory Alloy*," Biomaterials, 23(24), 4863-4871, (2002).

[26] S. Shabalovskaya, J. Anderegg and J. Van Humbeeck, *"Critical overview of Nitinol surfaces and their modifications for medical applications,"* Acta Biomater., **4**, 447-467, (2008).

[27] C.M. Chan, S. Trigwell, T. Duerig, *"Oxidation of an NiTi Alloy,"* Surf. Interface Analysis, **15**, 349-354 (1990).

[28] D. Starosvetsky and I. Gotman, "*Corrosion Behavior of TiN Coated Ni-Ti Shape Memory Surgical Alloy*," Biomaterials, **22**, 1853-1859, (2001).

[29] C. Kao, S. Ding, Y. Chen, and T. Huang, *"The Anticorrision Ability of Titanium Nitride (TiN) Plating on an Orthodontic Metal Bracket and Its Biocompatibility,"* J. Biomed. Mater. Res. A., **63,** 786-792, (2002).

[30] Y. Cheng, C. Wei, K.Y. Gan and L.C. Zhao, *"Surface modification of TiNi alloy through tantalum immersion ion implantation,"* Surf. Coat. Tech., **176,** 261-265, (2004).

[31] M. Maitz and N. Shevchenko, *"Plasma-immersion ion-implanted Nitinol surface with depressed nickel concentration for implants in blood,"* J. Biomed. Mater. Res. A. , **76A**, 356-365, (2005).

[32] N. Shevchenko, M.T. Pham and M.F. Maitz, *"Studies of surface modified NiTi alloy,"* App. Surf. Sci. , **235,** 126-131, (2004).

[33] K.W.K. Yeung, R. Poon, X. Liu, J. Ho, C. Chung, P. Chu, W. Lu, D. Chan and K. Cheung, *"Investigation of nickel suppression and cytocompatibility of surface-treated nickel-titanium shape memory alloys by using plasma immersion ion implantation,"* J. Biomed. Mater. Res. A., **72(3),** 238-45, (2005).

[34] H. Pelletier, D. Muller, P. Mill and J. Grob, *"Structural and mechanical characterisation of boron and nitrogen implanted NiTi shape memory alloy,"* Surf. Coat. Tech., **158-159,** 309-317, (2002).

[35] I. Milosev and B. Kapun, *"The corrosion resistance of Nitinol alloy in simulated physiological solutions Part 2: The effect of surface treatment,"* Mat. Sci. and Engr., **32**, 1068-1077, (2012).

[36] H.C. Jiang and L.J. Rong. *"Effect of Hydroxyapatite Coating on Nickel Release of the Porous NiTi Shape Memory Alloy Fabricated by SHS Method,"* Surf. Coat. Tech., **201**, 1017-1021, (2006).

[37] J-K. Liu, T-M. Lee, I-H. Liu, *"Effect of Loading Force on the Dissolution Behavior and Surface Properties of Nickel-Titanium Orthodontic Archwires in Artificial Saliva,"* Am. J. Orthod. Dent. Orthop., **140 (2),** 166-176, (2011).

[38] R. Poon, P. Chu, K. Yeung, J. Chung, S.C. Tjong, C.L. Chu, W. Lu, K. Cheung and K. Luk. *"Effects of Pulsing Frequency on Shape Recovery and Investigation of Nickel Out-Diffusion After Mechanical Bending of Nitrogen Plasma Implanted NiTi Shape Memory Alloys,"* Surf. Coat. Tech., **201**, 8286-8290, (2007).

[39] M. Nakamura, S. Takeda, K. Imai, H. Oshima, D. Kawahara, H. Kosugi and Y. Hashimoto, *"Cell-to-Materials Interaction-An Approach to Elucidate Biocompatibility of Biomaterials* In Vitro,*"* Biomech. Mat. Prop., ASTM STP 1173, 167-179, (1994).

[40] C. Chu, R. Wang, Y. Pu, Y. Dong, C. Guo, X. Sheng, P. Lin and P. Chu, *"Surface Treatment of NiTi Shape Memory Alloy by Modified Advanced Oxidation Process,"* Trans. Nonferrous Met. Soc. China, **19,** 575-580, (2009).

[41] D. Starosvetsky and I. Gotman, "*TiN Coating Improves the Corrosion Behavior of Superelastic NiTi Surgical Alloy*," Surf. Coat. Tech., **148**, 268-76, (2001).

[42] J.E. Garay, U. Anselmi-Tamburini, and Z.A. Munir, *"Enhanced growth of intermetallic phases in the Ni-Ti system by current effects,"* Acta Mater., **51**, 4487-4495, (2003).

[43] Y. Zhou, Q. Wang, D.L. Sun and X.L. Han, *"Co-effect of heat and direct current on growth of intermetallic layers at the interface of Ti-Ni diffusion couples,"* J. of Alloys and Comp., **509,** 1201-1205, (2011).

[44] C. Trépanier, L. Zhu, J. Fino and A.R. Pelton, *"Corrosion resistance of oxidized Nitinol,"* in International Conference on Shape Memory and Superelastic Technologies, USA, 2003, 357–373, (2003).

[45] L. Zhu, J. Fino and A.R. Pelton, "*Oxidation of Nitinol*," in International Conference on Shape Memory and Superelastic Technologies, USA, 2003, 357–368, (2003).

[46] M.M. Hasan, A.S. M. A. Haseeb, H. H. Masjuki and R. Saidur, *"Adhesion and wear behavior of nanostructured titanium oxide thin films,"* Int. J. Mech. Mat. Engr., **5**, 5-10 (2010).

[47] Z. Abdolldhi, A.A. Ziaee M. and A. Afshar, *"Investigation of titanium oxide layer in thermal-electrochemical anodizing of Ti6Al4V alloy,"* Int. J. Chem. Bio. Engr., **2,** 44-47, (2009).

[48] J. Desmaison, P. Lefort and M. Billy, *"Oxidation mechanism of titanium nitride in oxygen,"* Oxidation of Metals, **13**, (1979).

[49] J.P. Espinós, A. Fernández and A.R. González-Elipe, *"Oxidation and diffusion processes in nickel-titanium oxide systems,"* Surface Sci. , **295**, 402-410, (1993).

[50] V. Schroeder, *"Evolution of the passive film on mechanically damaged Nitinol,"* J. Mater. Biomed. Mat. Res. B., **1,** 1-13, (2011).

APPENDIX A XPS PEAK INFORMATION

Table A-1. XPS peak information for the mechanically polished NiTi sample from Figure 8.

2-Theta (deg)	Height	Area
42.544	720	9777
61.790	135	1876

Table A-2. XPS peak information for the NiTi sample nitrided at 1000°C in Figure 10.

2-Theta (deg)	Height	Area
36.654	771	7013
41.450	438	3173
42.647	1915	17013
61.853	583	6270
74.154	263	2909

Table A-3. XPS peak information for the 800-N-700-O sample in Figure 13.

2-Theta (deg)	Height	Area
27.545	3456	27218
36.143	514	4301
39.198	219	1846
41.291	273	1962
44.055	248	2271
54.351	1119	9582
56.699	479	3945
64.145	186	1774
69.002	416	4178
69.757	106	899

Table A-4. XPS peak information for the 900-N-700-O sample in Figure 14.

2-Theta (deg)	Height	Area
27.497	2406	19120
36.056	796	6750
39.155	189	1353
41.252	359	2696
44.006	182	1648
54.394	1033	9384
56.655	377	3087
62.838	152	1252
64.046	159	1427
69.005	344	3541
69.759	176	1837

Table A-5. XPS peak information for the 1000-N-700-O sample in Figure 15.

2-Theta (deg)	Height	Area
27.499	1439	12183
36.103	1021	8445
39.160	170	1337
41.297	393	3039
44.096	166	1363
54.354	893	8060
56.701	260	2266
62.758	212	1714
69.053	358	3663
69.853	214	2027

Table A-6. XPS peak information for the 1000-N-700-O sample in Figure 32.

2-Theta (deg)	Height	Area
27.463	1606	12948
36.150	153	1299
39.241	73	201
41.292	77	416
42.435	111	876
43.598	188	1769
44.205	327	3798
46.598	250	1894
51.662	138	1299
53.001	65	418
54.441	318	2581
56.742	173	1509
62.668	34	441
63.923	32	744
69.044	136	1391

Table B-1. Release rates (mg/cm^2/day) for 800-N-700-O, 850-N-700-O, and 950-N-700-O samples.

Week	1	2	3	4	5	6	7	8	9	10	11	12	13
800-01	0.006	0.014	0.016	0.019	0.015	0.000	0.010	0.000	0.005	0.001	0.000	0.000	0.002
800-02	0.002	0.006	0.011	0.008	0.006	0.001	0.010	0.012	0.015	0.000	0.000	0.000	0.000
800-03	0.005	0.009	0.009	0.008	0.003	0.000	0.012	0.007	0.007	0.004	0.000	0.000	0.001
800-04	0.004	0.008	0.014	0.021	0.020	0.000	0.013	0.000	0.000	0.000	0.000	0.000	0.000
800-05	0.004	0.026	0.037	0.019	0.012	0.009	0.007	0.000	0.000	0.000	0.000	0.000	0.000
850-01	0.002	0.003	0.005	0.003	0.003	0.002	0.007	0.006	0.004	0.003	0.000	0.001	0.003
850-02	0.002	0.003	0.005	0.003	0.005	0.003	0.006	0.006	0.007	0.003	0.002	0.002	0.000
850-03	0.004	0.006	0.010	0.006	0.009	0.000	0.007	0.000	0.004	0.000	0.000	0.000	0.002
850-04	0.002	0.002	0.004	0.004	0.004	0.002	0.004	0.006	0.005	0.007	0.001	0.000	0.005
850-05	0.003	0.003	0.006	0.002	0.003	0.000	0.002	0.004	0.004	0.004	0.007	0.005	0.001
900-01	0.001	0.002	0.004	0.002	0.004	0.002	0.003	0.002	0.006	0.005	0.006	0.002	0.003
900-02	0.000	0.001	0.003	0.001	0.001	0.001	0.000	0.000	0.001	0.001	0.000	0.000	0.001
900-03	0.001	0.002	0.006	0.001	0.002	0.000	0.000	0.001	0.001	0.000	0.000	0.000	0.001
900-04	0.003	0.005	0.009	0.002	0.005	0.005	0.006	0.007	0.007	0.004	0.001	0.000	0.000
900-05	0.002	0.002	0.005	0.001	0.002	0.002	0.001	0.002	0.003	0.002	0.002	0.001	0.000
950-01	0.001	0.002	0.003	0.002	0.000	0.001	0.001	0.000	0.000	0.000	0.000	0.000	0.001
950-02	0.006	0.007	0.007	0.002	0.000	0.003	0.003	0.001	0.000	0.001	0.000	0.003	0.006
950-03	0.002	0.003	0.003	0.001	0.000	0.002	0.002	0.000	0.001	0.001	0.000	0.001	0.003
950-04	0.002	0.003	0.003	0.004	0.002	0.002	0.001	0.000	0.000	0.000	0.000	0.000	0.002
950-05	0.017	0.017	0.011	0.015	0.008	0.015	0.009	0.001	0.000	0.000	0.000	0.002	0.004

Table B-2. Release rates (mg/cm^2/day) for 1000-N-700-O, 700-O, and untreated samples.

Week	1	2	3	4	5	6	7	8	9	10	11	12	13
1000-N-01	0.001	0.000	0.000	0.000	0.001	0.000	0.001	0.000	0.000	0.000	0.000	0.000	0.001
1000-N-02	0.006	0.007	0.012	0.022	0.021	0.017	0.014	0.001	0.000	0.000	0.000	0.000	0.000
1000-N-03	0.007	0.010	0.016	0.014	0.000	0.001	0.000	0.001	0.000	0.000	0.000	0.000	0.002
1000-N-04	0.007	0.012	0.016	0.003	0.000	0.005	0.004	0.016	0.010	0.007	0.003	0.010	0.008
1000-N-05	0.003	0.005	0.006	0.003	0.002	0.003	0.002	0.003	0.002	0.000	0.000	0.004	0.006
700-O-01	0.003	0.006	0.005	0.003	0.000	0.001	0.002	0.002	0.000	0.000	0.000	0.000	0.001
700-O-02	0.002	0.003	0.002	0.002	0.000	0.001	0.001	0.002	0.000	0.000	0.000	0.000	0.002
700-O-03	0.002	0.004	0.004	0.003	0.000	0.002	0.003	0.004	0.000	0.001	0.000	0.000	0.001
700-O-04	0.004	0.007	0.007	0.008	0.005	0.005	0.002	0.005	0.000	0.000	0.000	0.001	0.003
700-O-05	0.002	0.004	0.011	0.005	0.000	0.001	0.000	0.002	0.000	0.000	0.000	0.000	0.002
Unt 01	0.003	0.000	0.000	0.000	0.001	0.000	0.000	0.000	0.000	0.001	0.000	0.000	0.000
Unt 02	0.003	0.000	0.000	0.000	0.001	0.000	0.000	0.000	0.000	0.000	0.000	0.000	0.000
Unt 03	0.003	0.000	0.000	0.000	0.001	0.000	0.000	0.000	0.000	0.000	0.000	0.000	0.000
Unt 04	0.003	0.000	0.000	0.000	0.001	0.000	0.000	0.000	0.000	0.000	0.000	0.000	0.000
Unt 05	0.003	0.000	0.000	0.000	0.001	0.000	0.000	0.000	0.000	0.000	0.000	0.000	0.000

Table C-1. Nickel concentration measurements for 800-N-700-O group.

Sample	Day 0	Day 1	Day 2	Day 3	Day 4	Day 5	Day 6	Day 7	Day 10	Day 14	Day 17	Day 21	Day 24	Day 28	Day 31	Day 35
800-N-01	0.00	0.00	0.00	0.00	0.14	0.24	0.70	0.98	2.29	3.39	4.82	6.20	7.58	9.47	10.79	12.04
800-N-02	0.00	0.00	0.00	0.00	0.00	0.05	0.20	0.35	0.75	1.33	2.12	3.29	3.72	4.70	5.35	5.81
800-N-03	0.00	0.00	0.00	0.00	0.09	0.25	0.63	0.86	1.77	2.48	3.30	4.12	4.43	5.51	5.90	6.10
800-N-04	0.00	0.00	0.00	0.00	0.15	0.26	0.44	0.62	1.18	2.00	3.09	4.53	5.94	8.18	9.68	11.71
800-N-05	0.00	0.00	0.00	0.00	0.00	0.11	0.42	0.70	2.53	5.32	7.97	11.79	13.28	15.11	17.19	17.18
	Day 38	Day 42	Day 45	Day 49	Day 52	Day 56	Day 59	Day 63	Day 66	Day 70	Day 73	Day 77	Day 80	Day 84	Day 87	Day 91
800-N-01	11.59	11.36	12.20	13.08	13.48	12.62	13.40	13.48	13.63	13.62	13.55	13.27	12.79	12.71	12.60	13.08
800-N-02	5.88	5.91	6.44	7.63	8.45	9.79	10.86	12.40	12.44	11.71	11.53	10.23	9.70	8.59	6.57	6.82
800-N-03	6.03	6.12	6.82	8.21	9.28	9.35	9.74	10.49	10.84	11.12	11.23	10.96	10.64	10.70	10.69	10.89
800-N-04	11.99	11.17	12.79	13.43	13.68	13.46	13.48	13.52	12.65	12.61	11.95	10.69	9.86	8.93	9.00	7.58
800-N-05	17.40	18.73	19.90	19.98	19.71	16.99	15.58	11.57	9.11	6.67	5.40	4.19	3.75	3.30	2.67	2.91

Table C-2. Nickel concentration measurements for 850-N-700-O group.

Sample	Day 0	Day 1	Day 2	Day 3	Day 4	Day 5	Day 6	Day 7	Day 10	Day 14	Day 17	Day 21	Day 24	Day 28	Day 31	Day 35
850-N-01	0.00	0.00	0.00	0.00	0.01	0.08	0.17	0.32	0.60	0.76	1.18	1.58	1.87	2.18	2.43	2.75
850-N-02	0.00	0.00	0.00	0.00	0.06	0.09	0.17	0.37	0.76	0.86	1.28	1.68	1.88	2.17	2.40	3.07
850-N-03	0.00	0.00	0.00	0.01	0.19	0.22	0.44	0.62	1.13	1.71	2.45	3.49	4.04	4.61	5.62	6.23
850-N-04	0.00	0.00	0.00	0.00	0.12	0.16	0.26	0.38	0.60	0.81	1.18	1.58	1.96	2.21	2.39	2.83
850-N-05	0.00	0.00	0.00	0.00	0.13	0.24	0.28	0.51	0.89	1.01	1.55	2.01	2.32	2.43	2.67	3.03
	Day 38	Day 42	Day 45	Day 49	Day 52	Day 56	Day 59	Day 63	Day 66	Day 70	Day 73	Day 77	Day 80	Day 84	Day 87	Day 91
850-N-01	2.90	3.09	3.36	4.29	4.96	5.29	5.34	6.01	6.06	6.45	6.70	6.48	6.54	6.65	6.76	7.11
850-N-02	3.26	3.53	3.89	4.56	5.12	5.67	5.69	6.92	7.18	7.49	7.61	7.76	7.86	8.16	7.31	7.74
850-N-03	6.62	6.18	7.06	7.49	7.59	7.49	7.47	8.23	7.73	8.17	8.10	7.79	7.43	7.28	7.45	7.63
850-N-04	3.11	3.21	3.56	3.97	4.40	5.08	5.10	5.98	6.34	7.28	7.52	7.45	7.38	7.35	7.34	8.24
850-N-05	3.29	2.98	3.23	3.37	3.72	4.15	4.39	4.80	4.97	5.46	6.00	6.63	7.12	7.45	7.01	7.54

Table C-3. Nickel concentration measurements for 900-N-700-O group.

Sample	Day 0	Day 1	Day 2	Day 3	Day 4	Day 5	Day 6	Day 7	Day 10	Day 14	Day 17	Day 21	Day 24	Day 28	Day 31	Day 35
900-N-01	0.00	0.00	0.00	0.00	0.00	0.01	0.08	0.19	0.44	0.61	0.98	1.33	1.60	1.74	2.03	2.39
900-N-02	0.00	0.00	0.00	0.00	0.00	0.00	0.00	0.00	0.12	0.16	0.45	0.67	0.83	0.81	0.83	0.96
900-N-03	0.00	0.00	0.00	0.00	0.00	0.00	0.00	0.13	0.37	0.51	1.09	1.49	1.72	1.69	1.77	2.02
900-N-04	0.00	0.00	0.00	0.00	0.05	0.19	0.36	0.46	0.88	1.27	2.10	2.88	3.42	3.30	3.87	4.15
900-N-05	0.00	0.00	0.00	0.00	0.10	0.26	0.37	0.43	0.68	0.81	1.30	1.64	1.81	1.91	2.00	2.21
	Day 38	Day 42	Day 45	Day 49	Day 52	Day 56	Day 59	Day 63	Day 66	Day 70	Day 73	Day 77	Day 80	Day 84	Day 87	Day 91
900-N-01	2.71	2.73	3.05	3.21	3.40	3.48	3.71	4.48	4.60	5.41	6.05	6.52	6.63	6.95	6.69	7.52
900-N-02	1.16	1.07	1.12	1.16	1.14	1.22	1.23	1.37	1.41	1.52	1.58	1.56	1.53	1.53	1.40	1.77
900-N-03	2.23	2.00	2.10	2.01	2.05	2.16	2.12	2.39	2.27	2.40	2.53	2.48	2.47	2.42	2.11	2.62
900-N-04	5.01	5.08	5.84	6.07	6.63	7.33	7.49	8.48	8.22	9.09	9.24	9.20	9.18	9.23	8.96	9.18
900-N-05	2.53	2.48	2.55	2.65	2.78	2.95	3.00	3.53	3.65	3.96	4.22	4.35	4.33	4.50	3.89	3.93

Table C-4. Nickel concentration measurements for 950-N-700-O group.

Sample	Day 0	Day 1	Day 2	Day 3	Day 4	Day 5	Day 6	Day 7	Day 10	Day 14	Day 17	Day 21	Day 24	Day 28	Day 31	Day 35
950-N-01	0.00	0.00	0.00	0.03	0.05	0.10	0.13	0.17	0.37	0.57	0.98	1.11	1.26	1.44	1.59	1.49
950-N-02	0.00	0.00	0.00	0.32	0.52	0.70	0.94	1.03	1.51	2.24	2.66	3.44	3.47	3.75	4.02	3.71
950-N-03	0.00	0.00	0.00	0.09	0.17	0.22	0.37	0.36	0.55	0.85	1.05	1.39	1.38	1.61	1.81	1.69
950-N-04	0.00	0.00	0.00	0.15	0.21	0.25	0.33	0.38	0.57	0.92	1.21	1.52	1.70	2.18	2.46	2.51
950-N-05	0.00	0.00	0.31	0.93	1.61	2.10	2.55	2.97	4.19	5.86	6.39	7.86	8.48	10.49	11.44	11.92
	Day 38	Day 42	Day 45	Day 49	Day 52	Day 56	Day 59	Day 63	Day 66	Day 70	Day 73	Day 77	Day 80	Day 84	Day 87	Day 91
950-N-01	1.63	1.60	1.53	1.75	1.45	1.70	1.57	1.64	1.67	1.62	1.47	1.44	1.24	1.44	1.53	1.70
950-N-02	4.10	4.25	4.27	4.74	4.29	4.91	4.74	4.86	4.97	5.02	4.76	4.79	4.11	5.30	5.22	6.27
950-N-03	1.90	1.96	1.90	2.24	1.95	2.27	2.28	2.37	2.51	2.50	2.35	2.43	2.08	2.59	2.65	3.10
950-N-04	2.69	2.87	2.78	3.09	2.78	3.04	2.89	2.91	2.97	2.91	2.70	2.63	2.18	2.66	2.75	3.02
950-N-05	12.87	14.55	14.85	16.07	15.05	16.29	15.75	15.67	15.28	14.68	14.70	13.85	11.21	14.26	13.53	14.88

Table C-5. Nickel concentration measurements for 1000-N-700-O group.

Sample	Day 0	Day 1	Day 2	Day 3	Day 4	Day 5	Day 6	Day 7	Day 10	Day 14	Day 17	Day 21	Day 24	Day 28	Day 31	Day 35
1000-N-01	0.00	0.00	0.09	0.23	0.16	0.15	0.19	0.16	0.16	0.19	0.28	0.26	0.12	0.17	0.29	0.26
1000-N-02	0.00	0.00	0.07	0.41	0.61	0.72	0.92	1.05	1.50	2.34	2.83	4.40	5.39	8.29	9.88	12.02
1000-N-03	0.00	0.01	0.33	0.61	0.77	0.96	1.12	1.29	1.90	2.97	3.85	5.68	6.44	8.18	9.14	8.18
1000-N-04	0.00	0.00	0.19	0.48	0.62	0.82	1.02	1.27	2.02	3.45	4.55	6.28	6.32	6.82	7.36	6.80
1000-N-05	0.00	0.00	0.00	0.21	0.23	0.37	0.45	0.60	0.90	1.52	1.90	2.64	2.80	3.18	3.47	3.48
	Day 38	Day 42	Day 45	Day 49	Day 52	Day 56	Day 59	Day 63	Day 66	Day 70	Day 73	Day 77	Day 80	Day 84	Day 87	Day 91
1000-N-01	0.25	0.23	0.11	0.33	0.21	0.21	0.11	0.22	0.25	0.26	0.15	0.13	0.08	0.04	0.15	0.19
1000-N-02	12.98	14.96	15.96	17.43	17.40	17.57	17.12	16.29	15.79	14.70	14.30	12.61	9.33	9.95	7.14	6.11
1000-N-03	8.66	8.41	8.22	8.14	7.72	8.37	7.87	7.72	7.77	7.39	7.07	7.04	5.80	7.13	6.96	7.47
1000-N-04	7.28	7.63	7.77	8.39	8.65	11.12	11.90	12.95	13.46	14.20	14.75	14.69	12.27	16.45	15.92	17.91
1000-N-05	3.71	3.97	4.03	4.29	4.11	4.78	4.82	5.10	5.38	5.18	5.23	5.11	4.28	5.75	5.90	6.73

Table C-6. Nickel concentration measurements for 700-O group.

Sample	Day 0	Day 1	Day 2	Day 3	Day 4	Day 5	Day 6	Day 7	Day 10	Day 14	Day 17	Day 21	Day 24	Day 28	Day 31	Day 35
700-O-01	0.00	0.00	0.11	0.15	0.16	0.34	0.38	0.53	0.93	1.61	2.04	2.45	2.66	3.05	3.31	2.83
700-O-02	0.00	0.00	0.03	0.07	0.12	0.19	0.15	0.29	0.39	0.80	0.98	1.20	1.28	1.47	1.59	1.44
700-O-03	0.00	0.00	0.05	0.09	0.12	0.22	0.21	0.41	0.50	1.03	1.27	1.79	2.00	2.32	2.59	2.31
700-O-04	0.00	0.00	0.15	0.18	0.22	0.33	0.41	0.68	0.92	1.90	2.32	3.19	3.67	4.53	5.25	5.48
700-O-05	0.00	0.00	0.09	0.11	0.15	0.25	0.18	0.43	0.45	1.16	1.64	3.14	3.56	4.01	4.31	3.60
	Day 38	Day 42	Day 45	Day 49	Day 52	Day 56	Day 59	Day 63	Day 66	Day 70	Day 73	Day 77	Day 80	Day 84	Day 87	Day 91
700-O-01	3.42	3.03	3.75	3.41	2.03	3.68	3.53	3.30	3.29	3.10	3.18	2.94	2.39	2.89	2.87	3.14
700-O-02	1.78	1.64	1.87	1.86	1.72	2.24	2.15	2.23	2.21	2.20	2.33	2.12	1.77	2.17	2.10	2.44
700-O-03	2.96	2.67	3.19	3.11	2.82	3.78	3.53	3.66	3.71	3.79	3.88	3.59	2.91	3.58	3.40	3.76
700-O-04	7.12	6.35	7.40	6.77	6.03	7.64	6.99	6.70	6.83	6.51	6.61	6.17	4.92	6.41	6.26	6.98
700-O-05	4.50	3.79	4.25	3.80	3.40	4.13	3.62	3.60	3.59	3.33	3.40	3.19	2.37	2.98	2.93	3.26

Table C-7. Nickel concentration measurements for Untreated group.

Sample	Day 0	Day 1	Day 2	Day 3	Day 4	Day 5	Day 6	Day 7	Day 10	Day 14	Day 17	Day 21	Day 24	Day 28	Day 31	Day 35
Unt 01	0.00	0.36	0.11	0.28	0.48	0.40	0.39	0.46	0.41	0.34	0.32	0.32	0.32	0.22	0.40	0.36
Unt 02	0.00	0.00	0.11	0.28	0.48	0.41	0.43	0.54	0.50	0.46	0.34	0.39	0.36	0.23	0.40	0.33
Unt 03	0.00	0.03	0.15	0.40	0.48	0.39	0.39	0.50	0.47	0.46	0.36	0.41	0.39	0.26	0.46	0.37
Unt 04	0.00	0.00	0.36	0.16	0.52	0.41	0.39	0.51	0.48	0.45	0.31	0.40	0.37	0.22	0.43	0.37
Unt 05	0.00	0.03	0.19	0.52	0.44	0.37	0.36	0.48	0.42	0.39	0.30	0.36	0.35	0.19	0.42	0.32
	Day 38	Day 42	Day 45	Day 49	Day 52	Day 56	Day 59	Day 63	Day 66	Day 70	Day 73	Day 77	Day 80	Day 84	Day 87	Day 91
Unt 01	0.34	0.24	0.25	0.29	0.30	0.26	0.27	0.10	0.32	0.22	0.24	0.17	0.24	0.19	0.26	0.24
Unt 02	0.35	0.26	0.17	0.29	0.28	0.28	0.21	0.13	0.31	0.21	0.19	0.16	0.21	0.18	0.23	0.23
Unt 03	0.39	0.30	0.21	0.33	0.27	0.29	0.22	0.16	0.33	0.21	0.21	0.15	0.21	0.17	0.23	0.22
Unt 04	0.39	0.31	0.21	0.33	0.27	0.31	0.22	0.22	0.35	0.23	0.21	0.19	0.23	0.21	0.24	0.23
Unt 05	0.37	0.31	0.18	0.30	0.24	0.31	0.19	0.19	0.32	0.20	0.19	0.18	0.16	0.18	0.19	0.19